

See discussions, stats, and author profiles for this publication at: <https://www.researchgate.net/publication/359840375>

Search for associated production of a Z boson with an invisibly decaying Higgs boson or dark matter candidates at $s = 13$ TeV with the ATLAS detector

Article in *Physics Letters B* · April 2022

DOI: 10.1016/j.physletb.2022.137066

CITATIONS

4

READS

34

2879 authors, including:



Adam Abed Abud

University of Liverpool

261 PUBLICATIONS 6,290 CITATIONS

[SEE PROFILE](#)



Asmaa Aboulhorma

Mohammed V University of Rabat

33 PUBLICATIONS 90 CITATIONS

[SEE PROFILE](#)



Basanta Acharya

Nepal College of Information Technology

951 PUBLICATIONS 37,579 CITATIONS

[SEE PROFILE](#)



Baida Achkar

Georg-August-Universität Göttingen

241 PUBLICATIONS 6,709 CITATIONS

[SEE PROFILE](#)

Some of the authors of this publication are also working on these related projects:



Mu3e experiment for lepton flavour violation [View project](#)



The Cherenkov Telescope Array (CTA) [View project](#)



Search for associated production of a Z boson with an invisibly decaying Higgs boson or dark matter candidates at $\sqrt{s} = 13$ TeV with the ATLAS detector



The ATLAS Collaboration*

ARTICLE INFO

Article history:

Received 17 November 2021
 Received in revised form 21 January 2022
 Accepted 18 March 2022
 Available online 4 April 2022
 Editor: M. Doser

ABSTRACT

A search for invisible decays of the Higgs boson as well as searches for dark matter candidates, produced together with a leptonically decaying Z boson, are presented. The analysis is performed using proton–proton collisions at a centre-of-mass energy of 13 TeV, delivered by the LHC, corresponding to an integrated luminosity of 139 fb^{-1} and recorded by the ATLAS experiment. Assuming Standard Model cross-sections for ZH production, the observed (expected) upper limit on the branching ratio of the Higgs boson to invisible particles is found to be 19% (19%) at the 95% confidence level. Exclusion limits are also set for simplified dark matter models and two-Higgs-doublet models with an additional pseudoscalar mediator.

© 2022 The Author(s). Published by Elsevier B.V. This is an open access article under the CC BY license (<http://creativecommons.org/licenses/by/4.0/>). Funded by SCOAP³.

Contents

1. Introduction	1
2. ATLAS detector	2
3. Data and simulated event samples	3
4. Object selection	3
5. Event selection	4
6. Background estimates and signal extraction	4
7. Systematic uncertainties	5
8. Results	7
9. Conclusion	9
Declaration of competing interest	11
Acknowledgements	11
References	11
The ATLAS Collaboration	13

1. Introduction

Understanding the nature of dark matter (DM) is one of the most important goals in particle physics today. Experiments at particle colliders such as the Large Hadron Collider (LHC) might provide sensitivity that complements searches for naturally occurring DM particles or their decay products [1–8] by attempting to produce and detect them in the laboratory. The nature of DM particles remains largely unknown, and there is no obvious candidate

in the Standard Model (SM) of particle physics. One of the most credited hypotheses is that DM candidates are weakly interacting massive particles (WIMPs, denoted by the symbol χ). At hadron colliders, searches for WIMP-like DM production rely on one or more visible particles being produced in association with the invisible DM candidates, whose experimental signature would be the missing transverse momentum ($E_{\text{T}}^{\text{miss}}$) in the collision event.

Several models have been proposed in the past decades, with different assumptions about the DM couplings to SM particles and related production processes. As DM particles must be massive, searches for physics beyond the SM in which DM couples to the Higgs boson are strongly motivated. The Higgs boson was discov-

* E-mail address: atlas.publications@cern.ch.

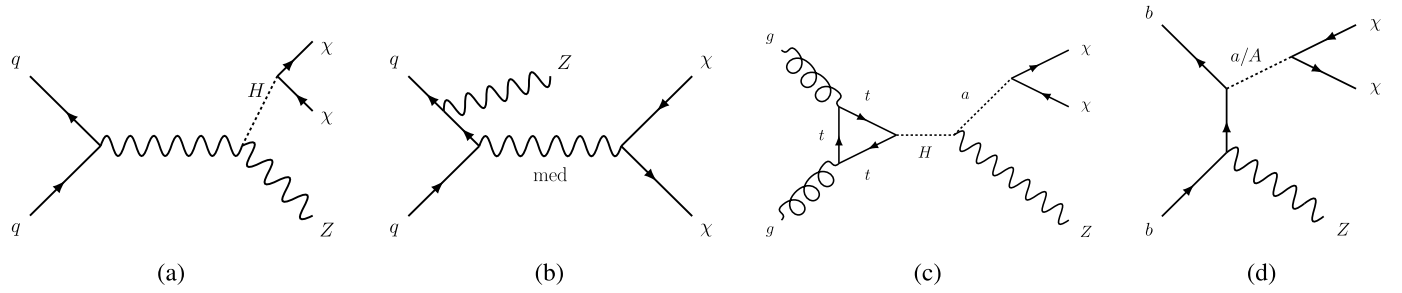


Fig. 1. Example Feynman diagrams of the probed processes: (a) associated production of a Higgs boson and a Z boson, where the Higgs boson decays into DM particles, (b) production of a Z boson and a mediator from a quark initial state in the simplified DM models, and (c) gg - and (d) bb -initiated 2HDM+ a diagrams.

ered in 2012 by the ATLAS and CMS Collaborations at the LHC, with a mass of approximately 125 GeV [9,10]. If the DM particles are in the right mass range, they could even be produced in decays of the Higgs boson. The SM branching ratio prediction for Higgs boson decays into $ZZ \rightarrow 4\nu$ is only 0.1% [11]. Assuming SM production of the Higgs boson, its branching ratio to invisible particles, $\mathcal{B}(H \rightarrow \text{inv})$, can be constrained in the absence of a significant excess of such events above the expected background.

Searches for an excess in events with two electrons or muons¹ and missing transverse momentum (E_T^{miss}) are sensitive to Higgs boson decays into DM if the Higgs boson is produced in association with a Z boson that decays into leptons. The analysis is also sensitive to so-far undiscovered heavier scalars produced together with the Z boson and decaying into invisible particles.

Searches in the $Z + E_T^{\text{miss}}$ final state can also be used to probe simplified DM models [12,13], in which DM is produced through a mediator particle that also couples to quarks and as such searches for dijet resonances are the most sensitive [14,15]. In the analysis presented here, benchmark models are used, and these consider s-channel production of DM particles through vector or axial-vector mediators. The models are defined by five parameters: the mediator and DM particle masses, and the mediator couplings g_χ , g_q , and g_ℓ to the DM particles, quarks, and leptons, respectively. Exclusion limits are set in a plane spanning the DM and mediator masses, for chosen values of the mediator couplings.

Furthermore, the analysis tests two-Higgs-doublet models (2HDM) that include an additional pseudoscalar mediator a and are called 2HDM+ a [16–18]. The two Higgs doublets in the model are CP-conserving and of type II [19–22], and the lighter scalar is identified as the observed 125 GeV Higgs boson. Four benchmark scenarios are probed in various planes as a function of the mass of the pseudoscalar Higgs boson, m_A ; the mass of the additional pseudoscalar, m_a ; the ratio of the vacuum expectation values of the two Higgs doublets, $\tan\beta$; and $\sin\theta$, where θ is the mixing angle between the two CP-odd weak spin-0 eigenstates [17]. Example Feynman diagrams for all probed models are shown in Fig. 1.

The $Z + E_T^{\text{miss}}$ channel is one of the most sensitive for the $H \rightarrow \text{inv}$ search and the most sensitive channel over much of the parameter space for 2HDM+ a searches.

Previous results in the $Z + E_T^{\text{miss}}$ final state were obtained with partial Run-2 datasets by the ATLAS Collaboration. Using 36 fb⁻¹ of data, ATLAS set a 95% confidence level (CL) upper limit of 67% on the Higgs boson branching ratio to invisible particles, with an expected limit of 39% in the absence of signal [23]. The same paper also reported exclusion limits for the simplified DM models mentioned above. Combining different Higgs boson production channels and different LHC runs, including 36 fb⁻¹ from Run 2, ATLAS set an upper limit of 26% (17% expected) on the Higgs boson branching ratio to invisible particles [24]. The CMS Collaboration

published results in the $Z + E_T^{\text{miss}}$ final state based on 137 fb⁻¹ of Run-2 data, including limits on the branching ratio for invisible decays of the Higgs boson (29% observed vs 25% expected), simplified DM models and 2HDM+ a models [25]. CMS also combined results from different production modes and LHC runs to set an upper limit of 19% (15% expected) on the Higgs boson branching ratio to invisible particles [26]. Constraints on 2HDM+ a models were also set by the ATLAS and CMS Collaborations using various final states [18,25,27,28].

The analysis strategy is outlined briefly in the following. Using the full LHC Run-2 dataset of 139 fb⁻¹ recorded with the ATLAS detector, events in this search are required to have two oppositely charged electrons or muons, consistent with originating from a Z boson decay, as well as significant E_T^{miss} . The same event selection is applied in both the $ZH \rightarrow \ell\ell + \text{inv}$ search and the other DM searches. A boosted decision tree (BDT) is trained so that its output is used as the discriminating observable in the search for invisible Higgs boson decays, while the searches in the context of simplified DM models and 2HDM+ a models are based on an observable representing the transverse mass distribution of the dominant ZZ background. Background distributions are estimated using simulated samples, and a simultaneous fit is performed in the signal region and three background control regions to constrain the systematic uncertainties and determine the normalisation of some of the backgrounds. The sensitivity of the analysis is considerably improved in comparison with a projection of the previous analysis scaled to the present integrated luminosity, mainly due to the use of the BDT and the simultaneous fit of the signal and background control regions.

2. ATLAS detector

The ATLAS experiment [29] at the LHC is a multipurpose particle detector with a forward–backward symmetric cylindrical geometry and a near 4π coverage in solid angle.² It consists of an inner tracking detector surrounded by a thin superconducting solenoid providing a 2 T axial magnetic field, electromagnetic and hadronic calorimeters, and a muon spectrometer. The inner tracking detector covers the pseudorapidity range $|\eta| < 2.5$. It consists of silicon pixel, silicon microstrip, and transition radiation tracking detectors. Lead/liquid-argon (LAr) sampling calorimeters provide electromagnetic (EM) energy measurements with high granularity. A steel/scintillator-tile hadronic calorimeter covers the central pseudorapidity range ($|\eta| < 1.7$). The endcap and forward regions are

² ATLAS uses a right-handed coordinate system with its origin at the nominal interaction point (IP) in the centre of the detector and the z-axis along the beam pipe. The x-axis points from the IP to the centre of the LHC ring, and the y-axis points upwards. Cylindrical coordinates (r, ϕ) are used in the transverse plane, ϕ being the azimuthal angle around the z-axis. The pseudorapidity is defined in terms of the polar angle θ as $\eta = -\ln \tan(\theta/2)$. Angular distance is measured in units of $\Delta R = \sqrt{(\Delta\eta)^2 + (\Delta\phi)^2}$.

¹ In this Letter, ‘lepton’ or ℓ refers to an electron or muon.

instrumented with LAr calorimeters for both the EM and hadronic energy measurements up to $|\eta| = 4.9$. The muon spectrometer surrounds the calorimeters and is based on three large superconducting air-core toroidal magnets with eight coils each. The field integral of the toroids ranges between 2.0 and 6.0 Tm across most of the detector. The muon spectrometer includes a system of precision chambers for tracking and fast detectors for triggering. A two-level trigger system is used to select events [30]. The first-level trigger is implemented in hardware and uses a subset of the detector information to accept events at a rate below 100 kHz. This is followed by a software-based trigger that reduces the accepted event rate to 1 kHz on average depending on the data-taking conditions. An extensive software suite [31] is used in the reconstruction and analysis of real and simulated data, in detector operations, and in the trigger and data acquisition systems of the experiment.

3. Data and simulated event samples

The presented analysis is performed using data from pp collisions, produced at $\sqrt{s} = 13$ TeV by the LHC and recorded with the ATLAS detector between 2015 and 2018. Data quality requirements [32] are applied to ensure that all detector subsystems were operational. The data correspond to an integrated luminosity of 139 fb^{-1} . The data sample was collected using a set of single-electron [33] and single-muon [34] triggers which require the presence of an electron (muon) with transverse energy E_T (transverse momentum p_T) above thresholds in the range of 20–26 GeV depending on the lepton flavour and data-taking period [35]. The trigger selections also impose object quality and isolation requirements. There must be a geometrical match between a trigger lepton and a lepton selected in the offline analysis as described in Section 4.

Simulated Monte Carlo (MC) samples are used to optimise the analysis selection, to estimate the signal, and as input to the background estimation. Unless otherwise mentioned, the NNPDF3.0 parton distribution function (PDF) set [36] was used for the hard interaction and the events were passed through the ATLAS detector response simulation [37] within the GEANT4 framework [38]. The profiles of the additional inelastic pp interactions (pile-up) in the simulation match those of each dataset between 2015 and 2018, and were obtained by overlaying minimum-bias events, simulated using the soft QCD processes of PYTHIA8.186 [39] with the NNPDF2.3LO PDF set [40] and a set of parameters called the A3 tune [41]. For all samples, except those generated with SHERPA [42], the EVTGEN 1.2.0 [43] program was used to simulate the properties of the b - and c -hadron decays.

Associated production of a Higgs boson and a Z boson was simulated with POWHEG Box v2 [44], including both the qq/qg and gg initial states. A Higgs boson mass of 125 GeV was assumed. The $qq/qg \rightarrow ZH$ process was calculated at next-to-leading order (NLO) in QCD, and the MINLO technique [45] was used to merge 0-jet and 1-jet events. The $gg \rightarrow ZH$ contribution was modelled at leading order (LO) in QCD. The parton-level events were passed to PYTHIA 8.212 [46] with the AZNLO tune [47] to model the Higgs boson decay into four neutrinos as invisible decays, and also the parton showering, hadronisation, and multiple parton interactions (MPI). The samples were normalised to next-to-next-to-leading order (NNLO) in QCD with electroweak (EW) corrections (for $qq/qg \rightarrow ZH$) or to NLO+next-to-leading logarithms (NLO+NLL) in QCD (for $gg \rightarrow ZH$) [11,48–55]. In addition, parameterised EW corrections were applied as a function of the transverse momentum of the Z boson for the $qq/qg \rightarrow ZH$ process [11]. Allowing the Z boson to decay into electron, muon or τ -lepton pairs, and assuming a Higgs boson branching ratio to invisible particles of 100%, the production cross-section times branching ratio is $77.0 \pm 1.5 \text{ fb}$ for $qq/qg \rightarrow ZH$ and $12.4 \pm 2.8 \text{ fb}$ for $gg \rightarrow ZH$ [11].

For the simplified DM models, the s-channel process $pp \rightarrow Z(\ell\ell)\chi\bar{\chi}$ events were simulated with MADGRAPH5_AMC@NLO 2.2.2 at NLO in QCD [56], and fed into PYTHIA 8.212 with the A14 tune [57]. Vector and axial-vector mediator samples were produced for various mediator and DM masses, with the mediator couplings to DM and quarks set to $g_\chi = 1.0$ and $g_q = 0.25$, respectively [12,13]. Only the leptophobic case is probed, i.e. the mediator coupling to leptons was set to $g_\ell = 0$. These samples were passed through a faster detector simulation using a parameterisation of the calorimeter response [37].

MADGRAPH 5 was used to generate the 2HDM+ a signals, from both the gg and bb initial states, at LO in QCD, in combination with PYTHIA 8.244 and the A14 tune. The model contains 14 parameters, including the DM mass, the masses of the five Higgs bosons, the ratio of the vacuum expectation values of the two Higgs doublets ($\tan\beta$), various couplings, and the mixing angles α and θ between the CP-even and CP-odd weak eigenstates, respectively. The bb -initiated production process is particularly important for high values of $\tan\beta$. Parameters and scanning planes were chosen following the recommendations in Ref. [17].

Diboson and triboson backgrounds were simulated with SHERPA 2.2.2, including the parton showering, hadronisation and MPI, based on the default SHERPA tunes. The $ZZ \rightarrow \ell\ell\nu\nu$ and $ZZ \rightarrow 4\ell$ events were simulated for both the qq/qg and gg initial states and include electrons and muons from τ -lepton decays. The $qq/qg \rightarrow ZZ$ matrix elements were calculated at NLO in QCD for up to one jet, and at LO for two or three jets, with the COMIX [58] and OPEN-LOOPS [59–61] matrix-element generators. The merging with the SHERPA parton shower [62] was performed using the MEPS@NLO prescription [63]. NLO EW corrections [59,64–67] were applied as a function of E_T^{miss} or the p_T of one of the Z bosons in the 4ℓ final state, using the average of additive and multiplicative approaches [67]. The $gg \rightarrow ZZ$ process was modelled at LO for up to one jet. NLO corrections for the $gg \rightarrow \ell\ell\nu\nu$ continuum process are calculated using the MATRIX package [60,68,69] with improvements in the calculation of the loop amplitudes [70]. The WZ , WW (including $gg \rightarrow WW$), and VVV contributions were modelled as well, with the same matrix-element accuracies as the ZZ contributions. The generation includes off-shell effects, $gg \rightarrow H$ contributions and interference between processes [60].

The Z + jets background was modelled with SHERPA 2.2.1, with matrix elements calculated at NLO in QCD for up to two jets and at LO for three or four jets. Top-quark pair ($t\bar{t}$) and single top-quark (Wt , s-channel and t-channel) production was simulated using POWHEG Box v2 (v1 for t-channel production) at NLO in QCD [44, 71–75], interfaced to Pythia 8.230 with the A14 tune. The predictions were normalised to NNLO+next-to-next-to-leading-logarithm (NNLO+NNLL) cross-section calculations [76–79]. Associated production of a top-quark pair and a W or Z boson, $t\bar{t} + V$, was simulated with MADGRAPH5_AMC@NLO 2.2.3, and interfaced to PYTHIA 8.210 with the A14 tune. In this case, predictions were normalised to NLO cross-section calculations [11,56].

4. Object selection

Selected events are required to contain at least one vertex with a minimum of two associated tracks with $p_T > 500 \text{ MeV}$ [80]. The primary vertex is chosen to be the vertex reconstructed with the largest Σp_T^2 of its associated tracks. The event quality is checked to remove events with noise bursts or coherent noise in the calorimeters [32].

Electron candidates are reconstructed by matching inner-detector tracks to clusters of energy deposited in the EM calorimeter. Electrons must have $p_T > 7 \text{ GeV}$ and $|\eta| < 2.47$. The associated track must have $|d_0|/\sigma_{d_0} < 5$ and $|z_0|\sin\theta < 0.5 \text{ mm}$, where d_0 (z_0) is the transverse (longitudinal) impact parameter relative to

the primary vertex, σ_{d_0} is the uncertainty in d_0 , and θ is the polar angle of the track. Candidates are identified with a likelihood method and must satisfy ‘medium’ identification criteria [81], while ‘loose’ criteria are used to veto additional electrons in each analysis region. The likelihood relies on the shape of the EM shower measured in the calorimeter, the quality of the track reconstruction, and the quality of the match between the track and the cluster. The energy of the EM clusters associated with the electrons is calibrated in successive steps using a combination of simulation-based and data-driven correction factors. The electron reconstruction, identification, and energy calibration algorithms, as well as their performance, including the associated systematic uncertainties, are studied in Ref. [81]. Muon candidates are reconstructed in the range $|\eta| < 2.5$ by combining tracks in the inner detector with tracks in the muon spectrometer. All muon candidates must have $p_T > 7$ GeV, $|d_0|/\sigma_{d_0} < 3$, and $|z_0|\sin\theta < 0.5$ mm. In order to improve the momentum resolution, further quality requirements are placed on the muons. ‘Medium’ quality requirements [82] are used for candidate muons and ‘loose’ criteria are used to veto additional muons. The algorithms and efficiency of the muon reconstruction and identification, as well as the momentum calibration, including the associated systematic uncertainties, are estimated as described in Refs. [82,83]. To suppress hadronic and non-prompt lepton background, electron and muon candidates are required to satisfy the particle-flow isolation criteria, which are based on tracking and calorimeter measurements [83].

Jets in the range $|\eta| < 4.5$ and $p_T > 20$ GeV are reconstructed with a particle-flow algorithm, which combines energy deposits in the calorimeter with inner-detector tracks [84], using the anti- k_r algorithm [85,86] with a radius parameter R of 0.4. A jet-vertex-tagging technique based on a multivariate likelihood [87] is applied to jets with $|\eta| < 2.4$ and $p_T < 60$ GeV to suppress jets that are not associated with the primary vertex of the event. Jets are further calibrated according to in situ measurements of the jet energy scale [88]. Jets in the range $|\eta| < 2.5$ are identified as b -jets with the MV2c10 algorithm, described in Ref. [89]. The b -jet identification efficiency is about 85% with a rejection factor of about 25 for light-flavour jets, as measured in a sample of simulated $t\bar{t}$ events.

Overlaps between reconstructed objects are accounted for with a removal procedure that is mainly based on the angular separation between the different final-state objects. The procedure is the same as the one described in Ref. [90].

The \vec{E}_T^{miss} of the event is computed as the negative vectorial sum of the transverse momenta of electrons, muons, jets and a track-based soft term [91] that accounts for the contribution from prompt particles that are not contained in the other objects. The E_T^{miss} significance [92] is defined as $S_{E_T^{\text{miss}}} = E_T^{\text{miss}}/(\sigma_L\sqrt{1-\rho_{\text{LT}}^2})$, where the parameters σ_L and ρ_{LT} are calculated from MC simulation and shown to describe the data well; the quantity σ_L denotes the resolution of the p_T of the system and ρ_{LT} is a correlation factor between resolutions of the p_T components parallel and perpendicular to the E_T^{miss} vector.

Further related quantities used in the analysis are H_T , the scalar sum of p_T for all leptons and those jets with $p_T > 30$ GeV, and $f_{\text{soft}} = \left|1 - \frac{|\vec{E}_T^{\text{miss}} + \sum \vec{p}_T^{\text{jets}}|}{p_T^{\ell\ell}}\right|$, a measure of the fraction of the event’s p_T carried by the soft term, where $\sum \vec{p}_T^{\text{jets}}$ is the vectorial sum of the transverse momenta of all jets in the event with $p_T > 30$ GeV and $p_T^{\ell\ell}$ is the p_T of the $\ell\ell$ system.

5. Event selection

Events are selected in a signal region (SR) designed to capture as many signal events as possible, and three control regions (CR) which are used to constrain the most important background pro-

cesses, and which are expected to have negligible contamination from signal events.

Events in the SR are required to have exactly two oppositely charged electrons or muons with an invariant mass consistent with the mass of the Z boson. The leptons must have $p_T^\ell > 20, 30$ GeV when ordered in increasing p_T . The lepton pair is required to have an invariant mass $m_{\ell\ell}$ in the range $76 < m_{\ell\ell} < 106$ GeV. In order to select events in the SR consistent with invisible particles recoiling against the Z boson, events are required to have $E_T^{\text{miss}} > 90$ GeV, $S_{E_T^{\text{miss}}} > 9$ and a separation of $\Delta R_{\ell\ell} < 1.8$ between the leptons.

An $e\mu$ CR is defined in exactly the same way as the SR apart from requiring the two leptons to have different flavours. This CR helps constrain the sum of the non-resonant backgrounds from $t\bar{t}$, single top-quark, WW and $Z \rightarrow \tau\tau$ events. The $e\mu$ CR is about 98% pure in non-resonant background.

A CR containing exactly four leptons, the 4ℓ CR, is used to constrain the ZZ background. Its events must contain two pairs of same-flavour oppositely charged leptons, with the four leptons required to have $p_T^\ell > 7, 15, 15, 27$ GeV when ordered in increasing p_T . If all four leptons are of the same flavour, the chosen pairing combination is the one minimising the quantity $|m_{\ell\ell 1} - m_Z| + |m_{\ell\ell 2} - m_Z|$, where the indices 1 and 2 denote the lepton pairs and m_Z is taken to be 91.19 GeV. Both lepton pairs must satisfy $76 < m_{\ell\ell} < 106$ GeV. In order to mimic the SR, the quantities $E_T^{\text{miss}'}$ and $S_{E_T^{\text{miss}'}}$ are calculated in the same way as E_T^{miss} and $S_{E_T^{\text{miss}}}$, but one pair of leptons, which is chosen at random, is treated as invisible and excluded from the calculation. The selection criteria are the same as for the SR, i.e. $E_T^{\text{miss}'} > 90$ GeV, $S_{E_T^{\text{miss}'}} > 9$ and $\Delta R_{\ell\ell} < 1.8$, where the final requirement is imposed on the remaining lepton pair. The 4ℓ CR is almost 100% pure in ZZ events.

A CR containing exactly three leptons, the 3ℓ CR, is used to constrain the WZ background. In order to select the Z boson in the event, two of the leptons must have opposite charge, the same flavour, $p_T^\ell > 20, 30$ GeV and $76 < m_{\ell\ell} < 106$ GeV. If there are two combinations that pass these requirements, the one closer in mass to m_Z is taken. To select events consistent with a W boson decay, it is required that the third lepton has $p_T^\ell > 20$ GeV, the event has $E_T^{\text{miss}} > 30$ GeV and $S_{E_T^{\text{miss}}} > 3$, and the transverse mass of the W boson candidate satisfies $m_T^W = \sqrt{2p_T^\ell E_T^{\text{miss}}(1 - \cos\Delta\phi(\ell, E_T^{\text{miss}}))} > 60$ GeV, where $\Delta\phi(\ell, E_T^{\text{miss}})$ is the azimuthal angle between the third lepton and \vec{E}_T^{miss} . The 3ℓ CR is about 93% pure in WZ events.

Events with one or more identified b -jets are removed in all regions to suppress events containing top quarks.

Considering all signal events in which the Z boson decays into an electron, muon or τ -lepton pair, the SR selection has an acceptance times efficiency of $\sim 8\%$ ($\sim 19\%$) for quark-induced (gluon-induced) $ZH \rightarrow \ell\ell + \text{inv}$, resulting in an expectation of 120 events for $\mathcal{B}(H \rightarrow \text{inv}) = 10\%$. For an example signal point in the simplified DM model ($m_\chi = 1$ GeV, $m_{\text{med}} = 900$ GeV), the acceptance times efficiency is $\sim 20\%$ with 145 events expected. For a gg -induced 2HDM+a signal point ($\tan\beta = 1.0$, $\sin\theta = 0.7$, $m_A = 600$ GeV, $m_a = 400$ GeV, $m_\chi = 10$ GeV), it is $\sim 32\%$ with 182 events expected. For all signal models the acceptance times efficiency is very similar for the dielectron and dimuon selections.

6. Background estimates and signal extraction

The signal and all backgrounds are estimated through simultaneous likelihood fits in the signal and control regions, using MC simulation as input. The dominant background in the SR is the ZZ background, followed by WZ , $Z + \text{jets}$, and the non-resonant backgrounds (WW , $t\bar{t}$, single top-quark and $Z \rightarrow \tau\tau$), which are

treated together. Small contributions arising from triboson production, $t\bar{t} + V$ and $ZZ \rightarrow 4\ell$, where two of the leptons are not reconstructed, are referred to as ‘Other’ in the following. The ZZ and non-resonant backgrounds have the same topology as the signal (two leptons and E_T^{miss}). The SM Higgs boson decay $ZZ \rightarrow 4\nu$ is included as part of the signal, while other decays are estimated to be small and neglected. The WZ background enters the SR if one of the leptons is not reconstructed. In most of the $Z + \text{jets}$ background, significant E_T^{miss} arises through mismeasurement of the energy of the jets or is due to neutrinos or muons that are missed by the reconstruction, coming from semileptonic heavy-flavour decays. The normalisation of the MC simulation prediction for $Z + \text{jets}$ was cross-checked using events with $S_{E_T^{\text{miss}}} < 9$, which has a high purity for this process. A sample of $\gamma + \text{jets}$ events, which has similar production diagrams to $Z + \text{jets}$, was used to check how well the MC simulation described the shape of the data. In both cases the MC simulation prediction and data were observed to agree within the statistical and systematic errors.

The data are compared with expectation by performing simultaneous maximum-likelihood fits, using the HistFitter framework [93], to distributions in the signal and control regions. A separate fit is performed for each signal hypothesis. Confidence intervals are based on a profile-likelihood-ratio test statistic [94], assuming asymptotic distributions for the test statistic. The CL_s method [94] is used to set exclusion limits. The systematic uncertainties affecting the signal and background distribution normalisations and shapes across categories are parameterised by making the likelihood function depend on dedicated nuisance parameters, constrained by additional Gaussian probability terms, which are correlated between the regions. The normalisations of the signal, of the WZ background and of the sum of non-resonant backgrounds are allowed to float in the fits, as their respective CRs have large numbers of events. The individual components of the non-resonant background are allowed to vary independently within their systematic uncertainties. As the 4ℓ CR has low statistics the normalisation of the ZZ background, like those of the other backgrounds ($Z + \text{jets}$, triboson production, $t\bar{t} + V$, $ZZ \rightarrow 4\ell$), can vary only within the systematic uncertainties.

The sensitivity of the $H \rightarrow \text{inv}$ search is increased by using a BDT that is coded in the TMVA package [95] to improve the separation between signal and background events. The BDT uses a set of kinematic distributions that are selected because they have a different shape for signal and background. These are combined into a single output variable that provides better signal/background separation than any of the individual inputs alone. Eight variables are used: E_T^{miss}/H_T , $S_{E_T^{\text{miss}}}$, H_T , f_{soft} , $m_{\ell\ell}$, $\Delta R_{\ell\ell}$, $y_{\ell\ell}$ (the rapidity of the $\ell\ell$ system), and $\Delta\phi(\ell\ell, \vec{E}_T^{\text{miss}})$ (the azimuthal angle between the p_T of the $\ell\ell$ system and \vec{E}_T^{miss}). Other variables were considered but they did not improve the sensitivity significantly. The BDT was trained in the SR using simulated events for the $ZH \rightarrow \ell\ell + \text{inv}$ signal and for the sum of all backgrounds. The BDT output distribution is used in the profile likelihood fit for the SR and $e\mu$ CR. The E_T^{miss} distribution is used for the 3ℓ and 4ℓ CRs as the shapes of many of the BDT input variables for the background processes differ significantly between the CRs and SR. Example post-fit distributions in the CRs are shown in Figs. 2(a)–2(c), after the $ZH \rightarrow \ell\ell + \text{inv}$ simultaneous fit to the SR and CRs. It can be seen that the data are well described by the expectation. The fit uses the same binning as shown in these plots.

For the searches considering the simplified DM models or 2HDM+ a models, the transverse mass distribution is used in the maximum-likelihood fits for the SR and the $e\mu$ CR. The quantity

$$m_T = \sqrt{\left[\sqrt{m_Z^2 + (p_T^{\ell\ell})^2} + \sqrt{m_Z^2 + (E_T^{\text{miss}})^2} \right]^2 - \left[\vec{p}_T^{\ell\ell} + \vec{E}_T^{\text{miss}} \right]^2}$$

is the transverse mass of the dominant ZZ background, and gives good separation between signal and background for the majority of the DM and 2HDM+ a signals considered in this analysis. BDTs were not used for the DM and 2HDM+ a searches, due to the complexity of training over many mass points. It was found that the m_T distribution provides better sensitivity over much of the probed parameter space than a BDT trained for one signal point. The m_T distribution is only used in the fit for $m_T > 200$ GeV. Fig. 2(d) shows that the background estimate is in good agreement with the data for the m_T distribution in the $e\mu$ CR after a simultaneous fit to the signal and control regions in the context of the simplified DM models (axial-vector signal with $(m_\chi, m_{\text{med}}) = (150, 900)$ GeV). As in the $H \rightarrow \text{inv}$ search, the E_T^{miss} distribution is used for the 3ℓ and 4ℓ CRs.

7. Systematic uncertainties

Signal and background expectations are subject to statistical, detector-related and theoretical uncertainties. The shapes of the observable distributions, the acceptances in signal and control regions, and the overall background sample normalisations that are not free to float in the fit can be affected when varying the simulation to estimate the impact of systematic uncertainties. As discussed in Section 6, the uncertainties are treated as nuisance parameters in the fits and correlated between signal and control regions, which helps to constrain many of them, and reduces their impact. The post-fit impact of the systematic uncertainties can be found in Section 8.

Among the systematic uncertainties, the uncertainties in modelling the backgrounds, especially the dominant $ZZ \rightarrow \ell\ell\nu\nu$ background, have the largest impact. Uncertainties in the factorisation of NLO EW corrections and higher-order QCD corrections to the $ZZ \rightarrow \ell\ell\nu\nu$ background [59,64–66] are taken from the deviation of the additive and multiplicative approaches from their average [67]. For all diboson backgrounds, uncertainties due to missing higher orders in the QCD calculation are estimated by varying the renormalisation and factorisation scales by a factor of two, either independently or correlated and taking the largest variation as the uncertainty, while the effects of PDF and α_s uncertainties are calculated using the PDF4LHC prescription [96]. The impact of the choice of parton shower and hadronisation model is evaluated by comparing the samples from the nominal generator set-up with samples produced with varied resummation and CKKW matching procedure [97,98], and a different recoil scheme tuned in SHERPA.

The effects of QCD uncertainties on the $Z + \text{jets}$ background are also non-negligible. They are estimated by varying the renormalisation and factorisation scales by a factor of two. PDF uncertainties are also included. Modelling uncertainties in the $t\bar{t}$ and single-top-quark backgrounds are subdominant; their estimation is performed by varying the generator used for the hard scatter, as well as the renormalisation and factorisation scales, the parton shower model, α_s , and the PDF sets. The modelling uncertainties of the remaining background processes are also evaluated but have no impact on the final result.

For the $ZH \rightarrow \ell\ell + \text{inv}$ signal, the uncertainty due to missing higher orders in QCD is estimated in bins of the kinematic observables using a scheme similar to the one discussed in Ref. [99]. The PDF uncertainties are evaluated using the PDF4LHC prescription [96]. To estimate the impact of using a different parton shower model, the default PYTHIA 8 parton shower algorithm is replaced with HERWIG 7 [100]. Uncertainties due to the EW corrections are estimated by taking the difference between the additive and multiplicative corrections. The effects of QCD scale uncertainties for the simplified DM model and the 2HDM+ a prediction are evaluated by varying the scales as described for the diboson backgrounds. The parton shower uncertainty is estimated with the eigenvariations

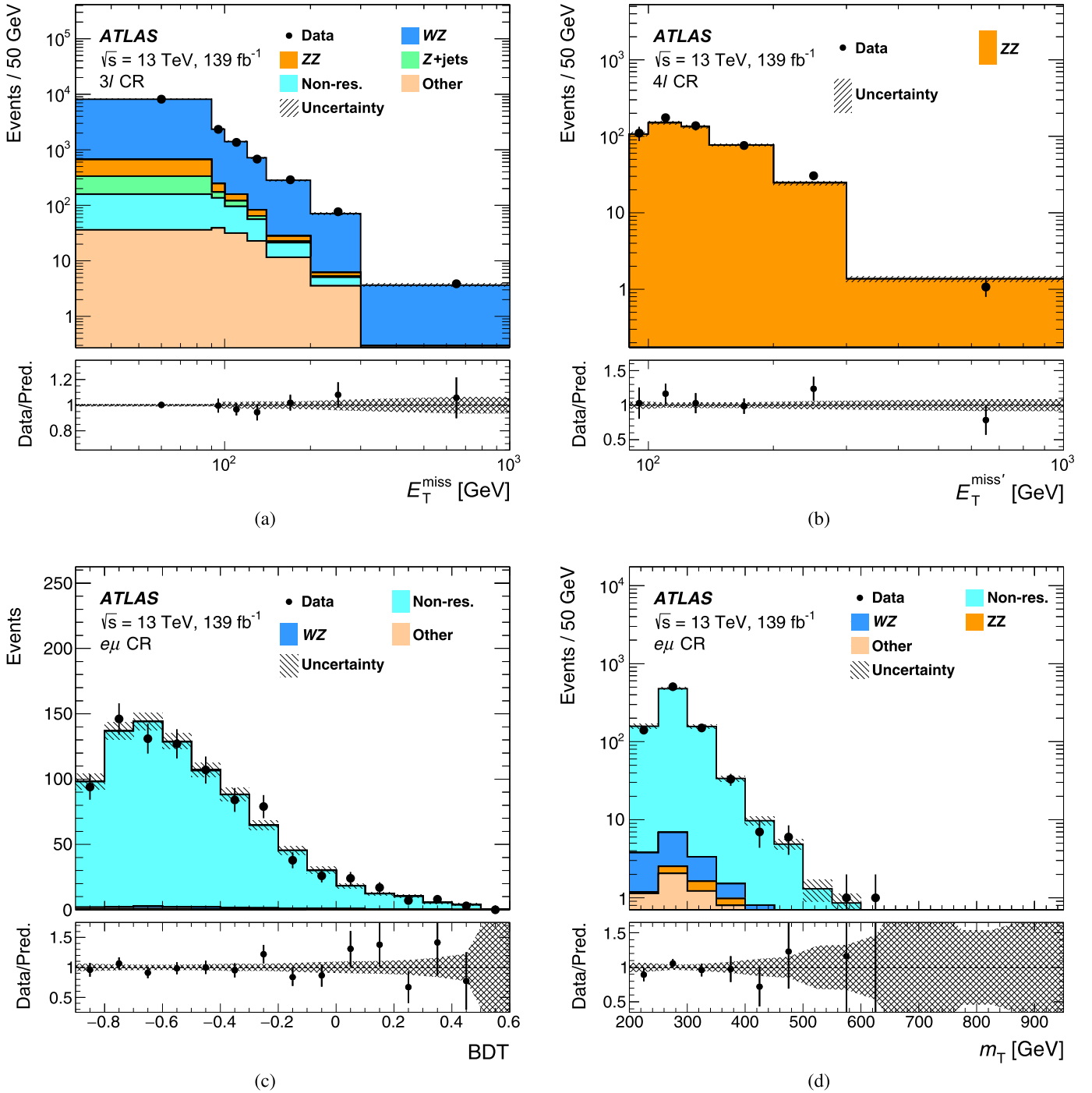


Fig. 2. Distributions in data compared with simulated events in the different CRs after (a, b, c) the simultaneous $ZH \rightarrow \ell\ell + \text{inv}$ fit and (d) a fit in the context of the simplified DM models (axial-vector signal with $(m_\chi, m_{\text{med}}) = (150, 900)$ GeV): (a) E_T^{miss} distribution in the 3ℓ CR, (b) $E_T^{\text{miss}'}$ distribution in the 4ℓ CR, (c) BDT distribution in the $e\mu$ CR, (d) m_T distribution in the $e\mu$ CR. As defined in the text, ‘Non-res.’ includes WW , $t\bar{t}$, single-top and $Z \rightarrow \tau\tau$ processes, while ‘Other’ stands for triboson, $t\bar{t} + V$, and $ZZ \rightarrow 4\ell$ production. Events recorded below (above) the x -range of the BDT plot are included in the first (last) bin shown. The bottom panel in each figure shows the ratio of the observed data to the predicted yields. The shaded bands in top and bottom panels represent the total statistical and systematic error of the background.

of the A14 tune. The PDF uncertainty includes variations of the NNPDF 3.0 set, as well as a comparison with two alternative PDF sets.

The detector-related uncertainties affecting signal and background predictions are dominated by jet reconstruction uncertainties. Uncertainties in the jet energy scale (JES) [88] arise from the calibration and are derived as function of the jet p_T and η . Further contributions emerge from the jet flavour composition and the pile-up conditions. Uncertainties in the jet energy resolution (JER) depend on the jet p_T and η and arise both from the method

used to derive the resolution and from the difference between simulation and data [88]. Uncertainties in the lepton identification and lepton energy/momentum scale and resolution are included in the fits. These are derived using simulated and measured events with $Z \rightarrow \ell\ell$, $J/\psi \rightarrow \ell\ell$ and $W \rightarrow \ell\nu$ decays [81,83]. The uncertainties in the lepton and jet energy scales are propagated to the uncertainty in the E_T^{miss} [91]. Additionally, the uncertainties from the momentum scale and resolution of the track-based soft term are included. The uncertainty in the combined 2015–2018

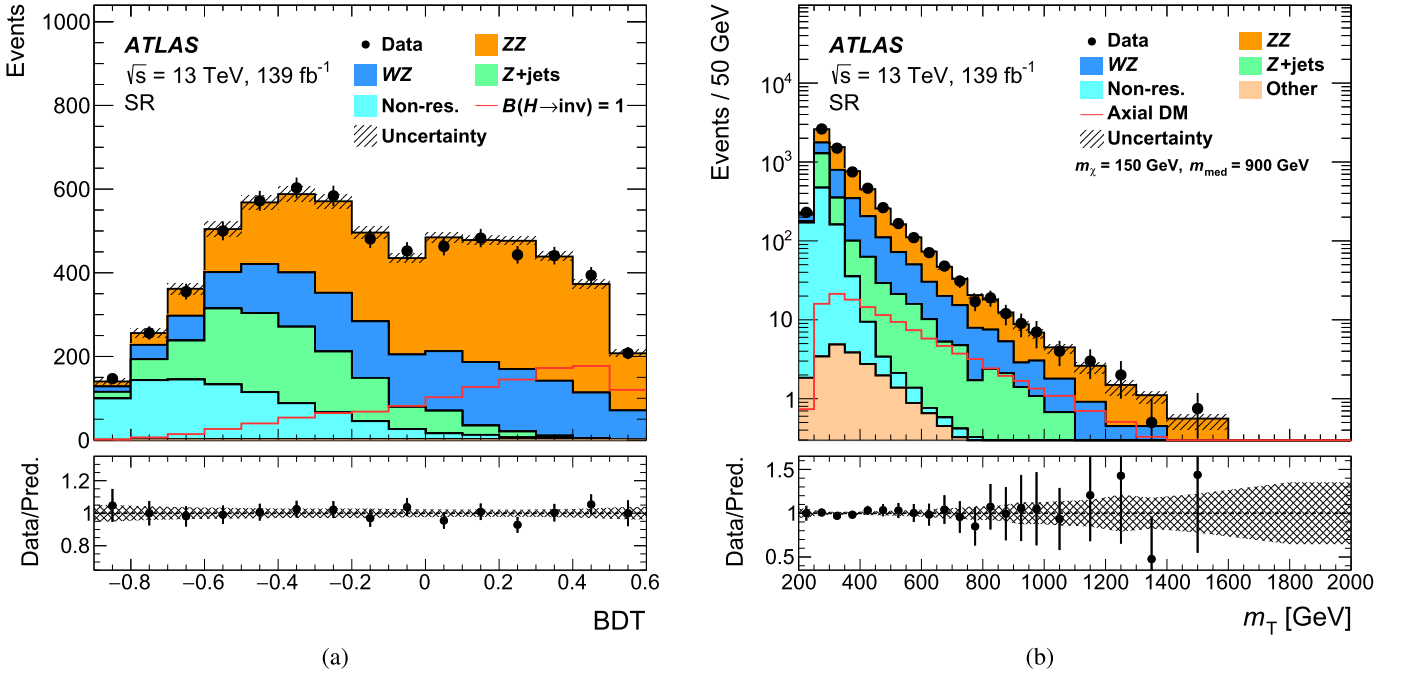


Fig. 3. (a) BDT and (b) m_T distributions in the signal region, after the respective simultaneous fits. The $H \rightarrow \text{inv}$ signal, with a branching ratio of $\mathcal{B} = 100\%$, is shown in (a) and an example DM axial-vector signal with $(m_\chi, m_{\text{med}}) = (150, 900)$ GeV is shown in (b). As defined in the text, ‘Non-res.’ includes WW , $t\bar{t}$, single top-quark and $Z \rightarrow \tau\tau$ processes, while ‘Other’ stands for triboson, $t\bar{t} + V$, and $ZZ \rightarrow 4\ell$ production. Events recorded below (above) the x -range of the BDT plot are included in the first (last) bin shown. The bottom panel in each figure shows the ratio of the observed data to the predicted yields. The shaded bands in top and bottom panels represent the total statistical and systematic error of the background.

Table 1

Summary of signal and control region yields after the simultaneous fit for the $ZH \rightarrow \ell\ell + \text{inv}$ signal. Also given is the total post-fit uncertainty of each number. As defined in the text, ‘Non-resonant’ includes WW , $t\bar{t}$, single top-quark and $Z \rightarrow \tau\tau$ processes. Note the uncertainty on the total expectation does not equal the sum of the uncertainties of individual contributions added in quadrature, due to correlations between the uncertainties.

	SR	$e\mu$ CR	3ℓ CR	4ℓ CR
Observed events	6382	891	11622	314
Expected yields after fit	6385 ± 81	895 ± 29	11620 ± 110	296 ± 11
$ZH \rightarrow \ell\ell + \text{inv}$	4 ± 110	-	-	-
$ZZ \rightarrow \ell\ell\nu\nu$	2681 ± 110	0.763 ± 0.064	2.61 ± 0.18	-
WZ	1595 ± 34	11.6 ± 1.1	10623 ± 150	-
Z + jets	1111 ± 100	0.79 ± 0.30	235 ± 89	-
Non-resonant	881 ± 39	876 ± 29	220 ± 31	-
$ZZ \rightarrow 4\ell$	85.8 ± 5.5	0.621 ± 0.056	443 ± 40	295 ± 11
$t\bar{t} + V$	12.7 ± 2.8	1.76 ± 0.41	53 ± 12	-
Triboson	13.0 ± 6.2	3.1 ± 1.4	44 ± 20	0.48 ± 0.23

integrated luminosity is 1.7% [101], obtained using the LUCID-2 detector [102].

8. Results

Fig. 3 shows the BDT and m_T distributions of the selected data events, compared with the estimated backgrounds after the simultaneous fits described in Section 6 are performed. For the $ZH \rightarrow \ell\ell + \text{inv}$ case, Table 1 gives the number of observed events as well as the signal and background expectations after the simultaneous fit. The numbers for the DM fits are very similar, with some differences in the $e\mu$ CR as the m_T distribution is only used in the fit for $m_T > 200$ GeV.

The data are in good agreement with the background expectation. Assuming SM Higgs production cross-sections and their uncertainties, the best-fit branching ratio of Higgs boson decays into invisible particles is $\mathcal{B}(H \rightarrow \text{inv}) = (0.3 \pm 9.0)\%$, which corresponds to an observed 95% CL upper limit of 19%. The corresponding expected upper limit is 19%. The analysis improvements and reduced systematic uncertainties lead to this limit being 45% lower than a

projection of the previous expected limit [23] scaled to the present integrated luminosity. The observed normalisation factors for the WZ and $e\mu$ backgrounds are 0.971 ± 0.060 and 0.92 ± 0.10 respectively. Table 2 shows the contributions of the statistical and systematic uncertainties to the total uncertainty of the best-fit $\mathcal{B}(H \rightarrow \text{inv})$. As discussed in Section 7, the dominant uncertainty is due to the ZZ modelling. Uncertainties in the jet reconstruction are important as well.

Fig. 4 shows the exclusion limits for the simplified DM models assuming either an axial-vector or vector mediator, with the chosen mediator couplings $g_\chi = 1.0$, $g_q = 0.25$, and $g_\ell = 0$. The bottom-left region inside the solid black contour is excluded at the 95% CL. The dashed red line labelled ‘Relic density’ corresponds to combinations of DM and mediator mass values that are consistent with a DM density of $\Omega h^2 = 0.118$ and a standard thermal history, as computed in Ref. [13]. The dashed magenta line indicates the previous ATLAS result from a 36.1 fb^{-1} dataset [23]. The present analysis enlarges the excluded area significantly. Axial-vector and vector mediators with masses of up to 950 GeV are excluded now,

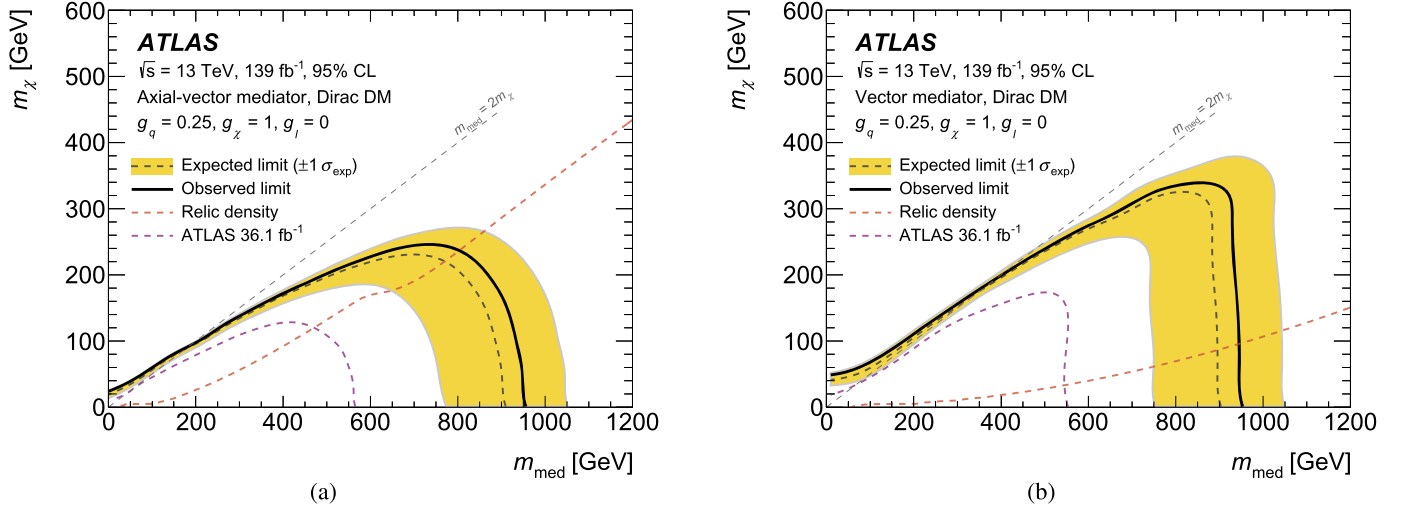


Fig. 4. Exclusion limits for simplified DM models with $g_\chi = 1.0$, $g_q = 0.25$, and $g_\ell = 0$, when assuming (a) an axial-vector mediator or (b) a vector mediator. The region below the solid black line is excluded at the 95% CL. The dashed black line indicates the expected limit in the absence of signal, and the yellow band the corresponding $\pm 1\sigma$ uncertainty band. The dashed red line labelled ‘Relic density’ corresponds to combinations of DM and mediator mass values that are consistent with a DM density of $\Omega h^2 = 0.118$ and a standard thermal history, as computed in Ref. [13]. Below the line, annihilation processes described by the simplified model mostly predict too high a relic density while regions with too low a relic density are mostly found for m_{med} closer to the DM mass. The dashed magenta line indicates the previous ATLAS result from a 36.1 fb^{-1} dataset [23].

Table 2

Summary of the uncertainties $\Delta\mathcal{B}$ on the best-fit $\mathcal{B}(H \rightarrow \text{inv})$, obtained by fixing the corresponding nuisance parameters to their best-fit values, and subtracting the square of the resulting uncertainty from the square of the total uncertainty to evaluate $(\Delta\mathcal{B})^2$. The statistical uncertainty component is obtained by fixing all nuisance parameters to their best-fit values. Note the total uncertainty does not equal the sum of the individual contributions added in quadrature due to correlations between the systematic uncertainties.

Uncertainty source	$\Delta\mathcal{B}$ [%]
Statistical uncertainty	5.1
Systematic uncertainties	7.4
Theory uncertainties	4.9
Signal modelling	0.4
ZZ modelling	4.4
Non-ZZ background modelling	2.1
Experimental uncertainties (excl. MC stat.)	4.6
Luminosity, pile-up	1.5
Jets, E_T^{miss}	4.0
Flavour tagging	0.4
Electrons, muons	1.2
MC statistical uncertainty	1.6
Total uncertainty	9.0

while DM masses of up to 250 GeV are excluded in the axial-vector case and up to 350 GeV in the case of a vector mediator.

Eight scans are produced for the 2HDM+ a models, following the recommendations in Ref. [17], including the requirement $m_A = m_H = m_{H^\pm}$. They are shown in Figs. 5 and 6. The hashed red area indicates that the width of one of the Higgs bosons is larger than 20% of its mass [16]. The experimental exclusion in those areas is subject to additional theoretical uncertainties, as the dependence of the width on the virtuality of the additional Higgs bosons could significantly alter the inclusive production cross-sections (one of the limitations of the models). For all presented scans, the exclusion limit is stronger for a mixing parameter value of $\sin\theta = 0.7$ because the cross-sections are larger than for $\sin\theta = 0.35$.

Figs. 5(a) and 5(b) show $\tan\beta$ vs m_a limit contours with $m_A = 600 \text{ GeV}$, while Figs. 5(c) and 5(d) show $\tan\beta$ vs m_A contours for $m_a = 250 \text{ GeV}$. Compared to previous limits shown by the dashed magenta line [18] in Fig. 5(a), the contours now extend upwards beyond $\tan\beta = 3$ due to the inclusion of bb -induced signal contributions (see Fig. 1(d) for an example diagram). The interplay

between those and the gg -fusion processes (Fig. 1(c)) affects the shapes, as the $\tan\beta$ dependence of the coupling of $H/A/a$ to top quarks (present in gg -fusion) differs from that to bottom quarks. The relative difference between m_A and m_a also affects the shape through the $H \rightarrow Z + a$ process.

The (m_A, m_a) exclusion limits are shown in Figs. 5(e) and 5(f). Compared to the 36.1 fb^{-1} exclusion limit shown by the dashed magenta line [18] in Fig. 5(e), the highest excluded m_A has improved from 1 TeV to $\sim 1.4 \text{ TeV}$ for $m_a = 100 \text{ GeV}$, and the highest excluded m_a has increased from 340 GeV to 480 GeV for $m_A \sim 1.05 \text{ TeV}$. Sensitivity is lost when $m_a + m_Z > m_H$, as particles are not produced on-shell anymore. For the scan in Fig. 5(f), points in parameter space evaluated with signal samples that underwent the simulation of the ATLAS detector response were augmented by points obtained through a reweighting of these samples based on generator-level distributions of key observables, namely p_T^Z (the transverse momentum of the Z boson), $p_T^{\chi\chi}$ (the transverse momentum of the $\chi\chi$ system), and $\Delta\phi(Z, \chi\chi)$ (the azimuthal angle between the Z boson and $\chi\chi$ system), similar to the procedure used in Ref. [103]. Fig. 6 shows upper limits on the signal strength, $\mu_{\text{upper}}^{95\%}$, as a function of $\sin\theta$ for models with $(m_A, m_a) = (600, 200) \text{ GeV}$ and $(1000, 350) \text{ GeV}$. Any $\sin\theta$ value for which $\mu_{\text{upper}}^{95\%} < 1$ is excluded.³ The dashed red line indicates the limit from the previous analysis [18].

Within the context of appropriate models, both the $\mathcal{B}(H \rightarrow \text{inv})$ limit and the limits on the simplified DM model (Fig. 4) can be compared with limits from direct-detection DM experiments. For consistent comparisons, the 90% CL is used, which corresponds to $\mathcal{B}(H \rightarrow \text{inv}) = 16\%$. The translation of the $H \rightarrow \text{inv}$ result into a WIMP-nucleon scattering cross-section $\sigma_{\text{WIMP-N}}$ in the Higgs portal model [104] relies on an effective field theory approach and assumes that Higgs boson decays into a pair of DM particles are kinematically possible and that the DM particle is a scalar or a Majorana fermion [105–107]. In this translation, the nuclear form factor $f_N = 0.308 \pm 0.018$ [108] is used. The simplified models with an axial-vector mediator can be translated to spin-dependent

³ $\mu_{\text{upper}}^{95\%}$ can be interpreted as $\sigma_{\text{upper}}^{95\%}/\sigma_{\text{theory}}$, where $\sigma_{\text{upper}}^{95\%}$ is the upper limit on the cross-section of the signal model, and σ_{theory} is the nominal cross-section of the signal model.

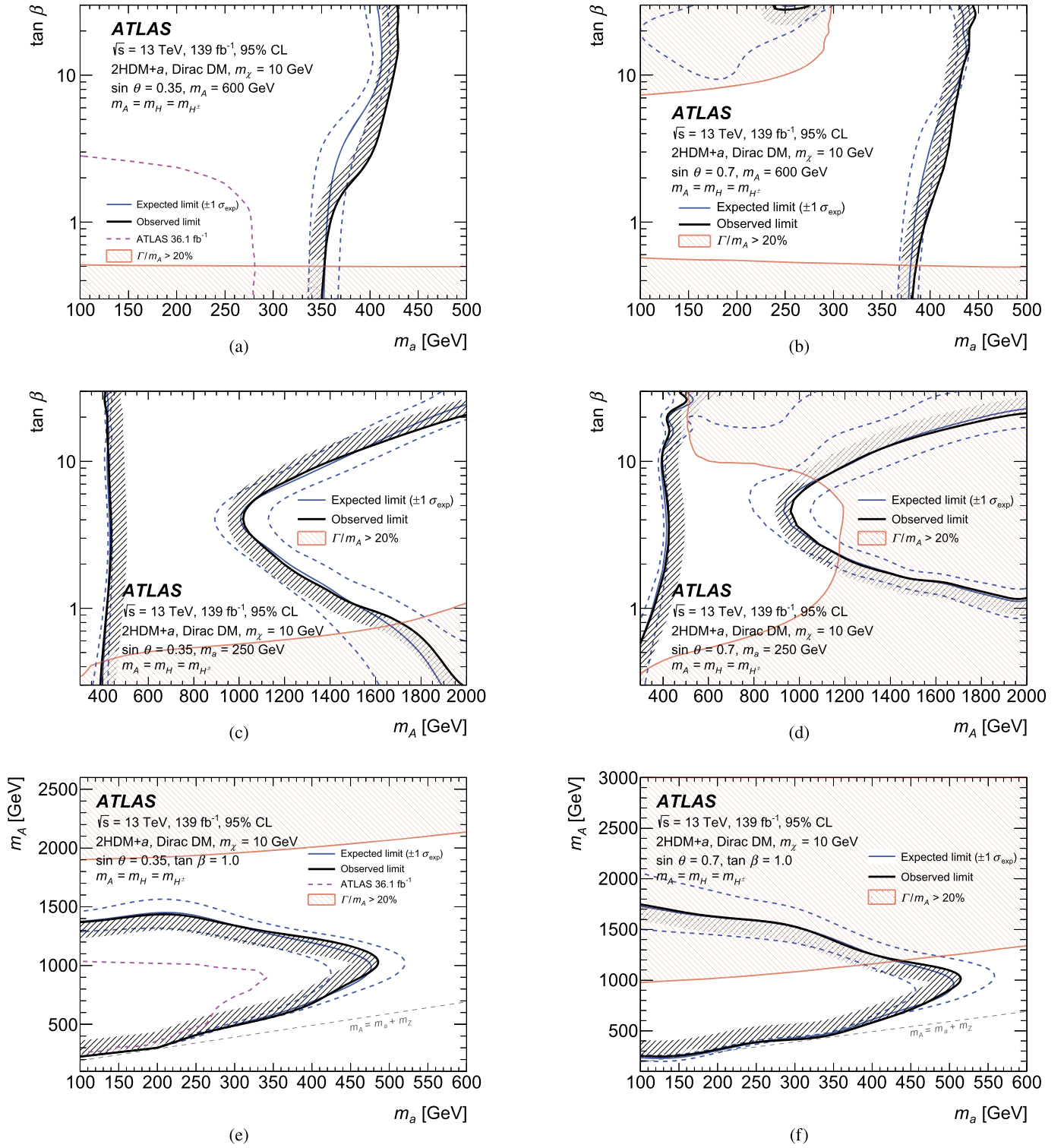


Fig. 5. Exclusion limits within the context of 2HDM+a models with different parameter choices and in various planes [17]. Subfigures (a, b) show the $\tan \beta$ vs m_a exclusion limits with $m_A = 600 \text{ GeV}$, (c, d) the $\tan \beta$ vs m_a exclusion limits with $m_a = 250 \text{ GeV}$, and (e, f) the m_A vs m_a exclusion limit with $\tan \beta = 1.0$. The region contained by the solid black line and the hashed black contour is excluded at the 95% CL. The solid blue line indicates the expected limit in the absence of signal, and the dashed blue lines the corresponding $\pm 1\sigma$ uncertainty band. Subfigures (a, c, e) assume $\sin \theta = 0.35$, while (b, d, f) assume $\sin \theta = 0.7$. Where included, the dashed magenta lines represent the 36.1 fb^{-1} results from Ref. [18]. The hashed red area indicates that the width of one of the Higgs bosons is larger than 20% of its mass.

WIMP–proton scattering, while the vector mediator induces spin-independent WIMP–nucleon interactions [12]. Figs. 7 and 8 show the complementarity of the collider and direct-detection experiments: the limits obtained in this analysis are particularly competitive for low DM masses, where experiments relying on recoil measurements have limited sensitivity.

9. Conclusion

This article presents a search for invisible decays of the Higgs boson as well as searches for dark matter candidates, produced together with a leptonically decaying Z boson. The analysis was performed using proton–proton collisions at a centre-of-mass energy

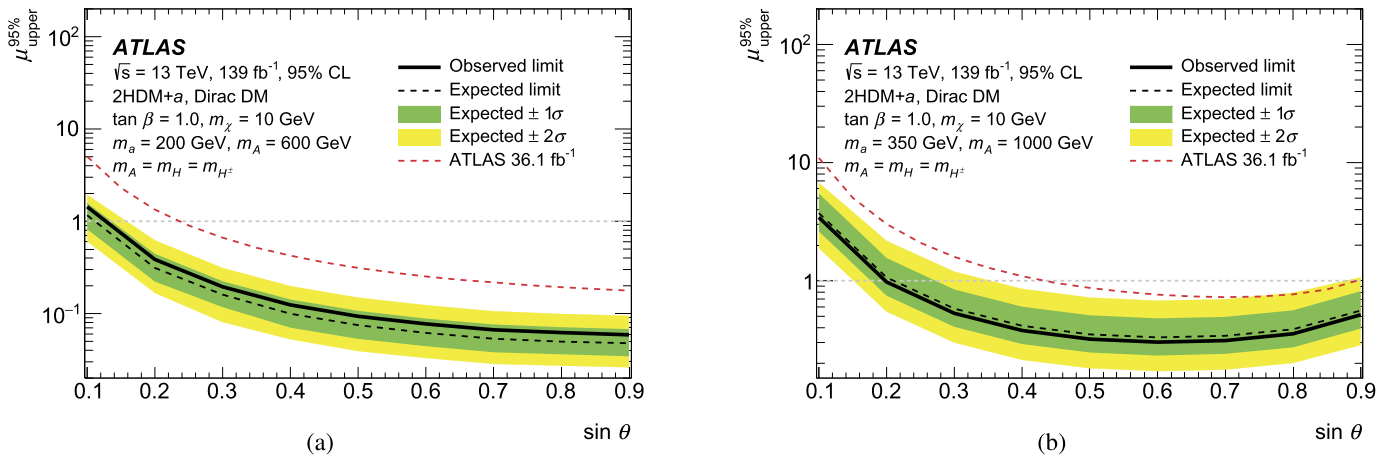


Fig. 6. $\sin\theta$ exclusion limits for 2HDM+a signals with $\tan\beta = 1.0$ and $m_\chi = 10$ GeV. The solid black line shows the observed limit, while the dashed black line indicates the expected limit in the absence of signal, with the corresponding 1σ and 2σ uncertainty bands in green and yellow. The dashed red line shows the result from the 36.1 fb^{-1} analysis [18]. The region below $\mu_{\text{upper}}^{95\%} = 1$ is excluded at the 95% CL. In (a), $m_A = 600$ GeV and $m_a = 200$ GeV, while in (b) $m_A = 1000$ GeV and $m_a = 350$ GeV.

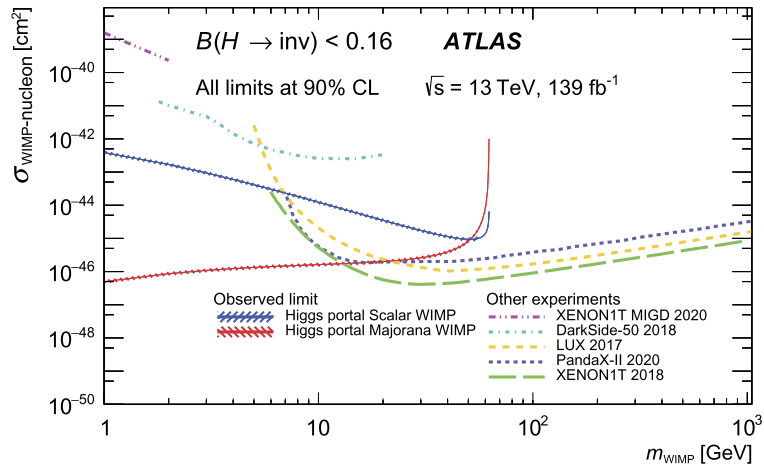


Fig. 7. Comparison between the 90% CL upper limits on the spin-independent WIMP–nucleon scattering cross-section from direct-detection experiments [1–5] and a reinterpretation of the $B(H \rightarrow \text{inv})$ limit obtained in this analysis, as a function of the WIMP mass. Higgs portal scenarios are assumed, where the 125 GeV Higgs boson decays into a pair of DM particles [104] that are either scalars or Majorana fermions. The uncertainties from the nuclear form factor are indicated by the hatched band. The regions above the limit contours are excluded in the $\sigma_{\text{WIMP-N}}$ range shown in the plot.

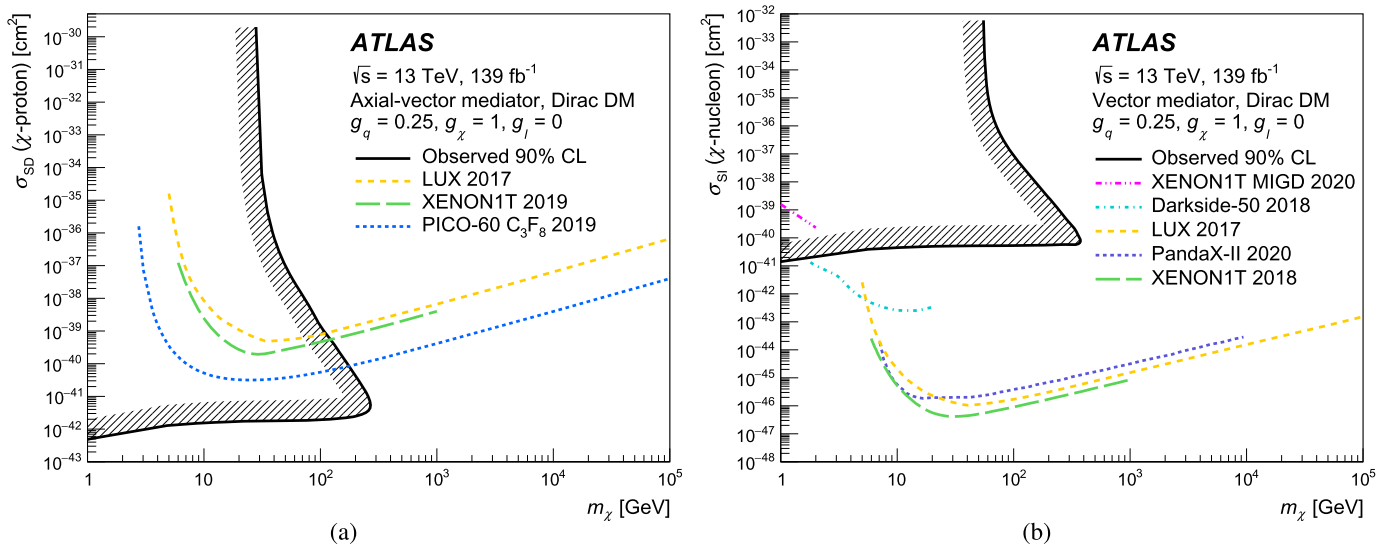


Fig. 8. Comparison of the upper limits at 90% CL from direct-detection experiments [1–8] with the exclusion obtained in the simplified DM models in the plane of the dark matter mass and (a) the spin-dependent WIMP–proton scattering cross-section or (b) the spin-independent WIMP–nucleon scattering cross-section [12]. The area within the shaded lines is excluded by this analysis in the context of the simplified models.

of 13 TeV, delivered by the LHC, corresponding to an integrated luminosity of 139 fb^{-1} and recorded by the ATLAS experiment. Assuming Standard Model cross-sections for ZH production, the upper limit in the branching ratio of the Higgs boson to invisible particles was constrained to 19%, at the 95% confidence level. The corresponding expected limit of 19% represents an improvement of about 45% in comparison with a projection of the previous analysis scaled to the present integrated luminosity. Exclusion limits were also set for simplified dark matter models and 2HDM+ a models for a number of benchmark parameters, improving on previously set combined constraints obtained with a 36 fb^{-1} dataset.

Declaration of competing interest

The authors declare that they have no known competing financial interests or personal relationships that could have appeared to influence the work reported in this paper.

Acknowledgements

We thank CERN for the very successful operation of the LHC, as well as the support staff from our institutions without whom ATLAS could not be operated efficiently.

We acknowledge the support of ANPCyT, Argentina; YerPhI, Armenia; ARC, Australia; BMWFW and FWF, Austria; ANAS, Azerbaijan; SSTC, Belarus; CNPq and FAPESP, Brazil; NSERC, NRC and CFI, Canada; CERN; ANID, Chile; CAS, MOST and NSFC, China; Min-ciencias, Colombia; MEYS CR, Czech Republic; DNRF and DNSRC, Denmark; IN2P3-CNRS and CEA-DRF/IRFU, France; SRNSFG, Georgia; BMBF, HGF and MPG, Germany; GSRI, Greece; RGC and Hong Kong SAR, China; ISF and Benozio Center, Israel; INFN, Italy; MEXT and JSPS, Japan; CNRST, Morocco; NWO, Netherlands; RCN, Norway; MEiN, Poland; FCT, Portugal; MNE/IFA, Romania; JINR, MES of Russia and NRC KI, Russian Federation; MESTD, Serbia; MSSR, Slovakia; ARRS and MIZŠ, Slovenia; DSI/NRF, South Africa; MICINN, Spain; SRC and Wallenberg Foundation, Sweden; SERI, SNSF and Canton of Bern and Canton of Geneva, Switzerland; MOST, Taiwan; TAEK, Turkey; STFC, United Kingdom; DOE and NSF, United States of America. In addition, individual groups and members have received support from BCKDF, Canarie, Compute Canada and CRC, Canada; COST, ERC, ERDF, Horizon 2020 and Marie Skłodowska-Curie Actions, European Union; Investissements d'Avenir Labex, Investissements d'Avenir Idex and ANR, France; DFG and AvH Foundation, Germany; Herakleitos, Thales and Aristeia programmes co-financed by EU-ESF and the Greek NSRF, Greece; BSF-NSF and GIF, Israel; Norwegian Financial Mechanism 2014-2021, Norway; NCN and NAWA, Poland; La Caixa Banking Foundation, CERCA Programme Generalitat de Catalunya and PROMETEO and GenT Programmes Generalitat Valenciana, Spain; Göran Gustafssons Stiftelse, Sweden; The Royal Society and Leverhulme Trust, United Kingdom.

The crucial computing support from all WLCG partners is acknowledged gratefully, in particular from CERN, the ATLAS Tier-1 facilities at TRIUMF (Canada), NDGF (Denmark, Norway, Sweden), CC-IN2P3 (France), KIT/GridKA (Germany), INFN-CNAF (Italy), NL-T1 (Netherlands), PIC (Spain), ASGC (Taiwan), RAL (UK) and BNL (USA), the Tier-2 facilities worldwide and large non-WLCG resource providers. Major contributors of computing resources are listed in Ref. [109].

References

[1] D.S. Akerib, et al., Results from a search for dark matter in the complete LUX exposure, *Phys. Rev. Lett.* 118 (2017) 021303, <https://doi.org/10.1103/PhysRevLett.118.021303>, arXiv:1608.07648 [astro-ph.CO].
 [2] E. Aprile, et al., Dark matter search results from a one ton-year exposure of XENON1T, *Phys. Rev. Lett.* 121 (2018) 111302, <https://doi.org/10.1103/PhysRevLett.121.111302>, arXiv:1805.12562 [astro-ph.CO].

[3] P. Agnes, et al., Low-mass dark matter search with the darkside-50 experiment, *Phys. Rev. Lett.* 121 (2018) 081307, <https://doi.org/10.1103/PhysRevLett.121.081307>, arXiv:1802.06994 [astro-ph.HE].
 [4] E. Aprile, et al., Search for light dark matter interactions enhanced by the Migdal effect or bremsstrahlung in XENON1T, *Phys. Rev. Lett.* 123 (2019) 241803, <https://doi.org/10.1103/PhysRevLett.123.241803>, arXiv:1907.12771 [hep-ex].
 [5] Q. Wang, et al., Results of dark matter search using the full PandaX-II exposure, *Chin. Phys. C* 44 (2020) 125001, <https://doi.org/10.1088/1674-1137/abb658>, arXiv:2007.15469 [astro-ph.CO].
 [6] D.S. Akerib, et al., Limits on spin-dependent WIMP-nucleon cross section obtained from the complete LUX exposure, *Phys. Rev. Lett.* 118 (2017) 251302, <https://doi.org/10.1103/PhysRevLett.118.251302>, arXiv:1705.03380 [astro-ph.CO].
 [7] C. Amole, et al., Dark matter search results from the complete exposure of the PICO-60 C_3F_8 bubble chamber, *Phys. Rev. D* 100 (2019) 022001, <https://doi.org/10.1103/PhysRevD.100.022001>, arXiv:1902.04031 [astro-ph.CO].
 [8] E. Aprile, et al., Constraining the spin-dependent WIMP-nucleon cross sections with XENON1T, *Phys. Rev. Lett.* 122 (2019) 141301, <https://doi.org/10.1103/PhysRevLett.122.141301>, arXiv:1902.03234 [astro-ph.CO].
 [9] ATLAS Collaboration, Observation of a new particle in the search for the Standard Model Higgs boson with the ATLAS detector at the LHC, *Phys. Lett. B* 716 (2012) 1, <https://doi.org/10.1016/j.physletb.2012.08.020>, arXiv:1207.7214 [hep-ex].
 [10] CMS Collaboration, Observation of a new boson at a mass of 125 GeV with the CMS experiment at the LHC, *Phys. Lett. B* 716 (2012) 30, <https://doi.org/10.1016/j.physletb.2012.08.021>, arXiv:1207.7235 [hep-ex].
 [11] D. de Florian, et al., *Handbook of LHC Higgs Cross Sections: 4. Deciphering the Nature of the Higgs Sector*, 2016, arXiv:1610.07922 [hep-ph].
 [12] A. Boveia, et al., Recommendations on presenting LHC searches for missing transverse energy signals using simplified s-channel models of dark matter, arXiv:1603.04156 [hep-ex], 2016.
 [13] A. Albert, et al., Recommendations of the LHC Dark Matter Working Group: comparing LHC searches for dark matter mediators in visible and invisible decay channels and calculations of the thermal relic density, *Phys. Dark Universe* 26 (2019) 100377, <https://doi.org/10.1016/j.dark.2019.100377>, arXiv:1703.05703 [hep-ex].
 [14] CMS Collaboration, Search for narrow and broad dijet resonances in proton-proton collisions at $\sqrt{s} = 13$ TeV and constraints on dark matter mediators and other new particles, *J. High Energy Phys.* 08 (2018) 130, [https://doi.org/10.1007/JHEP08\(2018\)130](https://doi.org/10.1007/JHEP08(2018)130), arXiv:1806.00843 [hep-ex].
 [15] ATLAS Collaboration, Search for new resonances in mass distributions of jet pairs using 139 fb^{-1} of pp collisions at $\sqrt{s} = 13$ TeV with the ATLAS detector, *J. High Energy Phys.* 03 (2020) 145, [https://doi.org/10.1007/JHEP03\(2020\)145](https://doi.org/10.1007/JHEP03(2020)145), arXiv:1910.08447 [hep-ex].
 [16] M. Bauer, U. Haisch, F. Kahlhoefer, Simplified dark matter models with two Higgs doublets: I. Pseudoscalar mediators, *J. High Energy Phys.* 05 (2017) 138, [https://doi.org/10.1007/JHEP05\(2017\)138](https://doi.org/10.1007/JHEP05(2017)138), arXiv:1701.07427 [hep-ph].
 [17] T. Abe, et al., LHC Dark Matter Working Group: next-generation spin-0 dark matter models, *Phys. Dark Universe* 27 (2020) 100351, <https://doi.org/10.1016/j.dark.2019.100351>, arXiv:1810.09420 [hep-ex].
 [18] ATLAS Collaboration, Constraints on mediator-based dark matter and scalar dark energy models using $\sqrt{s} = 13$ TeV pp collision data collected by the ATLAS detector, *J. High Energy Phys.* 05 (2019) 142, [https://doi.org/10.1007/JHEP05\(2019\)142](https://doi.org/10.1007/JHEP05(2019)142), arXiv:1903.01400 [hep-ex].
 [19] J.R. Andersen, et al., *Handbook of LHC Higgs Cross Sections: 3. Higgs Properties*, 2013, arXiv:1307.1347 [hep-ph].
 [20] T.D. Lee, A theory of spontaneous T violation, in: G. Feinberg (Ed.), *Phys. Rev. D* 8 (1973) 1226, <https://doi.org/10.1103/PhysRevD.8.1226>.
 [21] J.F. Gunion, H.E. Haber, CP-conserving two-Higgs-doublet model: the approach to the decoupling limit, *Phys. Rev. D* 67 (2003) 075019, <https://doi.org/10.1103/PhysRevD.67.075019>, arXiv:hep-ph/0207010.
 [22] G.C. Branco, et al., Theory and phenomenology of two-Higgs-doublet models, *Phys. Rep.* 516 (2012) 1, <https://doi.org/10.1016/j.physrep.2012.02.002>, arXiv:1106.0034 [hep-ph].
 [23] ATLAS Collaboration, Search for an invisibly decaying Higgs boson or dark matter candidates produced in association with a Z boson in pp collisions at $\sqrt{s} = 13$ TeV with the ATLAS detector, *Phys. Lett. B* 776 (2018) 318, <https://doi.org/10.1016/j.physletb.2017.11.049>, arXiv:1708.09624 [hep-ex].
 [24] ATLAS Collaboration, Combination of searches for invisible Higgs boson decays with the ATLAS experiment, *Phys. Rev. Lett.* 122 (2019) 231801, <https://doi.org/10.1103/PhysRevLett.122.231801>, arXiv:1904.05105 [hep-ex].
 [25] CMS Collaboration, Search for dark matter produced in association with a leptonically decaying Z boson in proton-proton collisions at $\sqrt{s} = 13$ TeV, *Eur. Phys. J. C* 81 (2021) 13, <https://doi.org/10.1140/epjc/s10052-020-08739-5>, arXiv:2008.04735 [hep-ex].
 [26] CMS Collaboration, Search for invisible decays of a Higgs boson produced through vector boson fusion in proton-proton collisions at $\sqrt{s} = 13$ TeV, *Phys. Lett. B* 793 (2019) 520, <https://doi.org/10.1016/j.physletb.2019.04.025>, arXiv:1809.05937 [hep-ex].

- [27] CMS Collaboration, Search for dark matter produced in association with a Higgs boson decaying to a pair of bottom quarks in proton–proton collisions at $\sqrt{s} = 13$ TeV, *Eur. Phys. J. C* 79 (2019) 280, <https://doi.org/10.1140/epjc/s10052-019-6730-7>, arXiv:1811.06562 [hep-ex].
- [28] ATLAS Collaboration, Search for dark matter produced in association with a single top quark in $\sqrt{s} = 13$ TeV pp collisions with the ATLAS detector, *Eur. Phys. J. C* 81 (2021) 860, <https://doi.org/10.1140/epjc/s10052-021-09566-y>, arXiv:2011.09308 [hep-ex].
- [29] ATLAS Collaboration, The ATLAS experiment at the CERN Large Hadron Collider, *J. Instrum.* 3 (2008) S08003, <https://doi.org/10.1088/1748-0221/3/08/S08003>.
- [30] ATLAS Collaboration, Performance of the ATLAS trigger system in 2015, *Eur. Phys. J. C* 77 (2017) 317, <https://doi.org/10.1140/epjc/s10052-017-4852-3>, arXiv:1611.09661 [hep-ex].
- [31] ATLAS Collaboration, The ATLAS Collaboration software and firmware, ATLAS-SOFT-PUB-2021-001, <https://cds.cern.ch/record/2767187>, 2021.
- [32] ATLAS Collaboration, ATLAS data quality operations and performance for 2015–2018 data-taking, *J. Instrum.* 15 (2020) P04003, <https://doi.org/10.1088/1748-0221/15/04/P04003>, arXiv:1911.04632 [physics.ins-det].
- [33] ATLAS Collaboration, Performance of electron and photon triggers in ATLAS during LHC Run 2, *Eur. Phys. J. C* 80 (2020) 47, <https://doi.org/10.1140/epjc/s10052-019-7500-2>, arXiv:1909.00761 [hep-ex].
- [34] ATLAS Collaboration, Performance of the ATLAS muon triggers in Run 2, *J. Instrum.* 15 (2020) P09015, <https://doi.org/10.1088/1748-0221/15/09/P09015>, arXiv:2004.13447 [hep-ex].
- [35] ATLAS Collaboration, The ATLAS Inner Detector Trigger performance in pp collisions at 13 TeV during LHC Run 2, arXiv:2107.02485 [hep-ex], 2021.
- [36] R.D. Ball, et al., Parton distributions for the LHC run II, *J. High Energy Phys.* 04 (2015) 040, [https://doi.org/10.1007/JHEP04\(2015\)040](https://doi.org/10.1007/JHEP04(2015)040), arXiv:1410.8849 [hep-ph].
- [37] ATLAS Collaboration, The ATLAS simulation infrastructure, *Eur. Phys. J. C* 70 (2010) 823, <https://doi.org/10.1140/epjc/s10052-010-1429-9>, arXiv:1005.4568 [physics.ins-det].
- [38] GEANT4 Collaboration, S. Agostinelli, et al., GEANT4 – a simulation toolkit, *Nucl. Instrum. Methods A* 506 (2003) 250, [https://doi.org/10.1016/S0168-9002\(03\)01368-8](https://doi.org/10.1016/S0168-9002(03)01368-8).
- [39] T. Sjöstrand, S. Mrenna, P. Skands, A brief introduction to PYTHIA 8.1, *Comput. Phys. Commun.* 178 (2008) 852, <https://doi.org/10.1016/j.cpc.2008.01.036>, arXiv:0710.3820 [hep-ph].
- [40] R.D. Ball, et al., Parton distributions with LHC data, *Nucl. Phys. B* 867 (2013) 244, <https://doi.org/10.1016/j.nuclphysb.2012.10.003>, arXiv:1207.1303 [hep-ph].
- [41] ATLAS Collaboration, The Pythia 8 A3 tune description of ATLAS minimum bias and inelastic measurements incorporating the Donnachie–Landshoff diffractive model, ATLAS-PUB-2016-017, <https://cds.cern.ch/record/2206965>, 2016.
- [42] E. Bothmann, et al., Event generation with Sherpa 2.2, *SciPost Phys.* 7 (2019) 034, <https://doi.org/10.21468/SciPostPhys.7.3.034>, arXiv:1905.09127 [hep-ph].
- [43] D.J. Lange, The EvtGen particle decay simulation package, *Nucl. Instrum. Methods A* 462 (2001) 152, [https://doi.org/10.1016/S0168-9002\(01\)00089-4](https://doi.org/10.1016/S0168-9002(01)00089-4).
- [44] S. Alioli, P. Nason, C. Oleari, E. Re, A general framework for implementing NLO calculations in shower Monte Carlo programs: the POWHEG BOX, *J. High Energy Phys.* 06 (2010) 043, [https://doi.org/10.1007/JHEP06\(2010\)043](https://doi.org/10.1007/JHEP06(2010)043), arXiv:1002.2581 [hep-ph].
- [45] K. Hamilton, P. Nason, G. Zanderighi, MINLO: multi-scale improved NLO, *J. High Energy Phys.* 10 (2012) 155, [https://doi.org/10.1007/JHEP10\(2012\)155](https://doi.org/10.1007/JHEP10(2012)155), arXiv:1206.3572 [hep-ph].
- [46] T. Sjöstrand, et al., An introduction to PYTHIA 8.2, *Comput. Phys. Commun.* 191 (2015) 159, <https://doi.org/10.1016/j.cpc.2015.01.024>, arXiv:1410.3012 [hep-ph].
- [47] ATLAS Collaboration, Measurement of the Z/γ^* boson transverse momentum distribution in pp collisions at $\sqrt{s} = 7$ TeV with the ATLAS detector, *J. High Energy Phys.* 09 (2014) 145, [https://doi.org/10.1007/JHEP09\(2014\)145](https://doi.org/10.1007/JHEP09(2014)145), arXiv:1406.3660 [hep-ex].
- [48] M.L. Ciccolini, S. Dittmaier, M. Krämer, Electroweak radiative corrections to associated WH and ZH production at hadron colliders, *Phys. Rev. D* 68 (2003) 073003, arXiv:hep-ph/0306234.
- [49] O. Brein, A. Djouadi, R. Harlander, NNLO QCD corrections to the Higgs-strahlung processes at hadron colliders, *Phys. Lett. B* 579 (2004) 149, <https://doi.org/10.1016/j.physletb.2003.10.112>, arXiv:hep-ph/0307206.
- [50] O. Brein, R. Harlander, M. Wiesemann, T. Zirke, Top-quark mediated effects in hadronic Higgs-strahlung, *Eur. Phys. J. C* 72 (2012) 1868, <https://doi.org/10.1140/epjc/s10052-012-1868-6>, arXiv:1111.0761 [hep-ph].
- [51] L. Attenkamp, S. Dittmaier, R.V. Harlander, H. Zehak, T.J.E. Zirke, Gluon-induced Higgs-strahlung at next-to-leading order QCD, *J. High Energy Phys.* 02 (2013) 078, [https://doi.org/10.1007/JHEP02\(2013\)078](https://doi.org/10.1007/JHEP02(2013)078), arXiv:1211.5015 [hep-ph].
- [52] A. Denner, S. Dittmaier, S. Kallweit, A. Mück, HAWK 2.0: a Monte Carlo program for Higgs production in vector-boson fusion and Higgs strahlung at hadron colliders, *Comput. Phys. Commun.* 195 (2015) 161, <https://doi.org/10.1016/j.cpc.2015.04.021>, arXiv:1412.5390 [hep-ph].
- [53] O. Brein, R.V. Harlander, T.J.E. Zirke, $vh@nnlo$ – Higgs Strahlung at hadron colliders, *Comput. Phys. Commun.* 184 (2013) 998, <https://doi.org/10.1016/j.cpc.2012.11.002>, arXiv:1210.5347 [hep-ph].
- [54] R.V. Harlander, A. Kulesza, V. Theeuwes, T. Zirke, Soft gluon resummation for gluon-induced Higgs Strahlung, *J. High Energy Phys.* 11 (2014) 082, [https://doi.org/10.1007/JHEP11\(2014\)082](https://doi.org/10.1007/JHEP11(2014)082), arXiv:1410.0217 [hep-ph].
- [55] R.V. Harlander, J. Klappert, S. Liebler, L. Simon, $vh@nnlo-v2$: new physics in Higgs Strahlung, *J. High Energy Phys.* 05 (2018) 089, [https://doi.org/10.1007/JHEP05\(2018\)089](https://doi.org/10.1007/JHEP05(2018)089), arXiv:1802.04817 [hep-ph].
- [56] J. Alwall, et al., The automated computation of tree-level and next-to-leading order differential cross sections, and their matching to parton shower simulations, *J. High Energy Phys.* 07 (2014) 079, [https://doi.org/10.1007/JHEP07\(2014\)079](https://doi.org/10.1007/JHEP07(2014)079), arXiv:1405.0301 [hep-ph].
- [57] ATLAS Collaboration, ATLAS Pythia 8 tunes to 7 TeV data, ATLAS-PUB-2014-021, <https://cds.cern.ch/record/1966419>, 2014.
- [58] T. Gleisberg, S. Höche, Comix, a new matrix element generator, *J. High Energy Phys.* 12 (2008) 039, <https://doi.org/10.1088/1126-6708/2008/12/039>, arXiv:0808.3674 [hep-ph].
- [59] F. Buccioni, et al., OpenLoops 2, *Eur. Phys. J. C* 79 (2019) 866, <https://doi.org/10.1140/epjc/s10052-019-7306-2>, arXiv:1907.13071 [hep-ph].
- [60] F. Cascioli, P. Maierhöfer, S. Pozzorini, Scattering amplitudes with open loops, *Phys. Rev. Lett.* 108 (2012) 111601, <https://doi.org/10.1103/PhysRevLett.108.111601>, arXiv:1111.5206 [hep-ph].
- [61] A. Denner, S. Dittmaier, L. Hofer, COLLIER: a Fortran-based complex one-loop library in extended regularizations, *Comput. Phys. Commun.* 212 (2017) 220, <https://doi.org/10.1016/j.cpc.2016.10.013>, arXiv:1604.06792 [hep-ph].
- [62] S. Schumann, F. Krauss, A parton shower algorithm based on Catani–Seymour dipole factorisation, *J. High Energy Phys.* 03 (2008) 038, <https://doi.org/10.1088/1126-6708/2008/03/038>, arXiv:0709.1027 [hep-ph].
- [63] S. Höche, F. Krauss, M. Schönherr, F. Siegert, QCD matrix elements + parton showers. The NLO case, *J. High Energy Phys.* 04 (2013) 027, [https://doi.org/10.1007/JHEP04\(2013\)027](https://doi.org/10.1007/JHEP04(2013)027), arXiv:1207.5030 [hep-ph].
- [64] S. Kallweit, J.M. Lindert, P. Maierhöfer, S. Pozzorini, M. Schönherr, NLO electroweak automation and precise predictions for W+multijet production at the LHC, *J. High Energy Phys.* 04 (2015) 012, [https://doi.org/10.1007/JHEP04\(2015\)012](https://doi.org/10.1007/JHEP04(2015)012), arXiv:1412.5157 [hep-ph].
- [65] S. Kallweit, J.M. Lindert, S. Pozzorini, M. Schönherr, NLO QCD+EW predictions for $2\ell 2\nu$ diboson signatures at the LHC, *J. High Energy Phys.* 11 (2017) 120, [https://doi.org/10.1007/JHEP11\(2017\)120](https://doi.org/10.1007/JHEP11(2017)120), arXiv:1705.00598 [hep-ph].
- [66] M. Schönherr, An automated subtraction of NLO EW infrared divergences, *Eur. Phys. J. C* 78 (2018) 119, <https://doi.org/10.1140/epjc/s10052-018-5600-z>, arXiv:1712.07975 [hep-ph].
- [67] M. Grazzini, S. Kallweit, J.M. Lindert, S. Pozzorini, M. Wiesemann, NNLO QCD + NLO EW with Matrix+OpenLoops: precise predictions for vector-boson pair production, *J. High Energy Phys.* 02 (2020) 087, [https://doi.org/10.1007/JHEP02\(2020\)087](https://doi.org/10.1007/JHEP02(2020)087), arXiv:1912.00068 [hep-ph].
- [68] M. Grazzini, S. Kallweit, M. Wiesemann, Fully differential NNLO computations with MATRIX, *Eur. Phys. J. C* 78 (2018) 537, <https://doi.org/10.1140/epjc/s10052-018-5771-7>, arXiv:1711.06631 [hep-ph].
- [69] T. Gehrmann, A. Manteuffel, L. Tancredi, The two-loop helicity amplitudes for $q\bar{q} \rightarrow V_1 V_2 \rightarrow 4$ leptons, *J. High Energy Phys.* 09 (2015) 128, [https://doi.org/10.1007/JHEP09\(2015\)128](https://doi.org/10.1007/JHEP09(2015)128), arXiv:1503.04812.
- [70] M. Grazzini, S. Kallweit, M. Wiesemann, J.Y. Yook, ZZ production at the LHC: NLO QCD corrections to the loop-induced gluon fusion channel, *J. High Energy Phys.* 03 (2019) 070, [https://doi.org/10.1007/JHEP03\(2019\)070](https://doi.org/10.1007/JHEP03(2019)070), arXiv:1811.09593 [hep-ph].
- [71] S. Frixione, G. Ridolfi, P. Nason, A positive-weight next-to-leading-order Monte Carlo for heavy flavour hadroproduction, *J. High Energy Phys.* 09 (2007) 126, <https://doi.org/10.1088/1126-6708/2007/09/126>, arXiv:0707.3088 [hep-ph].
- [72] P. Nason, A new method for combining NLO QCD with shower Monte Carlo algorithms, *J. High Energy Phys.* 11 (2004) 040, <https://doi.org/10.1088/1126-6708/2004/11/040>, arXiv:hep-ph/0409146.
- [73] S. Frixione, P. Nason, C. Oleari, Matching NLO QCD computations with parton shower simulations: the POWHEG method, *J. High Energy Phys.* 11 (2007) 070, <https://doi.org/10.1088/1126-6708/2007/11/070>, arXiv:0709.2092 [hep-ph].
- [74] R. Frederix, E. Re, P. Torrielli, Single-top t -channel hadroproduction in the four-flavour scheme with POWHEG and aMC@NLO, *J. High Energy Phys.* 09 (2012) 130, [https://doi.org/10.1007/JHEP09\(2012\)130](https://doi.org/10.1007/JHEP09(2012)130), arXiv:1207.5391 [hep-ph].
- [75] E. Re, Single-top Wt -channel production matched with parton showers using the POWHEG method, *Eur. Phys. J. C* 71 (2011) 1547, <https://doi.org/10.1140/epjc/s10052-011-1547-z>, arXiv:1009.2450 [hep-ph].
- [76] M. Czakon, A. Mitov, Top++: a program for the calculation of the top-pair cross-section at hadron colliders, *Comput. Phys. Commun.* 185 (2014) 2930, <https://doi.org/10.1016/j.cpc.2014.06.021>, arXiv:1112.5675 [hep-ph].
- [77] N. Kidonakis, Next-to-next-to-leading-order collinear and soft gluon corrections for t -channel single top quark production, *Phys. Rev. D* 83 (2011) 091503, <https://doi.org/10.1103/PhysRevD.83.091503>, arXiv:1103.2792 [hep-ph].

- [78] N. Kidonakis, Two-loop soft anomalous dimensions for single top quark associated production with a W^- or H^- , Phys. Rev. D 82 (2010) 054018, <https://doi.org/10.1103/PhysRevD.82.054018>, arXiv:1005.4451 [hep-ph].
- [79] N. Kidonakis, Next-to-next-to-leading logarithm resummation for s -channel single top quark production, Phys. Rev. D 81 (2010) 054028, <https://doi.org/10.1103/PhysRevD.81.054028>, arXiv:1001.5034 [hep-ph].
- [80] ATLAS Collaboration, Vertex reconstruction performance of the ATLAS detector at $\sqrt{s} = 13$ TeV, ATL-PHYS-PUB-2015-026, 2015, <https://cds.cern.ch/record/2037717>.
- [81] ATLAS Collaboration, Electron and photon performance measurements with the ATLAS detector using the 2015–2017 LHC proton–proton collision data, J. Instrum. 14 (2019) P12006, <https://doi.org/10.1088/1748-0221/14/12/P12006>, arXiv:1908.00005 [hep-ex].
- [82] ATLAS Collaboration, Muon reconstruction performance of the ATLAS Detector in proton–proton collision data at $\sqrt{s} = 13$ TeV, Eur. Phys. J. C 76 (2016) 292, <https://doi.org/10.1140/epjc/s10052-016-4120-y>, arXiv:1603.05598 [hep-ex].
- [83] ATLAS Collaboration, Muon reconstruction and identification efficiency in ATLAS using the full Run 2 pp collision data set at $\sqrt{s} = 13$ TeV, Eur. Phys. J. C 81 (2021) 578, <https://doi.org/10.1140/epjc/s10052-021-09233-2>, arXiv:2012.00578 [hep-ex].
- [84] ATLAS Collaboration, Jet reconstruction and performance using particle flow with the ATLAS Detector, Eur. Phys. J. C 77 (2017) 466, <https://doi.org/10.1140/epjc/s10052-017-5031-2>, arXiv:1703.10485 [hep-ex].
- [85] M. Cacciari, G.P. Salam, G. Soyez, The anti- k_t jet clustering algorithm, J. High Energy Phys. 04 (2008) 063, <https://doi.org/10.1088/1126-6708/2008/04/063>, arXiv:0802.1189 [hep-ph].
- [86] M. Cacciari, G.P. Salam, G. Soyez, FastJet user manual, Eur. Phys. J. C 72 (2012) 1896, <https://doi.org/10.1140/epjc/s10052-012-1896-2>, arXiv:1111.6097 [hep-ph].
- [87] ATLAS Collaboration, Performance of pile-up mitigation techniques for jets in pp collisions at $\sqrt{s} = 8$ TeV using the ATLAS detector, Eur. Phys. J. C 76 (2016) 581, <https://doi.org/10.1140/epjc/s10052-016-4395-z>, arXiv:1510.03823 [hep-ex].
- [88] ATLAS Collaboration, Jet energy scale and resolution measured in proton–proton collisions at $\sqrt{s} = 13$ TeV with the ATLAS detector, Eur. Phys. J. C 81 (2021) 689, <https://doi.org/10.1140/epjc/s10052-021-09402-3>, arXiv:2007.02645 [hep-ex].
- [89] ATLAS Collaboration, Measurements of b -jet tagging efficiency with the ATLAS detector using $t\bar{t}$ events at $\sqrt{s} = 13$ TeV, J. High Energy Phys. 08 (2018) 089, [https://doi.org/10.1007/JHEP08\(2018\)089](https://doi.org/10.1007/JHEP08(2018)089), arXiv:1805.01845 [hep-ex].
- [90] ATLAS Collaboration, Search for heavy resonances decaying into a pair of Z bosons in the $e^+e^-e'^+e'^-$ and $e^+e^-e\nu\bar{\nu}$ final states using 139 fb $^{-1}$ of proton–proton collisions at $\sqrt{s} = 13$ TeV with the ATLAS detector, Eur. Phys. J. C 81 (2021) 332, <https://doi.org/10.1140/epjc/s10052-021-09013-y>, arXiv:2009.14791 [hep-ex].
- [91] ATLAS Collaboration, Performance of missing transverse momentum reconstruction with the ATLAS detector using proton–proton collisions at $\sqrt{s} = 13$ TeV, Eur. Phys. J. C 78 (2018) 903, <https://doi.org/10.1140/epjc/s10052-018-6288-9>, arXiv:1802.08168 [hep-ex].
- [92] ATLAS Collaboration, Object-based missing transverse momentum significance in the ATLAS Detector, ATLAS-CONF-2018-038, 2018, <https://cds.cern.ch/record/2630948>.
- [93] M. Baak, et al., HistFitter software framework for statistical data analysis, Eur. Phys. J. C 75 (2015) 153, <https://doi.org/10.1140/epjc/s10052-015-3327-7>, arXiv:1410.1280 [hep-ex].
- [94] G. Cowan, K. Cranmer, E. Gross, O. Vitells, Asymptotic formulae for likelihood-based tests of new physics, Eur. Phys. J. C 71 (2011) 1554, <https://doi.org/10.1140/epjc/s10052-011-1554-0>, arXiv:1007.1727 [physics.data-an], Erratum: Eur. Phys. J. C 73 (2013) 2501, <https://doi.org/10.1140/epjc/s10052-013-2501-z>.
- [95] A. Hoecker, et al., TMVA - toolkit for multivariate data analysis, arXiv:physics/0703039 [physics.data-an], 2007.
- [96] J. Butterworth, et al., PDF4LHC recommendations for LHC Run II, J. Phys. G 43 (2016) 023001, <https://doi.org/10.1103/PhysRevLett.118.021303>, arXiv:1510.03865 [hep-ph].
- [97] S. Catani, F. Krauss, B.R. Webber, R. Kuhn, QCD matrix elements + parton showers, J. High Energy Phys. 11 (2001) 063, <https://doi.org/10.1088/1126-6708/2001/11/063>, arXiv:hep-ph/0109231.
- [98] S. Höche, F. Krauss, S. Schumann, F. Siegert, QCD matrix elements and truncated showers, J. High Energy Phys. 05 (2009) 053, <https://doi.org/10.1088/1126-6708/2009/05/053>, arXiv:0903.1219 [hep-ph].
- [99] ATLAS Collaboration, Measurements of Higgs boson properties in the diphoton decay channel with 36 fb $^{-1}$ of pp collision data at $\sqrt{s} = 13$ TeV with the ATLAS detector, Phys. Rev. D 98 (2018) 052005, <https://doi.org/10.1103/PhysRevD.98.052005>, arXiv:1802.04146 [hep-ex].
- [100] J. Bellm, et al., Herwig 7.0/Herwig++ 3.0 release note, Eur. Phys. J. C 76 (2016) 196, <https://doi.org/10.1140/epjc/s10052-016-4018-8>, arXiv:1512.01178 [hep-ph].
- [101] ATLAS Collaboration, Luminosity determination in pp collisions at $\sqrt{s} = 13$ TeV using the ATLAS detector at the LHC, ATLAS-CONF-2019-021, 2019, <https://cds.cern.ch/record/2677054>.
- [102] G. Avoni, et al., The new LUCID-2 detector for luminosity measurement and monitoring in ATLAS, J. Instrum. 13 (2018) P07017, <https://doi.org/10.1088/1748-0221/13/07/P07017>.
- [103] ATLAS Collaboration, Search for dark matter in events with missing transverse momentum and a Higgs boson decaying into two photons in pp collisions at $\sqrt{s} = 13$ TeV with the ATLAS detector, J. High Energy Phys. 10 (2021) 013, [https://doi.org/10.1007/JHEP10\(2021\)013](https://doi.org/10.1007/JHEP10(2021)013), arXiv:2104.13240 [hep-ex].
- [104] ATLAS Collaboration, Search for invisible decays of a Higgs boson using vector-boson fusion in pp collisions at $\sqrt{s} = 8$ TeV with the ATLAS detector, J. High Energy Phys. 01 (2016) 172, [https://doi.org/10.1007/JHEP01\(2016\)172](https://doi.org/10.1007/JHEP01(2016)172), arXiv:1508.07869 [hep-ex].
- [105] O.J.P. Eboli, D. Zeppenfeld, Observing an invisible Higgs boson, Phys. Lett. B 495 (2000) 147, [https://doi.org/10.1016/S0370-2693\(00\)01213-2](https://doi.org/10.1016/S0370-2693(00)01213-2), arXiv:hep-ph/0009158.
- [106] P.J. Fox, R. Harnik, J. Kopp, Y. Tsai, Missing energy signatures of dark matter at the LHC, Phys. Rev. D 85 (2012) 056011, <https://doi.org/10.1103/PhysRevD.85.056011>, arXiv:1109.4398 [hep-ph].
- [107] A. De Simone, G.F. Giudice, A. Strumia, Benchmarks for dark matter searches at the LHC, J. High Energy Phys. 06 (2014) 081, [https://doi.org/10.1007/JHEP06\(2014\)081](https://doi.org/10.1007/JHEP06(2014)081), arXiv:1402.6287 [hep-ph].
- [108] M. Hoferichter, P. Klos, J. Menéndez, A. Schwenk, Improved limits for Higgs-portal dark matter from LHC searches, Phys. Rev. Lett. 119 (2017) 181803, <https://doi.org/10.1103/PhysRevLett.119.181803>, arXiv:1708.02245 [hep-ph].
- [109] ATLAS Computing Acknowledgements, tech. rep., CERN, <https://cds.cern.ch/record/2776662>, 2021.

The ATLAS Collaboration

G. Aad⁹⁸, B. Abbott¹²⁴, D.C. Abbott⁹⁹, A. Abed Abud³⁴, K. Abeling⁵¹, D.K. Abhayasinghe⁹¹, S.H. Abidi²⁷, A. Abouhorma^{33e}, H. Abramowicz¹⁵⁷, H. Abreu¹⁵⁶, Y. Abulaiti⁵, A.C. Abusleme Hoffman^{142a}, B.S. Acharya^{64a,64b,o}, B. Achkar⁵¹, L. Adam⁹⁶, C. Adam Bourdarios⁴, L. Adamczyk^{81a}, L. Adamek¹⁶², S.V. Addepalli²⁴, J. Adelman¹¹⁶, A. Adiguzel^{11c,ac}, S. Adorni⁵², T. Adye¹³⁹, A.A. Affolder¹⁴¹, Y. Afik³⁴, C. Agapopoulou⁶², M.N. Agarar¹², J. Agarwala^{68a,68b}, A. Aggarwal¹¹⁴, C. Agheorghiesei^{25c}, J.A. Aguilar-Saavedra^{135f,135a,ab}, A. Ahmad³⁴, F. Ahmadov^{77,z}, W.S. Ahmed¹⁰⁰, X. Ai⁴⁴, G. Aielli^{71a,71b}, I. Aizenberg¹⁷⁵, S. Akatsuka⁸³, M. Akbiyik⁹⁶, T.P.A. Åkesson⁹⁴, A.V. Akimov¹⁰⁷, K. Al Khoury³⁷, G.L. Alberghi^{21b}, J. Albert¹⁷¹, P. Albicocco⁴⁹, M.J. Alconada Verzini⁸⁶, S. Alderweireldt⁴⁸, M. Aleksa³⁴, I.N. Aleksandrov⁷⁷, C. Alexa^{25b}, T. Alexopoulos⁹, A. Alfonsi¹¹⁵, F. Alfonsi^{21b}, M. Alhroob¹²⁴, B. Ali¹³⁷, S. Ali¹⁵⁴, M. Aliev¹⁶¹, G. Alimonti^{66a}, C. Allaire³⁴, B.M.M. Allbrooke¹⁵², P.P. Allport¹⁹, A. Aloisio^{67a,67b}, F. Alonso⁸⁶, C. Alpigiani¹⁴⁴, E. Alunno Camelia^{71a,71b}, M. Alvarez Estevez⁹⁵, M.G. Alviggi^{67a,67b}, Y. Amaral Coutinho^{78b}, A. Ambler¹⁰⁰, L. Ambroz¹³⁰, C. Amelung³⁴, D. Amidei¹⁰², S.P. Amor Dos Santos^{135a}, S. Amoroso⁴⁴, K.R. Amos¹⁶⁹, C.S. Amrouche⁵², V. Ananiev¹²⁹,

C. Anastopoulos¹⁴⁵, N. Andari¹⁴⁰, T. Andeen¹⁰, J.K. Anders¹⁸, S.Y. Andreev^{43a,43b}, A. Andreazza^{66a,66b}, C.R. Anelli¹⁷¹, S. Angelidakis⁸, A. Angerami³⁷, A.V. Anisenkov^{117b,117a}, A. Annovi^{69a}, C. Antel⁵², M.T. Anthony¹⁴⁵, E. Antipov¹²⁵, M. Antonelli⁴⁹, D.J.A. Antrim¹⁶, F. Anulli^{70a}, M. Aoki⁷⁹, J.A. Aparisi Pozo¹⁶⁹, M.A. Aparo¹⁵², L. Aperio Bella⁴⁴, N. Aranzabal³⁴, V. Araujo Ferraz^{78a}, C. Arcangeletti⁴⁹, A.T.H. Arce⁴⁷, E. Arena⁸⁸, J.-F. Arguin¹⁰⁶, S. Argyropoulos⁵⁰, J.-H. Arling⁴⁴, A.J. Armbruster³⁴, A. Armstrong¹⁶⁶, O. Arnaez¹⁶², H. Arnold³⁴, Z.P. Arrubarrena Tame¹¹⁰, G. Artoni¹³⁰, H. Asada¹¹², K. Asai¹²², S. Asai¹⁵⁹, N.A. Asbah⁵⁷, E.M. Asimakopoulou¹⁶⁷, L. Asquith¹⁵², J. Assahsah^{33d}, K. Assamagan²⁷, R. Astalos^{26a}, R.J. Atkin^{31a}, M. Atkinson¹⁶⁸, N.B. Atlay¹⁷, H. Atmani^{58b}, P.A. Atmasiddha¹⁰², K. Augsten¹³⁷, S. Auricchio^{67a,67b}, V.A. Austrup¹⁷⁷, G. Avner¹⁵⁶, G. Avolio³⁴, M.K. Ayoub^{13c}, G. Azuelos^{106,aj}, D. Babal^{26a}, H. Bachacou¹⁴⁰, K. Bachas¹⁵⁸, A. Bachi³², F. Backman^{43a,43b}, A. Badea⁵⁷, P. Bagnaia^{70a,70b}, H. Bahrasemani¹⁴⁸, A.J. Bailey¹⁶⁹, V.R. Bailey¹⁶⁸, J.T. Baines¹³⁹, C. Bakalis⁹, O.K. Baker¹⁷⁸, P.J. Bakker¹¹⁵, E. Bakos¹⁴, D. Bakshi Gupta⁷, S. Balaji¹⁵³, R. Balasubramanian¹¹⁵, E.M. Baldin^{117b,117a}, P. Balek¹³⁸, E. Ballabene^{66a,66b}, F. Balli¹⁴⁰, L.M. Baltés^{59a}, W.K. Balunas¹³⁰, J. Balz⁹⁶, E. Banas⁸², M. Bandieramonte¹³⁴, A. Bandyopadhyay²², S. Bansal²², L. Barak¹⁵⁷, E.L. Barberio¹⁰¹, D. Barberis^{53b,53a}, M. Barbero⁹⁸, G. Barbour⁹², K.N. Barends^{31a}, T. Barillari¹¹¹, M.-S. Barisits³⁴, J. Barkeloo¹²⁷, T. Barklow¹⁴⁹, B.M. Barnett¹³⁹, R.M. Barnett¹⁶, A. Baroncelli^{58a}, G. Barone²⁷, A.J. Barr¹³⁰, L. Barranco Navarro^{43a,43b}, F. Barreiro⁹⁵, J. Barreiro Guimarães da Costa^{13a}, U. Barron¹⁵⁷, S. Barsov¹³³, F. Bartels^{59a}, R. Bartoldus¹⁴⁹, G. Bartolini⁹⁸, A.E. Barton⁸⁷, P. Bartos^{26a}, A. Basalae⁴⁴, A. Basan⁹⁶, M. Baselga⁴⁴, I. Bashta^{72a,72b}, A. Bassalat^{62,ag}, M.J. Basso¹⁶², C.R. Basson⁹⁷, R.L. Bates⁵⁵, S. Batlamous^{33e}, J.R. Batley³⁰, B. Batool¹⁴⁷, M. Battaglia¹⁴¹, M. Baucé^{70a,70b}, F. Bauer^{140,*}, P. Bauer²², H.S. Bawa²⁹, A. Bayirli^{11c}, J.B. Beacham⁴⁷, T. Beau¹³¹, P.H. Beauchemin¹⁶⁵, F. Becherer⁵⁰, P. Bechtel²², H.P. Beck^{18,q}, K. Becker¹⁷³, C. Becot⁴⁴, A.J. Beddall^{11a}, V.A. Bednyakov⁷⁷, C.P. Bee¹⁵¹, T.A. Beermann³⁴, M. Begalli^{78b}, M. Beger²⁷, A. Behera¹⁵¹, J.K. Behr⁴⁴, C. Beirao Da Cruz E Silva³⁴, J.F. Beirer^{51,34}, F. Beisiegel²², M. Belfkir⁴, G. Bella¹⁵⁷, L. Bellagamba^{21b}, A. Bellerive³², P. Bellos¹⁹, K. Beloborodov^{117b,117a}, K. Belotskiy¹⁰⁸, N.L. Belyaev¹⁰⁸, D. Benchekroun^{33a}, Y. Benhammou¹⁵⁷, D.P. Benjamin²⁷, M. Benoit²⁷, J.R. Bensinger²⁴, S. Bentvelsen¹¹⁵, L. Beresford³⁴, M. Beretta⁴⁹, D. Berge¹⁷, E. Bergeaas Kuutmann¹⁶⁷, N. Berger⁴, B. Bergmann¹³⁷, L.J. Bergsten²⁴, J. Beringer¹⁶, S. Berlendis⁶, G. Bernardi¹³¹, C. Bernius¹⁴⁹, F.U. Bernlochner²², T. Berry⁹¹, P. Berta¹³⁸, A. Berthold⁴⁶, I.A. Bertram⁸⁷, O. Bessidskaia Bylund¹⁷⁷, S. Bethke¹¹¹, A. Betti⁴⁰, A.J. Bevan⁹⁰, S. Bhatta¹⁵¹, D.S. Bhattacharya¹⁷², P. Bhattarai²⁴, V.S. Bhopatkar⁵, R. Bi¹³⁴, R.M. Bianchi¹³⁴, O. Biebel¹¹⁰, R. Bielski¹²⁷, N.V. Biesuz^{69a,69b}, M. Biglietti^{72a}, T.R.V. Billoud¹³⁷, M. Bindi⁵¹, A. Bingul^{11d}, C. Bini^{70a,70b}, S. Biondi^{21b,21a}, A. Biondini⁸⁸, C.J. Birch-sykes⁹⁷, G.A. Bird^{19,139}, M. Birman¹⁷⁵, T. Bisanz³⁴, J.P. Biswal², D. Biswas^{176,j}, A. Bitadze⁹⁷, C. Bittrich⁴⁶, K. Bjørke¹²⁹, I. Bloch⁴⁴, C. Blocker²⁴, A. Blue⁵⁵, U. Blumenschein⁹⁰, J. Blumenthal⁹⁶, G.J. Bobbink¹¹⁵, V.S. Bobrovnikov^{117b,117a}, M. Boehler⁵⁰, D. Bogavac¹², A.G. Bogdanchikov^{117b,117a}, C. Böhm^{43a}, V. Boisvert⁹¹, P. Bokan⁴⁴, T. Bold^{81a}, M. Bomben¹³¹, M. Bona⁹⁰, M. Boonekamp¹⁴⁰, C.D. Booth⁹¹, A.G. Borbély⁵⁵, H.M. Borecka-Bielska¹⁰⁶, L.S. Borgna⁹², G. Borissov⁸⁷, D. Bortoletto¹³⁰, D. Boscherini^{21b}, M. Bosman¹², J.D. Bossio Sola³⁴, K. Bouaouda^{33a}, J. Boudreau¹³⁴, E.V. Bouhova-Thacker⁸⁷, D. Boumediene³⁶, R. Bouquet¹³¹, A. Boveia¹²³, J. Boyd³⁴, D. Boye²⁷, I.R. Boyko⁷⁷, A.J. Bozson⁹¹, J. Bracinik¹⁹, N. Brahimi^{58d,58c}, G. Brandt¹⁷⁷, O. Brandt³⁰, F. Braren⁴⁴, B. Brau⁹⁹, J.E. Brau¹²⁷, W.D. Breaden Madden⁵⁵, K. Brendlinger⁴⁴, R. Brenner¹⁷⁵, L. Brenner³⁴, R. Brenner¹⁶⁷, S. Bressler¹⁷⁵, B. Brickwedde⁹⁶, D.L. Briglin¹⁹, D. Britton⁵⁵, D. Britzger¹¹¹, I. Brock²², R. Brock¹⁰³, G. Brooijmans³⁷, W.K. Brooks^{142e}, E. Brost²⁷, P.A. Bruckman de Renstrom⁸², B. Brüers⁴⁴, D. Bruncko^{26b}, A. Bruni^{21b}, G. Bruni^{21b}, M. Bruschi^{21b}, N. Bruscino^{70a,70b}, L. Bryngemark¹⁴⁹, T. Buanes¹⁵, Q. Buat¹⁵¹, P. Buchholz¹⁴⁷, A.G. Buckley⁵⁵, I.A. Budagov⁷⁷, M.K. Bugge¹²⁹, O. Bulekov¹⁰⁸, B.A. Bullard⁵⁷, S. Burdin⁸⁸, C.D. Burgard⁴⁴, A.M. Burger¹²⁵, B. Burghgrave⁷, J.T.P. Burr⁴⁴, C.D. Burton¹⁰, J.C. Burzynski¹⁴⁸, E.L. Busch³⁷, V. Büscher⁹⁶, P.J. Bussey⁵⁵, J.M. Butler²³, C.M. Buttar⁵⁵, J.M. Butterworth⁹², W. Buttinger¹³⁹, C.J. Buxo Vazquez¹⁰³, A.R. Buzykaev^{117b,117a}, G. Cabras^{21b}, S. Cabrera Urbán¹⁶⁹, D. Caforio⁵⁴, H. Cai¹³⁴, V.M.M. Cairo¹⁴⁹, O. Cakir^{3a}, N. Calace³⁴, P. Calafiura¹⁶, G. Calderini¹³¹, P. Calfayan⁶³, G. Callea⁵⁵, L.P. Caloba^{78b}, D. Calvet³⁶, S. Calvet³⁶, T.P. Calvet⁹⁸, M. Calvetti^{69a,69b}, R. Camacho Toro¹³¹, S. Camarda³⁴, D. Camarero Munoz⁹⁵, P. Camarri^{71a,71b}, M.T. Camerlingo^{72a,72b}, D. Cameron¹²⁹, C. Camincher¹⁷¹, M. Campanelli⁹², A. Camplani³⁸, V. Canale^{67a,67b}, A. Canesse¹⁰⁰, M. Cano Bret⁷⁵, J. Cantero¹²⁵, Y. Cao¹⁶⁸, F. Capocasa²⁴, M. Capua^{39b,39a},

A. Carbone^{66a,66b}, R. Cardarelli^{71a}, J.C.J. Cardenas⁷, F. Cardillo¹⁶⁹, G. Carducci^{39b,39a}, T. Carli³⁴,
 G. Carlino^{67a}, B.T. Carlson¹³⁴, E.M. Carlson^{171,163a}, L. Carminati^{66a,66b}, M. Carnesale^{70a,70b},
 R.M.D. Carney¹⁴⁹, S. Caron¹¹⁴, E. Carquin^{142e}, S. Carrá⁴⁴, G. Carratta^{21b,21a}, J.W.S. Carter¹⁶²,
 T.M. Carter⁴⁸, D. Casadei^{31c}, M.P. Casado^{12.g}, A.F. Casha¹⁶², E.G. Castiglia¹⁷⁸, F.L. Castillo^{59a},
 L. Castillo Garcia¹², V. Castillo Gimenez¹⁶⁹, N.F. Castro^{135a,135e}, A. Catinaccio³⁴, J.R. Catmore¹²⁹,
 A. Cattai³⁴, V. Cavaliere²⁷, N. Cavalli^{21b,21a}, V. Cavasinni^{69a,69b}, E. Celebi^{11b}, F. Celli¹³⁰,
 M.S. Centonze^{65a,65b}, K. Cerny¹²⁶, A.S. Cerqueira^{78a}, A. Cerri¹⁵², L. Cerrito^{71a,71b}, F. Cerutti¹⁶,
 A. Cervelli^{21b}, S.A. Cetin^{11b}, Z. Chadi^{33a}, D. Chakraborty¹¹⁶, M. Chala^{135f}, J. Chan¹⁷⁶, W.S. Chan¹¹⁵,
 W.Y. Chan⁸⁸, J.D. Chapman³⁰, B. Chargeishvili^{155b}, D.G. Charlton¹⁹, T.P. Charman⁹⁰, M. Chatterjee¹⁸,
 S. Chekanov⁵, S.V. Chekulaev^{163a}, G.A. Chelkov^{77,ae}, A. Chen¹⁰², B. Chen¹⁵⁷, B. Chen¹⁷¹, C. Chen^{58a},
 C.H. Chen⁷⁶, H. Chen^{13c}, H. Chen²⁷, J. Chen^{58c}, J. Chen²⁴, S. Chen¹³², S.J. Chen^{13c}, X. Chen^{58c},
 X. Chen^{13b}, Y. Chen^{58a}, Y.-H. Chen⁴⁴, C.L. Cheng¹⁷⁶, H.C. Cheng^{60a}, A. Cheplakov⁷⁷, E. Cheremushkina⁴⁴,
 E. Cherepanova⁷⁷, R. Cherkaoui El Moursli^{33e}, E. Cheu⁶, K. Cheung⁶¹, L. Chevalier¹⁴⁰, V. Chiarella⁴⁹,
 G. Chiarelli^{69a}, G. Chiodini^{65a}, A.S. Chisholm¹⁹, A. Chitan^{25b}, Y.H. Chiu¹⁷¹, M.V. Chizhov^{77,s}, K. Choi¹⁰,
 A.R. Chomont^{70a,70b}, Y. Chou⁹⁹, Y.S. Chow¹¹⁵, T. Chowdhury^{31f}, L.D. Christopher^{31f}, M.C. Chu^{60a},
 X. Chu^{13a,13d}, J. Chudoba¹³⁶, J.J. Chwastowski⁸², D. Cieri¹¹¹, K.M. Ciesla⁸², V. Cindro⁸⁹, I.A. Cioară^{25b},
 A. Ciocio¹⁶, F. Ciotto^{67a,67b}, Z.H. Citron^{175,k}, M. Citterio^{66a}, D.A. Ciubotaru^{25b}, B.M. Ciungu¹⁶²,
 A. Clark⁵², P.J. Clark⁴⁸, J.M. Clavijo Columbie⁴⁴, S.E. Clawson⁹⁷, C. Clement^{43a,43b}, L. Clissa^{21b,21a},
 Y. Coadou⁹⁸, M. Cobal^{64a,64c}, A. Coccaro^{53b}, J. Cochran⁷⁶, R.F. Coelho Barrue^{135a},
 R. Coelho Lopes De Sa⁹⁹, S. Coelli^{66a}, H. Cohen¹⁵⁷, A.E.C. Coimbra³⁴, B. Cole³⁷, J. Collot⁵⁶,
 P. Conde Muiño^{135a,135g}, S.H. Connell^{31c}, I.A. Connelly⁵⁵, E.I. Conroy¹³⁰, F. Conventi^{67a,ak}, H.G. Cooke¹⁹,
 A.M. Cooper-Sarkar¹³⁰, F. Cormier¹⁷⁰, L.D. Corpe³⁴, M. Corradi^{70a,70b}, E.E. Corrigan⁹⁴, F. Corriveau^{100,y},
 M.J. Costa¹⁶⁹, F. Costanza⁴, D. Costanzo¹⁴⁵, B.M. Cote¹²³, G. Cowan⁹¹, J.W. Cowley³⁰, K. Cranmer¹²¹,
 S. Crépe-Renaudin⁵⁶, F. Crescioli¹³¹, M. Cristinziani¹⁴⁷, M. Cristoforetti^{73a,73b,b}, V. Croft¹⁶⁵,
 G. Crosetti^{39b,39a}, A. Cueto³⁴, T. Cuhadar Donszelmann¹⁶⁶, H. Cui^{13a,13d}, A.R. Cukierman¹⁴⁹,
 W.R. Cunningham⁵⁵, F. Curcio^{39b,39a}, P. Czodrowski³⁴, M.M. Czurylo^{59b},
 M.J. Da Cunha Sargedas De Sousa^{58a}, J.V. Da Fonseca Pinto^{78b}, C. Da Via⁹⁷, W. Dabrowski^{81a}, T. Dado⁴⁵,
 S. Dahbi^{31f}, T. Dai¹⁰², C. Dallapiccola⁹⁹, M. Dam³⁸, G. D'amen²⁷, V. D'Amico^{72a,72b}, J. Damp⁹⁶,
 J.R. Dandoy¹³², M.F. Daneri²⁸, M. Danninger¹⁴⁸, V. Dao³⁴, G. Darbo^{53b}, S. Darmora⁵, A. Dattagupta¹²⁷,
 S. D'Auria^{66a,66b}, C. David^{163b}, T. Davidek¹³⁸, D.R. Davis⁴⁷, B. Davis-Purcell³², I. Dawson⁹⁰, K. De⁷,
 R. De Asmundis^{67a}, M. De Beurs¹¹⁵, S. De Castro^{21b,21a}, N. De Groot¹¹⁴, P. de Jong¹¹⁵, H. De la Torre¹⁰³,
 A. De Maria^{13c}, D. De Pedis^{70a}, A. De Salvo^{70a}, U. De Sanctis^{71a,71b}, M. De Santis^{71a,71b}, A. De Santo¹⁵²,
 J.B. De Vivie De Regie⁵⁶, D.V. Dedovich⁷⁷, J. Degens¹¹⁵, A.M. Deiana⁴⁰, J. Del Peso⁹⁵, Y. Delabat Diaz⁴⁴,
 F. Deliot¹⁴⁰, C.M. Delitzsch⁶, M. Della Pietra^{67a,67b}, D. Della Volpe⁵², A. Dell'Acqua³⁴, L. Dell'Asta^{66a,66b},
 M. Delmastro⁴, P.A. Delsart⁵⁶, S. Demers¹⁷⁸, M. Demichev⁷⁷, S.P. Denisov¹¹⁸, L. D'Eramo¹¹⁶,
 D. Derendarz⁸², J.E. Derkaoui^{33d}, F. Derue¹³¹, P. Dervan⁸⁸, K. Desch²², K. Dette¹⁶², C. Deutsch²²,
 P.O. Deviveiros³⁴, F.A. Di Bello^{70a,70b}, A. Di Ciaccio^{71a,71b}, L. Di Ciaccio⁴, A. Di Domenico^{70a,70b},
 C. Di Donato^{67a,67b}, A. Di Girolamo³⁴, G. Di Gregorio^{69a,69b}, A. Di Luca^{73a,73b}, B. Di Micco^{72a,72b},
 R. Di Nardo^{72a,72b}, C. Diaconu⁹⁸, F.A. Dias¹¹⁵, T. Dias Do Vale^{135a}, M.A. Diaz^{142a}, F.G. Diaz Capriles²²,
 J. Dickinson¹⁶, M. Didenko¹⁶⁹, E.B. Diehl¹⁰², J. Dietrich¹⁷, S. Díez Cornell⁴⁴, C. Diez Pardos¹⁴⁷,
 A. Dimitrievska¹⁶, W. Ding^{13b}, J. Dingfelder²², I.-M. Dinu^{25b}, S.J. Dittmeier^{59b}, F. Dittus³⁴, F. Djama⁹⁸,
 T. Djobava^{155b}, J.I. Djuvsland¹⁵, M.A.B. Do Vale¹⁴³, D. Dodsworth²⁴, C. Doglioni⁹⁴, J. Dolejsi¹³⁸,
 Z. Dolezal¹³⁸, M. Donadelli^{78c}, B. Dong^{58c}, J. Donini³⁶, A. D'onofrio^{13c}, M. D'Onofrio⁸⁸, J. Dopke¹³⁹,
 A. Doria^{67a}, M.T. Dova⁸⁶, A.T. Doyle⁵⁵, E. Drechsler¹⁴⁸, E. Dreyer¹⁴⁸, T. Dreyer⁵¹, A.S. Drobac¹⁶⁵,
 D. Du^{58a}, T.A. du Pree¹¹⁵, F. Dubinin¹⁰⁷, M. Dubovsky^{26a}, A. Dubreuil⁵², E. Duchovni¹⁷⁵, G. Duckeck¹¹⁰,
 O.A. Ducu^{34,25b}, D. Duda¹¹¹, A. Dudarev³⁴, M. D'uffizi⁹⁷, L. Duflot⁶², M. Dührssen³⁴, C. Dülse¹⁷⁷,
 A.E. Dumitriu^{25b}, M. Dunford^{59a}, S. Dungs⁴⁵, K. Dunne^{43a,43b}, A. Duperrin⁹⁸, H. Duran Yildiz^{3a},
 M. Düren⁵⁴, A. Durglishvili^{155b}, B. Dutta⁴⁴, B.L. Dwyer¹¹⁶, G.I. Dyckes¹⁶, M. Dyndal^{81a}, S. Dysch⁹⁷,
 B.S. Dziedzic⁸², B. Eckerova^{26a}, M.G. Eggleston⁴⁷, E. Egidio Purcino De Souza^{78b}, L.F. Ehrke⁵², T. Eifert⁷,
 G. Eigen¹⁵, K. Einsweiler¹⁶, T. Ekelof¹⁶⁷, Y. El Ghazali^{33b}, H. El Jarrari^{33e}, A. El Moussaouy^{33a},
 V. Ellajosyula¹⁶⁷, M. Ellert¹⁶⁷, F. Ellinghaus¹⁷⁷, A.A. Elliot⁹⁰, N. Ellis³⁴, J. Elmsheuser²⁷, M. Elsing³⁴,
 D. Emelianov¹³⁹, A. Emerman³⁷, Y. Enari¹⁵⁹, J. Erdmann⁴⁵, A. Ereditato¹⁸, P.A. Erland⁸², M. Errenst¹⁷⁷,
 M. Escalier⁶², C. Escobar¹⁶⁹, O. Estrada Pastor¹⁶⁹, E. Etzion¹⁵⁷, G. Evans^{135a}, H. Evans⁶³, M.O. Evans¹⁵²,

A. Ezhilov ¹³³, F. Fabbri ⁵⁵, L. Fabbri ^{21b,21a}, G. Facini ¹⁷³, V. Fadeyev ¹⁴¹, R.M. Fakhruddinov ¹¹⁸,
 S. Falciano ^{70a}, P.J. Falke ²², S. Falke ³⁴, J. Faltova ¹³⁸, Y. Fan ^{13a}, Y. Fang ^{13a}, G. Fanourakis ⁴²,
 M. Fanti ^{66a,66b}, M. Faraj ^{58c}, A. Farbin ⁷, A. Farilla ^{72a}, E.M. Farina ^{68a,68b}, T. Farooque ¹⁰³,
 S.M. Farrington ⁴⁸, P. Farthouat ³⁴, F. Fassi ^{33e}, D. Fassouliotis ⁸, M. Faucci Giannelli ^{71a,71b}, W.J. Fawcett ³⁰,
 L. Fayard ⁶², O.L. Fedin ^{133,p}, M. Feickert ¹⁶⁸, L. Feligioni ⁹⁸, A. Fell ¹⁴⁵, C. Feng ^{58b}, M. Feng ^{13b},
 M.J. Fenton ¹⁶⁶, A.B. Fenyuk ¹¹⁸, S.W. Ferguson ⁴¹, J. Ferrando ⁴⁴, A. Ferrari ¹⁶⁷, P. Ferrari ¹¹⁵, R. Ferrari ^{68a},
 D. Ferrere ⁵², C. Ferretti ¹⁰², F. Fiedler ⁹⁶, A. Filipčič ⁸⁹, F. Filthaut ¹¹⁴, M.C.N. Fiolhais ^{135a,135c,a},
 L. Fiorini ¹⁶⁹, F. Fischer ¹⁴⁷, W.C. Fisher ¹⁰³, T. Fitschen ¹⁹, I. Fleck ¹⁴⁷, P. Fleischmann ¹⁰², T. Flick ¹⁷⁷,
 B.M. Flierl ¹¹⁰, L. Flores ¹³², M. Flores ^{31d}, L.R. Flores Castillo ^{60a}, F.M. Follega ^{73a,73b}, N. Fomin ¹⁵,
 J.H. Foo ¹⁶², B.C. Forland ⁶³, A. Formica ¹⁴⁰, F.A. Förster ¹², A.C. Forti ⁹⁷, E. Fortin ⁹⁸, M.G. Foti ¹³⁰,
 L. Fountas ⁸, D. Fournier ⁶², H. Fox ⁸⁷, P. Francavilla ^{69a,69b}, S. Francescato ⁵⁷, M. Franchini ^{21b,21a},
 S. Franchino ^{59a}, D. Francis ³⁴, L. Franco ⁴, L. Franconi ¹⁸, M. Franklin ⁵⁷, G. Frattari ^{70a,70b}, A.C. Freegard ⁹⁰,
 P.M. Freeman ¹⁹, W.S. Freund ^{78b}, E.M. Freundlich ⁴⁵, D. Froidevaux ³⁴, J.A. Frost ¹³⁰, Y. Fu ^{58a},
 M. Fujimoto ¹²², E. Fullana Torregrosa ¹⁶⁹, J. Fuster ¹⁶⁹, A. Gabrielli ^{21b,21a}, A. Gabrielli ³⁴, P. Gadow ⁴⁴,
 G. Gagliardi ^{53b,53a}, L.G. Gagnon ¹⁶, G.E. Gallardo ¹³⁰, E.J. Gallas ¹³⁰, B.J. Gallop ¹³⁹, R. Gamboa Goni ⁹⁰,
 K.K. Gan ¹²³, S. Ganguly ¹⁵⁹, J. Gao ^{58a}, Y. Gao ⁴⁸, Y.S. Gao ^{29,m}, F.M. Garay Walls ^{142a}, C. García ¹⁶⁹,
 J.E. García Navarro ¹⁶⁹, J.A. García Pascual ^{13a}, M. Garcia-Sciveres ¹⁶, R.W. Gardner ³⁵, D. Garg ⁷⁵,
 R.B. Garg ¹⁴⁹, S. Gargiulo ⁵⁰, C.A. Garner ¹⁶², V. Garonne ¹²⁹, S.J. Gasiorowski ¹⁴⁴, P. Gaspar ^{78b},
 G. Gaudio ^{68a}, P. Gauzzi ^{70a,70b}, I.L. Gavrilenko ¹⁰⁷, A. Gavrilyuk ¹¹⁹, C. Gay ¹⁷⁰, G. Gaycken ⁴⁴, E.N. Gazis ⁹,
 A.A. Geanta ^{25b}, C.M. Gee ¹⁴¹, C.N.P. Gee ¹³⁹, J. Geisen ⁹⁴, M. Geisen ⁹⁶, C. Gemme ^{53b}, M.H. Genest ⁵⁶,
 S. Gentile ^{70a,70b}, S. George ⁹¹, W.F. George ¹⁹, T. Gerialis ⁴², L.O. Gerlach ⁵¹, P. Gessinger-Befurt ³⁴,
 M. Ghasemi Bostanabad ¹⁷¹, A. Ghosh ¹⁶⁶, A. Ghosh ⁷⁵, B. Giacobbe ^{21b}, S. Giagu ^{70a,70b},
 N. Giangiacomi ¹⁶², P. Giannetti ^{69a}, A. Giannini ^{67a,67b}, S.M. Gibson ⁹¹, M. Gignac ¹⁴¹, D.T. Gil ^{81b},
 B.J. Gilbert ³⁷, D. Gillberg ³², G. Gilles ¹¹⁵, N.E.K. Gillwald ⁴⁴, D.M. Gingrich ^{2,aj}, M.P. Giordani ^{64a,64c},
 P.F. Giraud ¹⁴⁰, G. Giugliarelli ^{64a,64c}, D. Giugni ^{66a}, F. Giuli ^{71a,71b}, I. Gkialas ^{8,h}, P. Gkoutoumis ⁹,
 L.K. Gladilin ¹⁰⁹, C. Glasman ⁹⁵, G.R. Gledhill ¹²⁷, M. Glisic ¹²⁷, I. Gnesi ^{39b,d}, M. Goblirsch-Kolb ²⁴,
 D. Godin ¹⁰⁶, S. Goldfarb ¹⁰¹, T. Golling ⁵², D. Golubkov ¹¹⁸, J.P. Gombas ¹⁰³, A. Gomes ^{135a,135b},
 R. Goncalves Gama ⁵¹, R. Gonçalves ^{135a,135c}, G. Gonella ¹²⁷, L. Gonella ¹⁹, A. Gongadze ⁷⁷, F. Gonnella ¹⁹,
 J.L. Gonski ³⁷, S. González de la Hoz ¹⁶⁹, S. Gonzalez Fernandez ¹², R. Gonzalez Lopez ⁸⁸,
 C. Gonzalez Renteria ¹⁶, R. Gonzalez Suarez ¹⁶⁷, S. Gonzalez-Sevilla ⁵², G.R. Gonzalvo Rodriguez ¹⁶⁹,
 R.Y. González Andana ^{142a}, L. Goossens ³⁴, N.A. Gorasia ¹⁹, P.A. Gorbounov ¹¹⁹, H.A. Gordon ²⁷, B. Gorini ³⁴,
 E. Gorini ^{65a,65b}, A. Gorišek ⁸⁹, A.T. Goshaw ⁴⁷, M.I. Gostkin ⁷⁷, C.A. Gottardo ¹¹⁴, M. Gouighri ^{33b},
 V. Goumarre ⁴⁴, A.G. Goussiou ¹⁴⁴, N. Govender ^{31c}, C. Goy ⁴, I. Grabowska-Bold ^{81a}, K. Graham ³²,
 E. Gramstad ¹²⁹, S. Grancagnolo ¹⁷, M. Grandi ¹⁵², V. Gratchev ¹³³, P.M. Gravila ^{25f}, F.G. Gravili ^{65a,65b},
 H.M. Gray ¹⁶, C. Greife ²², I.M. Gregor ⁴⁴, P. Grenier ¹⁴⁹, K. Grevtsov ⁴⁴, C. Grieco ¹², N.A. Grieser ¹²⁴,
 A.A. Grillo ¹⁴¹, K. Grimm ^{29,l}, S. Grinstein ^{12,v}, J.-F. Grivaz ⁶², S. Groh ⁹⁶, E. Gross ¹⁷⁵, J. Grosse-Knetter ⁵¹,
 C. Grud ¹⁰², A. Grummer ¹¹³, J.C. Grundy ¹³⁰, L. Guan ¹⁰², W. Guan ¹⁷⁶, C. Gubbels ¹⁷⁰, J. Guenther ³⁴,
 J.G.R. Guerrero Rojas ¹⁶⁹, F. Guescini ¹¹¹, D. Guest ¹⁷, R. Gugel ⁹⁶, A. Guida ⁴⁴, T. Guillemain ⁴, S. Guindon ³⁴,
 J. Guo ^{58c}, L. Guo ⁶², Y. Guo ¹⁰², R. Gupta ⁴⁴, S. Gurbuz ²², G. Gustavino ¹²⁴, M. Guth ⁵², P. Gutierrez ¹²⁴,
 L.F. Gutierrez Zagazeta ¹³², C. Gutschow ⁹², C. Guyot ¹⁴⁰, C. Gwenlan ¹³⁰, C.B. Gwilliam ⁸⁸, E.S. Haaland ¹²⁹,
 A. Haas ¹²¹, M. Habedank ⁴⁴, C. Haber ¹⁶, H.K. Hadavand ⁷, A. Hadeef ⁹⁶, S. Hadzic ¹¹¹, M. Haleem ¹⁷²,
 J. Haley ¹²⁵, J.J. Hall ¹⁴⁵, G. Halladjian ¹⁰³, G.D. Hallewell ⁹⁸, L. Halser ¹⁸, K. Hamano ¹⁷¹, H. Hamdaoui ^{33e},
 M. Hamer ²², G.N. Hamity ⁴⁸, K. Han ^{58a}, L. Han ^{13c}, L. Han ^{58a}, S. Han ¹⁶, Y.F. Han ¹⁶², K. Hanagaki ^{79,t},
 M. Hance ¹⁴¹, M.D. Hank ³⁵, R. Hankache ⁹⁷, E. Hansen ⁹⁴, J.B. Hansen ³⁸, J.D. Hansen ³⁸, M.C. Hansen ²²,
 P.H. Hansen ³⁸, K. Hara ¹⁶⁴, T. Harenberg ¹⁷⁷, S. Harkusha ¹⁰⁴, Y.T. Harris ¹³⁰, P.F. Harrison ¹⁷³,
 N.M. Hartman ¹⁴⁹, N.M. Hartmann ¹¹⁰, Y. Hasegawa ¹⁴⁶, A. Hasib ⁴⁸, S. Hassani ¹⁴⁰, S. Haug ¹⁸,
 R. Hauser ¹⁰³, M. Havranek ¹³⁷, C.M. Hawkes ¹⁹, R.J. Hawkins ³⁴, S. Hayashida ¹¹², D. Hayden ¹⁰³,
 C. Hayes ¹⁰², R.L. Hayes ¹⁷⁰, C.P. Hays ¹³⁰, J.M. Hays ⁹⁰, H.S. Hayward ⁸⁸, S.J. Haywood ¹³⁹, F. He ^{58a},
 Y. He ¹⁶⁰, Y. He ¹³¹, M.P. Heath ⁴⁸, V. Hedberg ⁹⁴, A.L. Heggelund ¹²⁹, N.D. Hehir ⁹⁰, C. Heidegger ⁵⁰,
 K.K. Heidegger ⁵⁰, W.D. Heidorn ⁷⁶, J. Heilman ³², S. Heim ⁴⁴, T. Heim ¹⁶, B. Heinemann ^{44,ah},
 J.G. Heinlein ¹³², J.J. Heinrich ¹²⁷, L. Heinrich ³⁴, J. Hejbal ¹³⁶, L. Helary ⁴⁴, A. Held ¹²¹, C.M. Helling ¹⁴¹,
 S. Hellman ^{43a,43b}, C. Helsens ³⁴, R.C.W. Henderson ⁸⁷, L. Henkelmann ³⁰, A.M. Henriques Correia ³⁴,
 H. Herde ¹⁴⁹, Y. Hernández Jiménez ¹⁵¹, H. Herr ⁹⁶, M.G. Herrmann ¹¹⁰, T. Herrmann ⁴⁶, G. Herten ⁵⁰,

R. Hertenberger¹¹⁰, L. Hervas³⁴, N.P. Hessey^{163a}, H. Hibi⁸⁰, S. Higashino⁷⁹, E. Higón-Rodríguez¹⁶⁹, K.H. Hiller⁴⁴, S.J. Hillier¹⁹, M. Hils⁴⁶, I. Hinchliffe¹⁶, F. Hinterkeuser²², M. Hirose¹²⁸, S. Hirose¹⁶⁴, D. Hirschbuehl¹⁷⁷, B. Hiti⁸⁹, O. Hladik¹³⁶, J. Hobbs¹⁵¹, R. Hobincu^{25e}, N. Hod¹⁷⁵, M.C. Hodgkinson¹⁴⁵, B.H. Hodgkinson³⁰, A. Hoecker³⁴, J. Hofer⁴⁴, D. Hohn⁵⁰, T. Holm²², T.R. Holmes³⁵, M. Holzbock¹¹¹, L.B.A.H. Hommels³⁰, B.P. Honan⁹⁷, J. Hong^{58c}, T.M. Hong¹³⁴, Y. Hong⁵¹, J.C. Honig⁵⁰, A. Hönle¹¹¹, B.H. Hooberman¹⁶⁸, W.H. Hopkins⁵, Y. Horii¹¹², L.A. Horyn³⁵, S. Hou¹⁵⁴, J. Howarth⁵⁵, J. Hoya⁸⁶, M. Hrabovsky¹²⁶, A. Hrynevich¹⁰⁵, T. Hryn'ova⁴, P.J. Hsu⁶¹, S.-C. Hsu¹⁴⁴, Q. Hu³⁷, S. Hu^{58c}, Y.F. Hu^{13a,13d,al}, D.P. Huang⁹², X. Huang^{13c}, Y. Huang^{58a}, Y. Huang^{13a}, Z. Hubacek¹³⁷, F. Hubaut⁹⁸, M. Huebner²², F. Huegging²², T.B. Huffman¹³⁰, M. Huhtinen³⁴, S.K. Huiberts¹⁵, R. Hulskens⁵⁶, N. Huseynov^{77,z}, J. Huston¹⁰³, J. Huth⁵⁷, R. Hyneman¹⁴⁹, S. Hyrych^{26a}, G. Iacobucci⁵², G. Iakovidis²⁷, I. Ibragimov¹⁴⁷, L. Iconomidou-Fayard⁶², P. Iengo³⁴, R. Iguchi¹⁵⁹, T. Iizawa⁵², Y. Ikegami⁷⁹, A. Ilg¹⁸, N. Ilic¹⁶², H. Imam^{33a}, T. Ingebretsen Carlson^{43a,43b}, G. Introzzi^{68a,68b}, M. Iodice^{72a}, V. Ippolito^{70a,70b}, M. Ishino¹⁵⁹, W. Islam¹⁷⁶, C. Issever^{17,44}, S. Istin^{11c,am}, J.M. Iturbe Ponce^{60a}, R. Iuppa^{73a,73b}, A. Ivina¹⁷⁵, J.M. Izen⁴¹, V. Izzo^{67a}, P. Jacka¹³⁶, P. Jackson¹, R.M. Jacobs⁴⁴, B.P. Jaeger¹⁴⁸, C.S. Jagfeld¹¹⁰, G. Jäkel¹⁷⁷, K. Jakobs⁵⁰, T. Jakoubek¹⁷⁵, J. Jamieson⁵⁵, K.W. Janas^{81a}, G. Jarlskog⁹⁴, A.E. Jaspan⁸⁸, N. Javadov^{77,z}, T. Javůrek³⁴, M. Javurkova⁹⁹, F. Jeanneau¹⁴⁰, L. Jeanty¹²⁷, J. Jejelava^{155a,aa}, P. Jenni^{50,e}, S. Jézéquel⁴, J. Jia¹⁵¹, Z. Jia^{13c}, Y. Jiang^{58a}, S. Jiggins⁴⁸, J. Jimenez Pena¹¹¹, S. Jin^{13c}, A. Jinaru^{25b}, O. Jinnouchi¹⁶⁰, H. Jivan^{31f}, P. Johansson¹⁴⁵, K.A. Johns⁶, C.A. Johnson⁶³, D.M. Jones³⁰, E. Jones¹⁷³, R.W.L. Jones⁸⁷, T.J. Jones⁸⁸, J. Jovicevic¹⁴, X. Ju¹⁶, J.J. Junggeburth³⁴, A. Juste Rozas^{12,v}, S. Kabana^{142d}, A. Kaczmarska⁸², M. Kado^{70a,70b}, H. Kagan¹²³, M. Kagan¹⁴⁹, A. Kahn³⁷, A. Kahn¹³², C. Kahra⁹⁶, T. Kaji¹⁷⁴, E. Kajomovitz¹⁵⁶, C.W. Kalderon²⁷, A. Kamenshchikov¹¹⁸, M. Kaneda¹⁵⁹, N.J. Kang¹⁴¹, S. Kang⁷⁶, Y. Kano¹¹², D. Kar^{31f}, K. Karava¹³⁰, M.J. Kareem^{163b}, I. Karkanas¹⁵⁸, S.N. Karpov⁷⁷, Z.M. Karpova⁷⁷, V. Kartvelishvili⁸⁷, A.N. Karyukhin¹¹⁸, E. Kasimi¹⁵⁸, C. Kato^{58d}, J. Katzy⁴⁴, K. Kawade¹⁴⁶, K. Kawagoe⁸⁵, T. Kawaguchi¹¹², T. Kawamoto¹⁴⁰, G. Kawamura⁵¹, E.F. Kay¹⁷¹, F.I. Kaya¹⁶⁵, S. Kazakos¹², V.F. Kazanin^{117b,117a}, Y. Ke¹⁵¹, J.M. Keaveney^{31a}, R. Keeler¹⁷¹, J.S. Keller³², A.S. Kelly⁹², D. Kelsey¹⁵², J.J. Kempster¹⁹, J. Kendrick¹⁹, K.E. Kennedy³⁷, O. Kepka¹³⁶, S. Kersten¹⁷⁷, B.P. Kerševan⁸⁹, S. Ketabchi Haghighat¹⁶², M. Khandoga¹³¹, A. Khanov¹²⁵, A.G. Kharlamov^{117b,117a}, T. Kharlamova^{117b,117a}, E.E. Khoda¹⁴⁴, T.J. Khoo¹⁷, G. Khorauli¹⁷², E. Khramov⁷⁷, J. Khubua^{155b}, S. Kido⁸⁰, M. Kiehn³⁴, A. Kilgallon¹²⁷, E. Kim¹⁶⁰, Y.K. Kim³⁵, N. Kimura⁹², A. Kirchhoff⁵¹, D. Kirchmeier⁴⁶, C. Kirfel²², J. Kirk¹³⁹, A.E. Kiryunin¹¹¹, T. Kishimoto¹⁵⁹, D.P. Kisliuk¹⁶², C. Kitsaki⁹, O. Kivernyk²², T. Klapdor-Kleingrothaus⁵⁰, M. Klassen^{59a}, C. Klein³², L. Klein¹⁷², M.H. Klein¹⁰², M. Klein⁸⁸, U. Klein⁸⁸, P. Klimek³⁴, A. Klimentov²⁷, F. Klimpel¹¹¹, T. Klingl²², T. Klioutchnikova³⁴, F.F. Klitzner¹¹⁰, P. Kluit¹¹⁵, S. Kluth¹¹¹, E. Kneringer⁷⁴, T.M. Knight¹⁶², A. Knue⁵⁰, D. Kobayashi⁸⁵, R. Kobayashi⁸³, M. Kobel⁴⁶, M. Kocian¹⁴⁹, T. Kodama¹⁵⁹, P. Kodys¹³⁸, D.M. Koeck¹⁵², P.T. Koenig²², T. Koffas³², N.M. Köhler³⁴, M. Kolb¹⁴⁰, I. Koletsou⁴, T. Komarek¹²⁶, K. Köneke⁵⁰, A.X.Y. Kong¹, T. Kono¹²², V. Konstantinides⁹², N. Konstantinidis⁹², B. Konya⁹⁴, R. Kopeliansky⁶³, S. Koperny^{81a}, K. Korcyl⁸², K. Kordas¹⁵⁸, G. Koren¹⁵⁷, A. Korn⁹², S. Korn⁵¹, I. Korolkov¹², E.V. Korolkova¹⁴⁵, N. Korotkova¹⁰⁹, B. Kortman¹¹⁵, O. Kortner¹¹¹, S. Kortner¹¹¹, W.H. Kostecka¹¹⁶, V.V. Kostyukhin^{147,161}, A. Kotsokechagia⁶², A. Kotwal⁴⁷, A. Koulouris³⁴, A. Kourkoumeli-Charalampidi^{68a,68b}, C. Kourkoumelis⁸, E. Kourlitis⁵, O. Kovanda¹⁵², R. Kowalewski¹⁷¹, W. Kozanecki¹⁴⁰, A.S. Kozhin¹¹⁸, V.A. Kramarenko¹⁰⁹, G. Kramberger⁸⁹, P. Kramer⁹⁶, D. Krasnopevtsev^{58a}, M.W. Krasny¹³¹, A. Krasznahorkay³⁴, J.A. Kremer⁹⁶, J. Kretzschmar⁸⁸, K. Kreul¹⁷, P. Krieger¹⁶², F. Krieter¹¹⁰, S. Krishnamurthy⁹⁹, A. Krishnan^{59b}, M. Krivos¹³⁸, K. Krizka¹⁶, K. Kroeninger⁴⁵, H. Kroha¹¹¹, J. Kroll¹³⁶, J. Kroll¹³², K.S. Krowpman¹⁰³, U. Kruchonak⁷⁷, H. Krüger²², N. Krumnack⁷⁶, M.C. Kruse⁴⁷, J.A. Krzysiak⁸², A. Kubota¹⁶⁰, O. Kuchinskaia¹⁶¹, S. Kudah^{3a}, D. Kuechler⁴⁴, J.T. Kuechler⁴⁴, S. Kuehn³⁴, T. Kuhl⁴⁴, V. Kukhtin⁷⁷, Y. Kulchitsky^{104,ad}, S. Kuleshov^{142c}, M. Kumar^{31f}, N. Kumari⁹⁸, M. Kuna⁵⁶, A. Kupco¹³⁶, T. Kupfer⁴⁵, O. Kuprash⁵⁰, H. Kurashige⁸⁰, L.L. Kurchaninov^{163a}, Y.A. Kurochkin¹⁰⁴, A. Kurova¹⁰⁸, M.G. Kurth^{13a,13d}, E.S. Kuwertz³⁴, M. Kuze¹⁶⁰, A.K. Kvam¹⁴⁴, J. Kvita¹²⁶, T. Kwan¹⁰⁰, K.W. Kwok^{60a}, C. Lacasta¹⁶⁹, F. Lacava^{70a,70b}, H. Lacker¹⁷, D. Lacour¹³¹, N.N. Lad⁹², E. Ladygin⁷⁷, R. Lafaye⁴, B. Laforge¹³¹, T. Lagouri^{142d}, S. Lai⁵¹, I.K. Lakomic^{81a}, N. Lalloue⁵⁶, J.E. Lambert¹²⁴, S. Lammers⁶³, W. Lampl⁶, C. Lampoudis¹⁵⁸, E. Lançon²⁷, U. Landgraf⁵⁰, M.P.J. Landon⁹⁰, V.S. Lang⁵⁰, J.C. Lange⁵¹, R.J. Langenberg⁹⁹, A.J. Lankford¹⁶⁶, F. Lanni²⁷, K. Lantzsch²², A. Lanza^{68a}, A. Lapertosa^{53b,53a}, J.F. Laporte¹⁴⁰, T. Lari^{66a}, F. Lasagni Manghi^{21b}, M. Lassnig³⁴, V. Latonova¹³⁶, T.S. Lau^{60a}, A. Laudrain⁹⁶

A. Laurier³², M. Lavorgna^{67a,67b}, S.D. Lawlor⁹¹, Z. Lawrence⁹⁷, M. Lazzaroni^{66a,66b}, B. Le⁹⁷, B. Leban⁸⁹,
 A. Lebedev⁷⁶, M. LeBlanc³⁴, T. LeCompte⁵, F. Ledroit-Guillon⁵⁶, A.C.A. Lee⁹², G.R. Lee¹⁵, L. Lee⁵⁷,
 S.C. Lee¹⁵⁴, S. Lee⁷⁶, L.L. Leeuw^{31c}, B. Lefebvre^{163a}, H.P. Lefebvre⁹¹, M. Lefebvre¹⁷¹, C. Leggett¹⁶,
 K. Lehmann¹⁴⁸, N. Lehmann¹⁸, G. Lehmann Miotto³⁴, W.A. Leight⁴⁴, A. Leisos^{158,u}, M.A.L. Leite^{78c},
 C.E. Leitgeb⁴⁴, R. Leitner¹³⁸, K.J.C. Leney⁴⁰, T. Lenz²², S. Leone^{69a}, C. Leonidopoulos⁴⁸, A. Leopold¹⁵⁰,
 C. Leroy¹⁰⁶, R. Les¹⁰³, C.G. Lester³⁰, M. Levchenko¹³³, J. Levêque⁴, D. Levin¹⁰², L.J. Levinson¹⁷⁵,
 D.J. Lewis¹⁹, B. Li^{13b}, B. Li^{58b}, C. Li^{58a}, C-Q. Li^{58c,58d}, H. Li^{58a}, H. Li^{58b}, H. Li^{58b}, J. Li^{58c}, K. Li¹⁴⁴,
 L. Li^{58c}, M. Li^{13a,13d}, Q.Y. Li^{58a}, S. Li^{58d,58c,c}, T. Li^{58b}, X. Li⁴⁴, Y. Li⁴⁴, Z. Li^{58b}, Z. Li¹³⁰, Z. Li¹⁰⁰, Z. Li⁸⁸,
 Z. Liang^{13a}, M. Liberatore⁴⁴, B. Liberti^{71a}, K. Lie^{60c}, J. Lieber Marin^{78b}, K. Lin¹⁰³, R.A. Linck⁶³,
 R.E. Lindley⁶, J.H. Lindon², A. Linss⁴⁴, E. Lipeles¹³², A. Lipniacka¹⁵, T.M. Liss^{168,ai}, A. Lister¹⁷⁰,
 J.D. Little⁷, B. Liu^{13a}, B.X. Liu¹⁴⁸, J.B. Liu^{58a}, J.K.K. Liu³⁵, K. Liu^{58d,58c}, M. Liu^{58a}, M.Y. Liu^{58a}, P. Liu^{13a},
 X. Liu^{58a}, Y. Liu⁴⁴, Y. Liu^{13c,13d}, Y.L. Liu¹⁰², Y.W. Liu^{58a}, M. Livan^{68a,68b}, J. Llorente Merino¹⁴⁸,
 S.L. Lloyd⁹⁰, E.M. Lobodzinska⁴⁴, P. Loch⁶, S. Loffredo^{71a,71b}, T. Lohse¹⁷, K. Lohwasser¹⁴⁵,
 M. Lokajicek¹³⁶, J.D. Long¹⁶⁸, I. Longarini^{70a,70b}, L. Longo³⁴, R. Longo¹⁶⁸, I. Lopez Paz¹²,
 A. Lopez Solis⁴⁴, J. Lorenz¹¹⁰, N. Lorenzo Martinez⁴, A.M. Lory¹¹⁰, A. Lösle⁵⁰, X. Lou^{43a,43b}, X. Lou^{13a},
 A. Lounis⁶², J. Love⁵, P.A. Love⁸⁷, J.J. Lozano Bahilo¹⁶⁹, G. Lu^{13a}, M. Lu^{58a}, S. Lu¹³², Y.J. Lu⁶¹,
 H.J. Lubatti¹⁴⁴, C. Luci^{70a,70b}, F.L. Lucio Alves^{13c}, A. Lucotte⁵⁶, F. Luehring⁶³, I. Luise¹⁵¹, L. Luminari^{70a},
 O. Lundberg¹⁵⁰, B. Lund-Jensen¹⁵⁰, N.A. Luongo¹²⁷, M.S. Lutz¹⁵⁷, D. Lynn²⁷, H. Lyons⁸⁸, R. Lysak¹³⁶,
 E. Lytken⁹⁴, F. Lyu^{13a}, V. Lyubushkin⁷⁷, T. Lyubushkina⁷⁷, H. Ma²⁷, L.L. Ma^{58b}, Y. Ma⁹²,
 D.M. Mac Donell¹⁷¹, G. Maccarrone⁴⁹, C.M. Macdonald¹⁴⁵, J.C. MacDonald¹⁴⁵, R. Madar³⁶,
 W.F. Mader⁴⁶, M. Madugoda Ralalage Don¹²⁵, N. Madysa⁴⁶, J. Maeda⁸⁰, T. Maeno²⁷, M. Maerker⁴⁶,
 V. Magerl⁵⁰, J. Magro^{64a,64c}, D.J. Mahon³⁷, C. Maidantchik^{78b}, A. Maio^{135a,135b,135d}, K. Maj^{81a},
 O. Majersky^{26a}, S. Majewski¹²⁷, N. Makovec⁶², V. Maksimovic¹⁴, B. Malaescu¹³¹, Pa. Malecki⁸²,
 V.P. Maleev¹³³, F. Malek⁵⁶, D. Malito^{39b,39a}, U. Mallik⁷⁵, C. Malone³⁰, S. Maltezos⁹, S. Malyukov⁷⁷,
 J. Mamuzic¹⁶⁹, G. Mancini⁴⁹, J.P. Mandalia⁹⁰, I. Mandić⁸⁹, L. Manhaes de Andrade Filho^{78a},
 I.M. Maniatis¹⁵⁸, M. Manisha¹⁴⁰, J. Manjarres Ramos⁴⁶, K.H. Mankinen⁹⁴, A. Mann¹¹⁰, A. Manousos⁷⁴,
 B. Mansoulie¹⁴⁰, I. Mantos¹⁵⁸, S. Manzoni¹¹⁵, A. Marantis^{158,u}, G. Marchiori¹³¹, M. Marcisovsky¹³⁶,
 L. Marcoccia^{71a,71b}, C. Marcon⁹⁴, M. Marjanovic¹²⁴, Z. Marshall¹⁶, S. Marti-Garcia¹⁶⁹, T.A. Martin¹⁷³,
 V.J. Martin⁴⁸, B. Martin dit Latour¹⁵, L. Martinelli^{70a,70b}, M. Martinez^{12,v}, P. Martinez Agullo¹⁶⁹,
 V.I. Martinez Outschoorn⁹⁹, S. Martin-Haugh¹³⁹, V.S. Martoiu^{25b}, A.C. Martyniuk⁹², A. Marzin³⁴,
 S.R. Maschek¹¹¹, L. Masetti⁹⁶, T. Mashimo¹⁵⁹, J. Masik⁹⁷, A.L. Maslennikov^{117b,117a}, L. Massa^{21b},
 P. Massarotti^{67a,67b}, P. Mastrandrea^{69a,69b}, A. Mastroberardino^{39b,39a}, T. Masubuchi¹⁵⁹, D. Matakias²⁷,
 T. Mathisen¹⁶⁷, A. Matic¹¹⁰, N. Matsuzawa¹⁵⁹, J. Maurer^{25b}, B. Maček⁸⁹, D.A. Maximov^{117b,117a},
 R. Mazini¹⁵⁴, I. Maznas¹⁵⁸, S.M. Mazza¹⁴¹, C. Mc Ginn²⁷, J.P. Mc Gowan¹⁰⁰, S.P. Mc Kee¹⁰²,
 T.G. McCarthy¹¹¹, W.P. McCormack¹⁶, E.F. McDonald¹⁰¹, A.E. McDougall¹¹⁵, J.A. MCFayden¹⁵²,
 G. Mchedlidze^{155b}, M.A. McKay⁴⁰, K.D. McLean¹⁷¹, S.J. McMahon¹³⁹, P.C. McNamara¹⁰¹,
 R.A. McPherson^{171,y}, J.E. Mdhului^{31f}, Z.A. Meadows⁹⁹, S. Meehan³⁴, T. Megy³⁶, S. Mehlhase¹¹⁰,
 A. Mehta⁸⁸, B. Meirose⁴¹, D. Melini¹⁵⁶, B.R. Mellado Garcia^{31f}, A.H. Melo⁵¹, F. Meloni⁴⁴, A. Melzer²²,
 E.D. Mendes Gouveia^{135a}, A.M. Mendes Jacques Da Costa¹⁹, H.Y. Meng¹⁶², L. Meng³⁴, S. Menke¹¹¹,
 M. Mentink³⁴, E. Meoni^{39b,39a}, C. Merlassino¹³⁰, P. Mermoud^{52,*}, L. Merola^{67a,67b}, C. Meroni^{66a},
 G. Merz¹⁰², O. Meshkov^{107,109}, J.K.R. Meshreki¹⁴⁷, J. Metcalfe⁵, A.S. Mete⁵, C. Meyer⁶³, J-P. Meyer¹⁴⁰,
 M. Michetti¹⁷, R.P. Middleton¹³⁹, L. Mijović⁴⁸, G. Mikenberg¹⁷⁵, M. Mikestikova¹³⁶, M. Mikuž⁸⁹,
 H. Mildner¹⁴⁵, A. Milic¹⁶², C.D. Milke⁴⁰, D.W. Miller³⁵, L.S. Miller³², A. Milov¹⁷⁵, D.A. Milstead^{43a,43b},
 T. Min^{13c}, A.A. Minaenko¹¹⁸, I.A. Minashvili^{155b}, L. Mince⁵⁵, A.I. Mincer¹²¹, B. Mindur^{81a}, M. Mineev⁷⁷,
 Y. Minegishi¹⁵⁹, Y. Mino⁸³, L.M. Mir¹², M. Miralles Lopez¹⁶⁹, M. Mironova¹³⁰, T. Mitani¹⁷⁴,
 V.A. Mitsou¹⁶⁹, M. Mittal^{58c}, O. Miu¹⁶², P.S. Miyagawa⁹⁰, Y. Miyazaki⁸⁵, A. Mizukami⁷⁹,
 J.U. Mjörnmark⁹⁴, T. Mkrtchyan^{59a}, M. Mlynarikova¹¹⁶, T. Moa^{43a,43b}, S. Mobius⁵¹, K. Mochizuki¹⁰⁶,
 P. Moder⁴⁴, P. Mogg¹¹⁰, A.F. Mohammed^{13a}, S. Mohapatra³⁷, G. Mokgatitswane^{31f}, B. Mondal¹⁴⁷,
 S. Mondal¹³⁷, K. Mönig⁴⁴, E. Monnier⁹⁸, L. Monsonis Romero¹⁶⁹, A. Montalbano¹⁴⁸,
 J. Montejo Berlingen³⁴, M. Montella¹²³, F. Monticelli⁸⁶, N. Morange⁶², A.L. Moreira De Carvalho^{135a},
 M. Moreno Llacer¹⁶⁹, C. Moreno Martinez¹², P. Morettini^{53b}, S. Morgenstern¹⁷³, D. Mori¹⁴⁸, M. Morii⁵⁷,
 M. Morinaga¹⁵⁹, V. Morisbak¹²⁹, A.K. Morley³⁴, A.P. Morris⁹², L. Morvaj³⁴, P. Moschovakos³⁴,
 B. Moser¹¹⁵, M. Mosidze^{155b}, T. Moskalets⁵⁰, P. Moskvitina¹¹⁴, J. Moss^{29,n}, E.J.W. Moyses⁹⁹,

S. Muanza⁹⁸, J. Mueller¹³⁴, R. Mueller¹⁸, D. Muenstermann⁸⁷, G.A. Mullier⁹⁴, J.J. Mullin¹³², D.P. Mungo^{66a,66b}, J.L. Munoz Martinez¹², F.J. Munoz Sanchez⁹⁷, M. Murin⁹⁷, P. Murin^{26b}, W.J. Murray^{173,139}, A. Murrone^{66a,66b}, J.M. Muse¹²⁴, M. Muškinja¹⁶, C. Mwewa²⁷, A.G. Myagkov^{118,ae}, A.J. Myers⁷, A.A. Myers¹³⁴, G. Myers⁶³, M. Myska¹³⁷, B.P. Nachman¹⁶, O. Nackenhorst⁴⁵, A. Nag Nag⁴⁶, K. Nagai¹³⁰, K. Nagano⁷⁹, J.L. Nagle²⁷, E. Nagy⁹⁸, A.M. Nairz³⁴, Y. Nakahama¹¹², K. Nakamura⁷⁹, H. Nanjo¹²⁸, F. Napolitano^{59a}, R. Narayan⁴⁰, E.A. Narayanan¹¹³, I. Naryshkin¹³³, M. Naseri³², C. Nass²², T. Naumann⁴⁴, G. Navarro^{20a}, J. Navarro-Gonzalez¹⁶⁹, R. Nayak¹⁵⁷, P.Y. Nechaeva¹⁰⁷, F. Nechansky⁴⁴, T.J. Neep¹⁹, A. Negri^{68a,68b}, M. Negrini^{21b}, C. Nellist¹¹⁴, C. Nelson¹⁰⁰, K. Nelson¹⁰², S. Nemecek¹³⁶, M. Nessi^{34,f}, M.S. Neubauer¹⁶⁸, F. Neuhaus⁹⁶, J. Neundorff⁴⁴, R. Newhouse¹⁷⁰, P.R. Newman¹⁹, C.W. Ng¹³⁴, Y.S. Ng¹⁷, Y.W.Y. Ng¹⁶⁶, B. Ngair^{33e}, H.D.N. Nguyen¹⁰⁶, R.B. Nickerson¹³⁰, R. Nicolaidou¹⁴⁰, D.S. Nielsen³⁸, J. Nielsen¹⁴¹, M. Niemeyer⁵¹, N. Nikiforou¹⁰, V. Nikolaenko^{118,ae}, I. Nikolic-Audit¹³¹, K. Nikolopoulos¹⁹, P. Nilsson²⁷, H.R. Nindhito⁵², A. Nisati^{70a}, N. Nishu², R. Nisius¹¹¹, T. Nitta¹⁷⁴, T. Nobe¹⁵⁹, D.L. Noel³⁰, Y. Noguchi⁸³, I. Nomidis¹³¹, M.A. Nomura²⁷, M.B. Norfolk¹⁴⁵, R.R.B. Norisam⁹², J. Novak⁸⁹, T. Novak⁴⁴, O. Novgorodova⁴⁶, L. Novotny¹³⁷, R. Novotny¹¹³, L. Nozka¹²⁶, K. Ntekas¹⁶⁶, E. Nurse⁹², F.G. Oakham^{32,aj}, J. Ocariz¹³¹, A. Ochi⁸⁰, I. Ochoa^{135a}, J.P. Ochoa-Ricoux^{142a}, S. Oda⁸⁵, S. Odaka⁷⁹, S. Oerdek¹⁶⁷, A. Ogrodnik^{81a}, A. Oh⁹⁷, C.C. Ohm¹⁵⁰, H. Oide¹⁶⁰, R. Oishi¹⁵⁹, M.L. Ojeda⁴⁴, Y. Okazaki⁸³, M.W. O'Keefe⁸⁸, Y. Okumura¹⁵⁹, A. Olariu^{25b}, L.F. Oleiro Seabra^{135a}, S.A. Olivares Pino^{142d}, D. Oliveira Damazio²⁷, D. Oliveira Goncalves^{78a}, J.L. Oliver¹⁶⁶, M.J.R. Olsson¹⁶⁶, A. Olszewski⁸², J. Olszowska⁸², Ö.O. Öncel²², D.C. O'Neil¹⁴⁸, A.P. O'Neill¹³⁰, A. Onofre^{135a,135e}, P.U.E. Onyisi¹⁰, R.G. Oreamuno Madriz¹¹⁶, M.J. Oreglia³⁵, G.E. Orellana⁸⁶, D. Orestano^{72a,72b}, N. Orlando¹², R.S. Orr¹⁶², V. O'Shea⁵⁵, R. Ospanov^{58a}, G. Otero y Garzon²⁸, H. Otono⁸⁵, P.S. Ott^{59a}, G.J. Ottino¹⁶, M. Ouchrif^{33d}, J. Ouellette²⁷, F. Ould-Saada¹²⁹, A. Ouraou^{140,*}, Q. Ouyang^{13a}, M. Owen⁵⁵, R.E. Owen¹³⁹, K.Y. Oyulmaz^{11c}, V.E. Ozcan^{11c}, N. Ozturk⁷, S. Ozturk^{11c}, J. Pacalt¹²⁶, H.A. Pacey³⁰, K. Pachal⁴⁷, A. Pacheco Pages¹², C. Padilla Aranda¹², S. Pagan Griso¹⁶, G. Palacino⁶³, S. Palazzo⁴⁸, S. Palestini³⁴, M. Palka^{81b}, P. Palni^{81a}, D.K. Panchal¹⁰, C.E. Pandini⁵², J.G. Panduro Vazquez⁹¹, P. Pani⁴⁴, G. Panizzo^{64a,64c}, L. Paolozzi⁵², C. Papadatos¹⁰⁶, S. Parajuli⁴⁰, A. Paramonov⁵, C. Paraskevopoulos⁹, D. Paredes Hernandez^{60b}, S.R. Paredes Saenz¹³⁰, B. Parida¹⁷⁵, T.H. Park¹⁶², A.J. Parker²⁹, M.A. Parker³⁰, F. Parodi^{53b,53a}, E.W. Parrish¹¹⁶, J.A. Parsons³⁷, U. Parzefall⁵⁰, L. Pascual Dominguez¹⁵⁷, V.R. Pascuzzi¹⁶, F. Pasquali¹¹⁵, E. Pasqualucci^{70a}, S. Passaggio^{53b}, F. Pastore⁹¹, P. Pasuwan^{43a,43b}, J.R. Pater⁹⁷, A. Pathak¹⁷⁶, J. Patton⁸⁸, T. Pauly³⁴, J. Pearkes¹⁴⁹, M. Pedersen¹²⁹, L. Pedraza Diaz¹¹⁴, R. Pedro^{135a}, T. Peiffer⁵¹, S.V. Peleganchuk^{117b,117a}, O. Penc¹³⁶, C. Peng^{60b}, H. Peng^{58a}, M. Penzin¹⁶¹, B.S. Peralva^{78a}, A.P. Pereira Peixoto^{135a}, L. Pereira Sanchez^{43a,43b}, D.V. Perepelitsa²⁷, E. Perez Codina^{163a}, M. Perganti⁹, L. Perini^{66a,66b}, H. Pernegger³⁴, S. Perrella³⁴, A. Perrevoort¹¹⁵, K. Peters⁴⁴, R.F.Y. Peters⁹⁷, B.A. Petersen³⁴, T.C. Petersen³⁸, E. Petit⁹⁸, V. Petousis¹³⁷, C. Petridou¹⁵⁸, P. Petroff⁶², F. Petrucci^{72a,72b}, A. Petrukhin¹⁴⁷, M. Pettee¹⁷⁸, N.E. Pettersson³⁴, K. Petukhova¹³⁸, A. Peyaud¹⁴⁰, R. Pezoa^{142e}, L. Pezzotti³⁴, G. Pezzullo¹⁷⁸, T. Pham¹⁰¹, P.W. Phillips¹³⁹, M.W. Phipps¹⁶⁸, G. Piacquadio¹⁵¹, E. Pianori¹⁶, F. Piazza^{66a,66b}, A. Picazio⁹⁹, R. Piegai²⁸, D. Pietreanu^{25b}, J.E. Pilcher³⁵, A.D. Pilkington⁹⁷, M. Pinamonti^{64a,64c}, J.L. Pinfold², C. Pitman Donaldson⁹², D.A. Pizzi³², L. Pizzimento^{71a,71b}, A. Pizzini¹¹⁵, M.-A. Pleier²⁷, V. Plesanovs⁵⁰, V. Pleskot¹³⁸, E. Plotnikova⁷⁷, P. Podberezko^{117b,117a}, R. Poettgen⁹⁴, R. Poggi⁵², L. Poggioli¹³¹, I. Pogrebnyak¹⁰³, D. Pohl²², I. Pokharel⁵¹, G. Polesello^{68a}, A. Poley^{148,163a}, A. Policicchio^{70a,70b}, R. Polifka¹³⁸, A. Polini^{21b}, C.S. Pollard¹³⁰, Z.B. Pollock¹²³, V. Polychronakos²⁷, D. Ponomarenko¹⁰⁸, L. Pontecorvo³⁴, S. Popa^{25a}, G.A. Popeneciu^{25d}, L. Portales⁴, D.M. Portillo Quintero^{163a}, S. Pospisil¹³⁷, P. Postolache^{25c}, K. Potamianos¹³⁰, I.N. Potrap⁷⁷, C.J. Potter³⁰, H. Potti¹, T. Poulsen⁴⁴, J. Poveda¹⁶⁹, T.D. Powell¹⁴⁵, G. Pownall⁴⁴, M.E. Pozo Astigarraga³⁴, A. Prades Ibanez¹⁶⁹, P. Pralavorio⁹⁸, M.M. Prapa⁴², S. Prell⁷⁶, D. Price⁹⁷, M. Primavera^{65a}, M.A. Principe Martin⁹⁵, M.L. Proffitt¹⁴⁴, N. Proklova¹⁰⁸, K. Prokofiev^{60c}, F. Prokoshin⁷⁷, S. Protopopescu²⁷, J. Proudfoot⁵, M. Przybycien^{81a}, D. Pudzha¹³³, P. Puzo⁶², D. Pyatiizbyantseva¹⁰⁸, J. Qian¹⁰², Y. Qin⁹⁷, T. Qiu⁹⁰, A. Quadt⁵¹, M. Queitsch-Maitland³⁴, G. Rabanal Bolanos⁵⁷, F. Ragusa^{66a,66b}, J.A. Raine⁵², S. Rajagopalan²⁷, K. Ran^{13a,13d}, D.F. Rassloff^{59a}, D.M. Rauch⁴⁴, S. Rave⁹⁶, B. Ravina⁵⁵, I. Ravinovich¹⁷⁵, M. Raymond³⁴, A.L. Read¹²⁹, N.P. Readioff¹⁴⁵, D.M. Rebuszi^{68a,68b}, G. Redlinger²⁷, K. Reeves⁴¹, D. Reikher¹⁵⁷, A. Reiss⁹⁶, A. Rej¹⁴⁷, C. Rembser³⁴, A. Renardi⁴⁴, M. Renda^{25b}, M.B. Rendel¹¹¹, A.G. Rennie⁵⁵, S. Resconi^{66a}, M. Ressegotti^{53b,53a}, E.D. Resseguie¹⁶, S. Rettie⁹², B. Reynolds¹²³, E. Reynolds¹⁹, M. Rezaei Estabragh¹⁷⁷, O.L. Rezanova^{117b,117a},

P. Reznicek¹³⁸, E. Ricci^{73a,73b}, R. Richter¹¹¹, S. Richter⁴⁴, E. Richter-Was^{81b}, M. Ridel¹³¹, P. Rieck¹¹¹, P. Riedler³⁴, O. Rifki⁴⁴, M. Rijssenbeek¹⁵¹, A. Rimoldi^{68a,68b}, M. Rimoldi⁴⁴, L. Rinaldi^{21b,21a}, T.T. Rinn¹⁶⁸, M.P. Rinnagel¹¹⁰, G. Ripellino¹⁵⁰, I. Riu¹², P. Rivadeneira⁴⁴, J.C. Rivera Vergara¹⁷¹, F. Rizatdinova¹²⁵, E. Rizvi⁹⁰, C. Rizzi⁵², B.A. Roberts¹⁷³, B.R. Roberts¹⁶, S.H. Robertson^{100,y}, M. Robin⁴⁴, D. Robinson³⁰, C.M. Robles Gajardo^{142e}, M. Robles Manzano⁹⁶, A. Robson⁵⁵, A. Rocchi^{71a,71b}, C. Roda^{69a,69b}, S. Rodriguez Bosca^{59a}, A. Rodriguez Rodriguez⁵⁰, A.M. Rodríguez Vera^{163b}, S. Roe³⁴, A.R. Roepe¹²⁴, J. Roggel¹⁷⁷, O. Røhne¹²⁹, R.A. Rojas¹⁷¹, B. Roland⁵⁰, C.P.A. Roland⁶³, J. Roloff²⁷, A. Romaniouk¹⁰⁸, M. Romano^{21b}, A.C. Romero Hernandez¹⁶⁸, N. Rompotis⁸⁸, M. Ronzani¹²¹, L. Roos¹³¹, S. Rosati^{70a}, B.J. Rosser¹³², E. Rossi¹⁶², E. Rossi⁴, E. Rossi^{67a,67b}, L.P. Rossi^{53b}, L. Rossini⁴⁴, R. Rosten¹²³, M. Rotaru^{25b}, B. Rottler⁵⁰, D. Rousseau⁶², D. Rousso³⁰, G. Rovelli^{68a,68b}, A. Roy¹⁰, A. Rozanov⁹⁸, Y. Rozen¹⁵⁶, X. Ruan^{31f}, A.J. Ruby⁸⁸, T.A. Ruggeri¹, F. Rühr⁵⁰, A. Ruiz-Martinez¹⁶⁹, A. Rummler³⁴, Z. Rurikova⁵⁰, N.A. Rusakovich⁷⁷, H.L. Russell³⁴, L. Rustige³⁶, J.P. Rutherford⁶, E.M. Rüttinger¹⁴⁵, M. Rybar¹³⁸, E.B. Rye¹²⁹, A. Ryzhov¹¹⁸, J.A. Sabater Iglesias⁴⁴, P. Sabatini¹⁶⁹, L. Sabetta^{70a,70b}, H.F-W. Sadrozinski¹⁴¹, R. Sadykov⁷⁷, F. Safai Tehrani^{70a}, B. Safarzadeh Samani¹⁵², M. Safdari¹⁴⁹, S. Saha¹⁰⁰, M. Sahinsoy¹¹¹, A. Sahu¹⁷⁷, M. Saimpert¹⁴⁰, M. Saito¹⁵⁹, T. Saito¹⁵⁹, D. Salamani³⁴, G. Salamanna^{72a,72b}, A. Salnikov¹⁴⁹, J. Salt¹⁶⁹, A. Salvador Salas¹², D. Salvatore^{39b,39a}, F. Salvatore¹⁵², A. Salzburger³⁴, D. Sammel⁵⁰, D. Sampsonidis¹⁵⁸, D. Sampsonidou^{58d,58c}, J. Sánchez¹⁶⁹, A. Sanchez Pineda⁴, V. Sanchez Sebastian¹⁶⁹, H. Sandaker¹²⁹, C.O. Sander⁴⁴, I.G. Sanderswood⁸⁷, J.A. Sandesara⁹⁹, M. Sandhoff¹⁷⁷, C. Sandoval^{20b}, D.P.C. Sankey¹³⁹, M. Sannino^{53b,53a}, A. Sansoni⁴⁹, C. Santoni³⁶, H. Santos^{135a,135b}, S.N. Santpur¹⁶, A. Santra¹⁷⁵, K.A. Saoucha¹⁴⁵, A. Saponov⁷⁷, J.G. Saraiva^{135a,135d}, J. Sardain⁹⁸, O. Sasaki⁷⁹, K. Sato¹⁶⁴, C. Sauer^{59b}, F. Sauerburger⁵⁰, E. Sauvan⁴, P. Savard^{162,aj}, R. Sawada¹⁵⁹, C. Sawyer¹³⁹, L. Sawyer⁹³, I. Sayago Galvan¹⁶⁹, C. Sbarra^{21b}, A. Sbrizzi^{21b,21a}, T. Scanlon⁹², J. Schaarschmidt¹⁴⁴, P. Schacht¹¹¹, D. Schaefer³⁵, U. Schäfer⁹⁶, A.C. Schaffer⁶², D. Schaile¹¹⁰, R.D. Schamberger¹⁵¹, E. Schanet¹¹⁰, C. Scharf¹⁷, N. Scharmberg⁹⁷, V.A. Schegelsky¹³³, D. Scheirich¹³⁸, F. Schenck¹⁷, M. Schernau¹⁶⁶, C. Schiavi^{53b,53a}, L.K. Schildgen²², Z.M. Schillaci²⁴, E.J. Schioppa^{65a,65b}, M. Schioppa^{39b,39a}, B. Schlag⁹⁶, K.E. Schleicher⁵⁰, S. Schlenker³⁴, K. Schmieden⁹⁶, C. Schmitt⁹⁶, S. Schmitt⁴⁴, L. Schoeffel¹⁴⁰, A. Schoening^{59b}, P.G. Scholer⁵⁰, E. Schopf¹³⁰, M. Schott⁹⁶, J. Schovancova³⁴, S. Schramm⁵², F. Schroeder¹⁷⁷, H-C. Schultz-Coulon^{59a}, M. Schumacher⁵⁰, B.A. Schumm¹⁴¹, Ph. Schune¹⁴⁰, A. Schwartzman¹⁴⁹, T.A. Schwarz¹⁰², Ph. Schwemling¹⁴⁰, R. Schwienhorst¹⁰³, A. Sciandra¹⁴¹, G. Sciolla²⁴, F. Scuri^{69a}, F. Scutti¹⁰¹, C.D. Sebastiani⁸⁸, K. Sedlaczek⁴⁵, P. Seema¹⁷, S.C. Seidel¹¹³, A. Seiden¹⁴¹, B.D. Seidlitz²⁷, T. Seiss³⁵, C. Seitz⁴⁴, J.M. Seixas^{78b}, G. Sekhniaidze^{67a}, S.J. Sekula⁴⁰, L. Selem⁴, N. Semprini-Cesari^{21b,21a}, S. Sen⁴⁷, C. Serfon²⁷, L. Serin⁶², L. Serkin^{64a,64b}, M. Sessa^{72a,72b}, H. Severini¹²⁴, S. Sevova¹⁴⁹, F. Sforza^{53b,53a}, A. Sfyrla⁵², E. Shabalina⁵¹, R. Shaheen¹⁵⁰, J.D. Shahinian¹³², N.W. Shaikh^{43a,43b}, D. Shaked Renous¹⁷⁵, L.Y. Shan^{13a}, M. Shapiro¹⁶, A. Sharma³⁴, A.S. Sharma¹, S. Sharma⁴⁴, P.B. Shatalov¹¹⁹, K. Shaw¹⁵², S.M. Shaw⁹⁷, P. Sherwood⁹², L. Shi⁹², C.O. Shimmin¹⁷⁸, Y. Shimogama¹⁷⁴, J.D. Shinner⁹¹, I.P.J. Shipsey¹³⁰, S. Shirabe⁵², M. Shiyakova⁷⁷, J. Shlomi¹⁷⁵, M.J. Shochet³⁵, J. Shojaii¹⁰¹, D.R. Shope¹⁵⁰, S. Shrestha¹²³, E.M. Shrif^{31f}, M.J. Shroff¹⁷¹, E. Shulga¹⁷⁵, P. Sicho¹³⁶, A.M. Sickles¹⁶⁸, E. Sideras Haddad^{31f}, O. Sidiropoulou³⁴, A. Sidoti^{21b}, F. Siegert⁴⁶, Dj. Sijacki¹⁴, J.M. Silva¹⁹, M.V. Silva Oliveira³⁴, S.B. Silverstein^{43a}, S. Simion⁶², R. Simoniello³⁴, N.D. Simpson⁹⁴, S. Simsek^{11b}, P. Sinervo¹⁶², V. Sinetckii¹⁰⁹, S. Singh¹⁴⁸, S. Singh¹⁶², S. Sinha⁴⁴, S. Sinha^{31f}, M. Sioli^{21b,21a}, I. Siral¹²⁷, S.Yu. Sivoklokov¹⁰⁹, J. Sjölin^{43a,43b}, A. Skaf⁵¹, E. Skorda⁹⁴, P. Skubic¹²⁴, M. Slawinska⁸², K. Sliwa¹⁶⁵, V. Smakhtin¹⁷⁵, B.H. Smart¹³⁹, J. Smiesko¹³⁸, S.Yu. Smirnov¹⁰⁸, Y. Smirnov¹⁰⁸, L.N. Smirnova^{109,r}, O. Smirnova⁹⁴, E.A. Smith³⁵, H.A. Smith¹³⁰, M. Smizanska⁸⁷, K. Smolek¹³⁷, A. Smykiewicz⁸², A.A. Snesarev¹⁰⁷, H.L. Snoek¹¹⁵, S. Snyder²⁷, R. Sobie^{171,y}, A. Soffer¹⁵⁷, F. Sohns⁵¹, C.A. Solans Sanchez³⁴, E.Yu. Soldatov¹⁰⁸, U. Soldevila¹⁶⁹, A.A. Solodkov¹¹⁸, S. Solomon⁵⁰, A. Soloshenko⁷⁷, O.V. Solovyanov¹¹⁸, V. Solovyev¹³³, P. Sommer¹⁴⁵, H. Son¹⁶⁵, A. Sonay¹², W.Y. Song^{163b}, A. Sopczak¹³⁷, A.L. Soppio⁹², F. Sopkova^{26b}, S. Sottocornola^{68a,68b}, R. Soualah^{64a,64c}, A.M. Soukharev^{117b,117a}, Z. Soumami^{33e}, D. South⁴⁴, S. Spagnolo^{65a,65b}, M. Spalla¹¹¹, M. Spangenberg¹⁷³, F. Spanò⁹¹, D. Sperlich⁵⁰, T.M. Spieker^{59a}, G. Spigo³⁴, M. Spina¹⁵², D.P. Spiteri⁵⁵, M. Spousta¹³⁸, A. Stabile^{66a,66b}, R. Stamen^{59a}, M. Stamenkovic¹¹⁵, A. Stampekis¹⁹, M. Standke²², E. Stanecka⁸², B. Stanislaus³⁴, M.M. Stanitzki⁴⁴, M. Stankaityte¹³⁰, B. Stapf⁴⁴, E.A. Starchenko¹¹⁸, G.H. Stark¹⁴¹, J. Stark⁹⁸, D.M. Starke^{163b}, P. Staroba¹³⁶, P. Starovoitov^{59a}, S. Stärz¹⁰⁰, R. Staszewski⁸²,

G. Stavropoulos⁴², P. Steinberg²⁷, A.L. Steinhebel¹²⁷, B. Stelzer^{148,163a}, H.J. Stelzer¹³⁴,
O. Stelzer-Chilton^{163a}, H. Stenzel⁵⁴, T.J. Stevenson¹⁵², G.A. Stewart³⁴, M.C. Stockton³⁴, G. Stoicea^{25b},
M. Stolarski^{135a}, S. Stonjek¹¹¹, A. Straessner⁴⁶, J. Strandberg¹⁵⁰, S. Strandberg^{43a,43b}, M. Strauss¹²⁴,
T. Strebler⁹⁸, P. Strizenec^{26b}, R. Ströhmer¹⁷², D.M. Strom¹²⁷, L.R. Strom⁴⁴, R. Stroynowski⁴⁰,
A. Strubig^{43a,43b}, S.A. Stucci²⁷, B. Stugu¹⁵, J. Stupak¹²⁴, N.A. Styles⁴⁴, D. Su¹⁴⁹, S. Su^{58a},
W. Su^{58d,144,58c}, X. Su^{58a}, K. Sugizaki¹⁵⁹, V.V. Sulim¹⁰⁷, M.J. Sullivan⁸⁸, D.M.S. Sultan⁵²,
L. Sultanaliyeva¹⁰⁷, S. Sultansoy^{3c}, T. Sumida⁸³, S. Sun¹⁰², S. Sun¹⁷⁶, X. Sun⁹⁷,
O. Sunneborn Gudnadottir¹⁶⁷, C.J.E. Suster¹⁵³, M.R. Sutton¹⁵², M. Svatos¹³⁶, M. Swiatlowski^{163a},
T. Swirski¹⁷², I. Sykora^{26a}, M. Sykora¹³⁸, T. Sykora¹³⁸, D. Ta⁹⁶, K. Tackmann^{44,w}, A. Taffard¹⁶⁶,
R. Tafirout^{163a}, R.H.M. Taibah¹³¹, R. Takashima⁸⁴, K. Takeda⁸⁰, T. Takeshita¹⁴⁶, E.P. Takeva⁴⁸,
Y. Takubo⁷⁹, M. Talby⁹⁸, A.A. Talyshev^{117b,117a}, K.C. Tam^{60b}, N.M. Tamir¹⁵⁷, A. Tanaka¹⁵⁹, J. Tanaka¹⁵⁹,
R. Tanaka⁶², J. Tang^{58c}, Z. Tao¹⁷⁰, S. Tapia Araya⁷⁶, S. Tapprogge⁹⁶, A. Tarek Abouelfadl Mohamed¹⁰³,
S. Tarem¹⁵⁶, K. Tariq^{58b}, G. Tarna^{25b}, G.F. Tartarelli^{66a}, P. Tas¹³⁸, M. Tasevsky¹³⁶, E. Tassi^{39b,39a},
G. Tateno¹⁵⁹, Y. Tayalati^{33e}, G.N. Taylor¹⁰¹, W. Taylor^{163b}, H. Teagle⁸⁸, A.S. Tee¹⁷⁶,
R. Teixeira De Lima¹⁴⁹, P. Teixeira-Dias⁹¹, H. Ten Kate³⁴, J.J. Teoh¹¹⁵, K. Terashi¹⁵⁹, J. Terron⁹⁵,
S. Terzo¹², M. Testa⁴⁹, R.J. Teuscher^{162,y}, N. Themistokleous⁴⁸, T. Theveneaux-Pelzer¹⁷,
O. Thielmann¹⁷⁷, D.W. Thomas⁹¹, J.P. Thomas¹⁹, E.A. Thompson⁴⁴, P.D. Thompson¹⁹, E. Thomson¹³²,
E.J. Thorpe⁹⁰, Y. Tian⁵¹, V.O. Tikhomirov^{107,af}, Yu.A. Tikhonov^{117b,117a}, S. Timoshenko¹⁰⁸, P. Tipton¹⁷⁸,
S. Tisserant⁹⁸, S.H. Tlou^{31f}, A. Tnourji³⁶, K. Todome^{21b,21a}, S. Todorova-Nova¹³⁸, S. Todt⁴⁶,
M. Togawa⁷⁹, J. Tojo⁸⁵, S. Tokár^{26a}, K. Tokushuku⁷⁹, E. Tolley¹²³, R. Tombs³⁰, M. Tomoto^{79,112},
L. Tompkins¹⁴⁹, P. Tornambe⁹⁹, E. Torrence¹²⁷, H. Torres⁴⁶, E. Torró Pastor¹⁶⁹, M. Toscani²⁸,
C. Toscirì³⁵, J. Toth^{98,x}, D.R. Tovey¹⁴⁵, A. Traet¹⁵, C.J. Treado¹²¹, T. Trefzger¹⁷², A. Tricoli²⁷,
I.M. Trigger^{163a}, S. Trincaz-Duvoid¹³¹, D.A. Trischuk¹⁷⁰, W. Trischuk¹⁶², B. Trocmé⁵⁶, A. Trofymov⁶²,
C. Troncon^{66a}, F. Trovato¹⁵², L. Truong^{31c}, M. Trzebinski⁸², A. Trzupek⁸², F. Tsai¹⁵¹, A. Tsiamis¹⁵⁸,
P.V. Tsiarehka^{104,ad}, A. Tsigotis^{158,u}, V. Tsiskaridze¹⁵¹, E.G. Tskhadadze^{155a}, M. Tsopoulou¹⁵⁸,
Y. Tsujikawa⁸³, I.I. Tsukerman¹¹⁹, V. Tsulaia¹⁶, S. Tsuno⁷⁹, O. Tsur¹⁵⁶, D. Tsybychev¹⁵¹, Y. Tu^{60b},
A. Tudorache^{25b}, V. Tudorache^{25b}, A.N. Tuna³⁴, S. Turchikhin⁷⁷, I. Turk Cakir^{3a}, R.J. Turner¹⁹,
R. Turra^{66a}, P.M. Tuts³⁷, S. Tzamarias¹⁵⁸, P. Tzanis⁹, E. Tzovara⁹⁶, K. Uchida¹⁵⁹, F. Ukegawa¹⁶⁴,
P.A. Ulloa Poblete^{142c}, G. Unal³⁴, M. Unal¹⁰, A. Undrus²⁷, G. Unel¹⁶⁶, F.C. Ungaro¹⁰¹, K. Uno¹⁵⁹,
J. Urban^{26b}, P. Urquijo¹⁰¹, G. Usai⁷, R. Ushioda¹⁶⁰, M. Usman¹⁰⁶, Z. Uysal^{11d}, V. Vacek¹³⁷,
B. Vachon¹⁰⁰, K.O.H. Vadla¹²⁹, T. Vafeiadis³⁴, C. Valderanis¹¹⁰, E. Valdes Santurio^{43a,43b}, M. Valente^{163a},
S. Valentinetti^{21b,21a}, A. Valero¹⁶⁹, R.A. Vallance¹⁹, A. Vallier⁹⁸, J.A. Valls Ferrer¹⁶⁹, T.R. Van Daalen¹⁴⁴,
P. Van Gemmeren⁵, S. Van Stroud⁹², I. Van Vulpen¹¹⁵, M. Vanadia^{71a,71b}, W. Vandelli³⁴,
M. Vandenbroucke¹⁴⁰, E.R. Vandewall¹²⁵, D. Vannicola¹⁵⁷, L. Vannoli^{53b,53a}, R. Vari^{70a}, E.W. Varnes⁶,
C. Varni¹⁶, T. Varol¹⁵⁴, D. Varouchas⁶², K.E. Varvell¹⁵³, M.E. Vasile^{25b}, L. Vaslin³⁶, G.A. Vasquez¹⁷¹,
F. Vazeille³⁶, D. Vazquez Furelos¹², T. Vazquez Schroeder³⁴, J. Veatch⁵¹, V. Vecchio⁹⁷, M.J. Veen¹¹⁵,
I. Veliscek¹³⁰, L.M. Veloce¹⁶², F. Veloso^{135a,135c}, S. Veneziano^{70a}, A. Ventura^{65a,65b}, A. Verbitskiy¹¹¹,
M. Verducci^{69a,69b}, C. Vergis²², M. Verissimo De Araujo^{78b}, W. Verkerke¹¹⁵, A.T. Vermeulen¹¹⁵,
J.C. Vermeulen¹¹⁵, C. Vernieri¹⁴⁹, P.J. Verschuur⁹¹, M. Vessella⁹⁹, M.L. Vesterbacka¹²¹,
M.C. Vetterli^{148,aj}, A. Vgenopoulos¹⁵⁸, N. Viaux Maira^{142e}, T. Vickey¹⁴⁵, O.E. Vickey Boeriu¹⁴⁵,
G.H.A. Viehhauser¹³⁰, L. Vigani^{59b}, M. Villa^{21b,21a}, M. Villaplana Perez¹⁶⁹, E.M. Villhauer⁴⁸,
E. Vilucchi⁴⁹, M.G. Vincker³², G.S. Virdee¹⁹, A. Vishwakarma⁴⁸, C. Vittori^{21b,21a}, I. Vivarelli¹⁵²,
V. Vladimirov¹⁷³, E. Voevodina¹¹¹, M. Vogel¹⁷⁷, P. Vokac¹³⁷, J. Von Ahnen⁴⁴, E. Von Toerne²²,
V. Vorobel¹³⁸, K. Vorobev¹⁰⁸, M. Vos¹⁶⁹, J.H. Vosseveld⁸⁸, M. Vozak⁹⁷, L. Vozdecky⁹⁰, N. Vranjes¹⁴,
M. Vranjes Milosavljevic¹⁴, V. Vrba^{137,*}, M. Vreeswijk¹¹⁵, N.K. Vu⁹⁸, R. Vuillermet³⁴, O.V. Vujanovic⁹⁶,
I. Vukotic³⁵, S. Wada¹⁶⁴, C. Wagner⁹⁹, W. Wagner¹⁷⁷, S. Wahdan¹⁷⁷, H. Wahlberg⁸⁶, R. Wakasa¹⁶⁴,
M. Wakida¹¹², V.M. Walbrecht¹¹¹, J. Walder¹³⁹, R. Walker¹¹⁰, S.D. Walker⁹¹, W. Walkowiak¹⁴⁷,
A.M. Wang⁵⁷, A.Z. Wang¹⁷⁶, C. Wang^{58a}, C. Wang^{58c}, H. Wang¹⁶, J. Wang^{60a}, P. Wang⁴⁰, R.-J. Wang⁹⁶,
R. Wang⁵⁷, R. Wang¹¹⁶, S.M. Wang¹⁵⁴, S. Wang^{58b}, T. Wang^{58a}, W.T. Wang⁷⁵, W.X. Wang^{58a},
X. Wang^{13c}, X. Wang¹⁶⁸, X. Wang^{58c}, Y. Wang^{58a}, Z. Wang¹⁰², C. Wanotayaroj³⁴, A. Warburton¹⁰⁰,
C.P. Ward³⁰, R.J. Ward¹⁹, N. Warrack⁵⁵, A.T. Watson¹⁹, M.F. Watson¹⁹, G. Watts¹⁴⁴, B.M. Waugh⁹²,
A.F. Webb¹⁰, C. Weber²⁷, M.S. Weber¹⁸, S.A. Weber³², S.M. Weber^{59a}, C. Wei^{58a}, Y. Wei¹³⁰,
A.R. Weidberg¹³⁰, J. Weingarten⁴⁵, M. Weirich⁹⁶, C. Weiser⁵⁰, T. Wenaus²⁷, B. Wendland⁴⁵,

T. Wengler³⁴, S. Wenig³⁴, N. Wermes²², M. Wessels^{59a}, K. Whalen¹²⁷, A.M. Wharton⁸⁷, A.S. White⁵⁷, A. White⁷, M.J. White¹, D. Whiteson¹⁶⁶, L. Wickremasinghe¹²⁸, W. Wiedenmann¹⁷⁶, C. Wiel⁴⁶, M. Wielers¹³⁹, N. Wieseotte⁹⁶, C. Wiglesworth³⁸, L.A.M. Wiik-Fuchs⁵⁰, D.J. Wilbern¹²⁴, H.G. Wilkens³⁴, L.J. Wilkins⁹¹, D.M. Williams³⁷, H.H. Williams¹³², S. Williams³⁰, S. Willocq⁹⁹, P.J. Windischhofer¹³⁰, I. Wingerter-Seez⁴, F. Winklmeier¹²⁷, B.T. Winter⁵⁰, M. Wittgen¹⁴⁹, M. Wobisch⁹³, A. Wolf⁹⁶, R. Wölker¹³⁰, J. Wollrath¹⁶⁶, M.W. Wolter⁸², H. Wolters^{135a,135c}, V.W.S. Wong¹⁷⁰, A.F. Wongel⁴⁴, S.D. Worm⁴⁴, B.K. Wosiek⁸², K.W. Woźniak⁸², K. Wraight⁵⁵, J. Wu^{13a,13d}, S.L. Wu¹⁷⁶, X. Wu⁵², Y. Wu^{58a}, Z. Wu^{140,58a}, J. Wuerzinger¹³⁰, T.R. Wyatt⁹⁷, B.M. Wynne⁴⁸, S. Xella³⁸, L. Xia^{13c}, M. Xia^{13b}, J. Xiang^{60c}, X. Xiao¹⁰², M. Xie^{58a}, X. Xie^{58a}, I. Xioutidis¹⁵², D. Xu^{13a}, H. Xu^{58a}, H. Xu^{58a}, L. Xu^{58a}, R. Xu¹³², T. Xu^{58a}, W. Xu¹⁰², Y. Xu^{13b}, Z. Xu^{58b}, Z. Xu¹⁴⁹, B. Yabsley¹⁵³, S. Yacoob^{31a}, N. Yamaguchi⁸⁵, Y. Yamaguchi¹⁶⁰, M. Yamatani¹⁵⁹, H. Yamauchi¹⁶⁴, T. Yamazaki¹⁶, Y. Yamazaki⁸⁰, J. Yan^{58c}, S. Yan¹³⁰, Z. Yan²³, H.J. Yang^{58c,58d}, H.T. Yang¹⁶, S. Yang^{58a}, T. Yang^{60c}, X. Yang^{58a}, X. Yang^{13a}, Y. Yang¹⁵⁹, Z. Yang^{102,58a}, W.-M. Yao¹⁶, Y.C. Yap⁴⁴, H. Ye^{13c}, J. Ye⁴⁰, S. Ye²⁷, I. Yeletsikh⁷⁷, M.R. Yexley⁸⁷, P. Yin³⁷, K. Yorita¹⁷⁴, K. Yoshihara⁷⁶, C.J.S. Young⁵⁰, C. Young¹⁴⁹, M. Yuan¹⁰², R. Yuan^{58b,i}, X. Yue^{59a}, M. Zaazoua^{33e}, B. Zabinski⁸², G. Zacharis⁹, E. Zaid⁴⁸, A.M. Zaitsev^{118,ae}, T. Zakareishvili^{155b}, N. Zakharchuk³², S. Zambito³⁴, D. Zanzi⁵⁰, S.V. Zeißner⁴⁵, C. Zeitnitz¹⁷⁷, J.C. Zeng¹⁶⁸, D.T. Zenger Jr²⁴, O. Zenin¹¹⁸, T. Ženiš^{26a}, S. Zenz⁹⁰, S. Zerradi^{33a}, D. Zerwas⁶², B. Zhang^{13c}, D.F. Zhang¹⁴⁵, G. Zhang^{13b}, J. Zhang⁵, K. Zhang^{13a}, L. Zhang^{13c}, M. Zhang¹⁶⁸, R. Zhang¹⁷⁶, S. Zhang¹⁰², X. Zhang^{58c}, X. Zhang^{58b}, Z. Zhang⁶², P. Zhao⁴⁷, T. Zhao^{58b}, Y. Zhao¹⁴¹, Z. Zhao^{58a}, A. Zhemchugov⁷⁷, Z. Zheng¹⁴⁹, D. Zhong¹⁶⁸, B. Zhou¹⁰², C. Zhou¹⁷⁶, H. Zhou⁶, N. Zhou^{58c}, Y. Zhou⁶, C.G. Zhu^{58b}, C. Zhu^{13a,13d}, H.L. Zhu^{58a}, H. Zhu^{13a}, J. Zhu¹⁰², Y. Zhu^{58a}, X. Zhuang^{13a}, K. Zhukov¹⁰⁷, V. Zhulanov^{117b,117a}, D. Zieminska⁶³, N.I. Zimine⁷⁷, S. Zimmermann^{50,*}, J. Zinsser^{59b}, M. Ziolkowski¹⁴⁷, L. Živković¹⁴, A. Zoccoli^{21b,21a}, K. Zoch⁵², T.G. Zorbas¹⁴⁵, O. Zormpa⁴², W. Zou³⁷, L. Zwalinski³⁴

¹ Department of Physics, University of Adelaide, Adelaide; Australia

² Department of Physics, University of Alberta, Edmonton AB; Canada

³ (a) Department of Physics, Ankara University, Ankara; (b) Istanbul Aydın University, Application and Research Center for Advanced Studies, Istanbul; (c) Division of Physics, TOBB

University of Economics and Technology, Ankara; Turkey

⁴ LAPP, Univ. Savoie Mont Blanc, CNRS/IN2P3, Annecy; France

⁵ High Energy Physics Division, Argonne National Laboratory, Argonne IL; United States of America

⁶ Department of Physics, University of Arizona, Tucson AZ; United States of America

⁷ Department of Physics, University of Texas at Arlington, Arlington TX; United States of America

⁸ Physics Department, National and Kapodistrian University of Athens, Athens; Greece

⁹ Physics Department, National Technical University of Athens, Zografou; Greece

¹⁰ Department of Physics, University of Texas at Austin, Austin TX; United States of America

¹¹ (a) Bahcesehir University, Faculty of Engineering and Natural Sciences, Istanbul; (b) Istanbul Bilgi University, Faculty of Engineering and Natural Sciences, Istanbul; (c) Department of

Physics, Bogazici University, Istanbul; (d) Department of Physics Engineering, Gaziantep University, Gaziantep; Turkey

¹² Institut de Física d'Altes Energies (IFAE), Barcelona Institute of Science and Technology, Barcelona; Spain

¹³ (a) Institute of High Energy Physics, Chinese Academy of Sciences, Beijing; (b) Physics Department, Tsinghua University, Beijing; (c) Department of Physics, Nanjing University, Nanjing;

(d) University of Chinese Academy of Science (UCAS), Beijing; China

¹⁴ Institute of Physics, University of Belgrade, Belgrade; Serbia

¹⁵ Department for Physics and Technology, University of Bergen, Bergen; Norway

¹⁶ Physics Division, Lawrence Berkeley National Laboratory and University of California, Berkeley CA; United States of America

¹⁷ Institut für Physik, Humboldt Universität zu Berlin, Berlin; Germany

¹⁸ Albert Einstein Center for Fundamental Physics and Laboratory for High Energy Physics, University of Bern, Bern; Switzerland

¹⁹ School of Physics and Astronomy, University of Birmingham, Birmingham; United Kingdom

²⁰ (a) Facultad de Ciencias y Centro de Investigaciones, Universidad Antonio Nariño, Bogotá; (b) Departamento de Física, Universidad Nacional de Colombia, Bogotá; Colombia

²¹ (a) Dipartimento di Fisica e Astronomia A. Righi, Università di Bologna; (b) INFN Sezione di Bologna; Italy

²² Physikalisches Institut, Universität Bonn, Bonn; Germany

²³ Department of Physics, Boston University, Boston MA; United States of America

²⁴ Department of Physics, Brandeis University, Waltham MA; United States of America

²⁵ (a) Transilvania University of Brasov, Brasov; (b) Horia Hulubei National Institute of Physics and Nuclear Engineering, Bucharest; (c) Department of Physics, Alexandru Ioan Cuza

University of Iasi, Iasi; (d) National Institute for Research and Development of Isotopic and Molecular Technologies, Physics Department, Cluj-Napoca; (e) University Politehnica Bucharest,

Bucharest; (f) West University in Timisoara, Timisoara; Romania

²⁶ (a) Faculty of Mathematics, Physics and Informatics, Comenius University, Bratislava; (b) Department of Subnuclear Physics, Institute of Experimental Physics of the Slovak Academy of

Sciences, Kosice; Slovak Republic

²⁷ Physics Department, Brookhaven National Laboratory, Upton NY; United States of America

²⁸ Departamento de Física (FCEN) and IFIBA, Universidad de Buenos Aires and CONICET, Buenos Aires; Argentina

²⁹ California State University, CA; United States of America

³⁰ Cavendish Laboratory, University of Cambridge, Cambridge; United Kingdom

³¹ (a) Department of Physics, University of Cape Town, Cape Town; (b) iThemba Labs, Western Cape; (c) Department of Mechanical Engineering Science, University of Johannesburg,

Johannesburg; (d) National Institute of Physics, University of the Philippines Diliman (Philippines); (e) University of South Africa, Department of Physics, Pretoria; (f) School of Physics,

University of the Witwatersrand, Johannesburg; South Africa

³² Department of Physics, Carleton University, Ottawa ON; Canada

³³ (a) Faculté des Sciences Ain Chock, Réseau Universitaire de Physique des Hautes Energies – Université Hassan II, Casablanca; (b) Faculté des Sciences, Université Ibn-Tofail, Kénitra;

(c) Faculté des Sciences Semlalia, Université Cadi Ayyad, LPHEA, Marrakech; (d) LPMR, Faculté des Sciences, Université Mohamed Premier, Oujda; (e) Faculté des sciences, Université

Mohammed V, Rabat; (f) Mohammed VI Polytechnic University, Ben Guerir; Morocco

³⁴ CERN, Geneva; Switzerland

³⁵ Enrico Fermi Institute, University of Chicago, Chicago IL; United States of America

- 36 LPC, Université Clermont Auvergne, CNRS/IN2P3, Clermont-Ferrand; France
- 37 Nevis Laboratory, Columbia University, Irvington NY; United States of America
- 38 Niels Bohr Institute, University of Copenhagen, Copenhagen; Denmark
- 39 (a) Dipartimento di Fisica, Università della Calabria, Rende; (b) INFN Gruppo Collegato di Cosenza, Laboratori Nazionali di Frascati; Italy
- 40 Physics Department, Southern Methodist University, Dallas TX; United States of America
- 41 Physics Department, University of Texas at Dallas, Richardson TX; United States of America
- 42 National Centre for Scientific Research "Demokritos", Agia Paraskevi; Greece
- 43 (a) Department of Physics, Stockholm University; (b) Oskar Klein Centre, Stockholm; Sweden
- 44 Deutsches Elektronen-Synchrotron DESY, Hamburg and Zeuthen; Germany
- 45 Fakultät Physik, Technische Universität Dortmund, Dortmund; Germany
- 46 Institut für Kern- und Teilchenphysik, Technische Universität Dresden, Dresden; Germany
- 47 Department of Physics, Duke University, Durham NC; United States of America
- 48 SUPA – School of Physics and Astronomy, University of Edinburgh, Edinburgh; United Kingdom
- 49 INFN e Laboratori Nazionali di Frascati, Frascati; Italy
- 50 Physikalisches Institut, Albert-Ludwigs-Universität Freiburg, Freiburg; Germany
- 51 II. Physikalisches Institut, Georg-August-Universität Göttingen, Göttingen; Germany
- 52 Département de Physique Nucléaire et Corpusculaire, Université de Genève, Genève; Switzerland
- 53 (a) Dipartimento di Fisica, Università di Genova, Genova; (b) INFN Sezione di Genova; Italy
- 54 II. Physikalisches Institut, Justus-Liebig-Universität Giessen, Giessen; Germany
- 55 SUPA – School of Physics and Astronomy, University of Glasgow, Glasgow; United Kingdom
- 56 LPSC, Université Grenoble Alpes, CNRS/IN2P3, Grenoble INP, Grenoble; France
- 57 Laboratory for Particle Physics and Cosmology, Harvard University, Cambridge MA; United States of America
- 58 (a) Department of Modern Physics and State Key Laboratory of Particle Detection and Electronics, University of Science and Technology of China, Hefei; (b) Institute of Frontier and Interdisciplinary Science and Key Laboratory of Particle Physics and Particle Irradiation (MOE), Shandong University, Qingdao; (c) School of Physics and Astronomy, Shanghai Jiao Tong University, Key Laboratory for Particle Astrophysics and Cosmology (MOE), SKLPPC, Shanghai; (d) Tsung-Dao Lee Institute, Shanghai; China
- 59 (a) Kirchhoff-Institut für Physik, Ruprecht-Karls-Universität Heidelberg, Heidelberg; (b) Physikalisches Institut, Ruprecht-Karls-Universität Heidelberg, Heidelberg; Germany
- 60 (a) Department of Physics, Chinese University of Hong Kong, Shatin, N.T., Hong Kong; (b) Department of Physics, University of Hong Kong, Hong Kong; (c) Department of Physics and Institute for Advanced Study, Hong Kong University of Science and Technology, Clear Water Bay, Kowloon, Hong Kong; China
- 61 Department of Physics, National Tsing Hua University, Hsinchu; Taiwan
- 62 IJCLab, Université Paris-Saclay, CNRS/IN2P3, 91405, Orsay; France
- 63 Department of Physics, Indiana University, Bloomington IN; United States of America
- 64 (a) INFN Gruppo Collegato di Udine, Sezione di Trieste, Udine; (b) ICTP, Trieste; (c) Dipartimento Politecnico di Ingegneria e Architettura, Università di Udine, Udine; Italy
- 65 (a) INFN Sezione di Lecce; (b) Dipartimento di Matematica e Fisica, Università del Salento, Lecce; Italy
- 66 (a) INFN Sezione di Milano; (b) Dipartimento di Fisica, Università di Milano, Milano; Italy
- 67 (a) INFN Sezione di Napoli; (b) Dipartimento di Fisica, Università di Napoli, Napoli; Italy
- 68 (a) INFN Sezione di Pavia; (b) Dipartimento di Fisica, Università di Pavia, Pavia; Italy
- 69 (a) INFN Sezione di Pisa; (b) Dipartimento di Fisica E. Fermi, Università di Pisa, Pisa; Italy
- 70 (a) INFN Sezione di Roma; (b) Dipartimento di Fisica, Sapienza Università di Roma, Roma; Italy
- 71 (a) INFN Sezione di Roma Tor Vergata; (b) Dipartimento di Fisica, Università di Roma Tor Vergata, Roma; Italy
- 72 (a) INFN Sezione di Roma Tre; (b) Dipartimento di Matematica e Fisica, Università Roma Tre, Roma; Italy
- 73 (a) INFN-TIFPA; (b) Università degli Studi di Trento, Trento; Italy
- 74 Institut für Astro- und Teilchenphysik, Leopold-Franzens-Universität, Innsbruck; Austria
- 75 University of Iowa, Iowa City IA; United States of America
- 76 Department of Physics and Astronomy, Iowa State University, Ames IA; United States of America
- 77 Joint Institute for Nuclear Research, Dubna; Russia
- 78 (a) Departamento de Engenharia Elétrica, Universidade Federal de Juiz de Fora (UFJF), Juiz de Fora; (b) Universidade Federal do Rio De Janeiro COPPE/EE/IF, Rio de Janeiro; (c) Instituto de Física, Universidade de São Paulo, São Paulo; Brazil
- 79 KEK, High Energy Accelerator Research Organization, Tsukuba; Japan
- 80 Graduate School of Science, Kobe University, Kobe; Japan
- 81 (a) AGH University of Science and Technology, Faculty of Physics and Applied Computer Science, Krakow; (b) Marian Smoluchowski Institute of Physics, Jagiellonian University, Krakow; Poland
- 82 Institute of Nuclear Physics Polish Academy of Sciences, Krakow; Poland
- 83 Faculty of Science, Kyoto University, Kyoto; Japan
- 84 Kyoto University of Education, Kyoto; Japan
- 85 Research Center for Advanced Particle Physics and Department of Physics, Kyushu University, Fukuoka; Japan
- 86 Instituto de Física La Plata, Universidad Nacional de La Plata and CONICET, La Plata; Argentina
- 87 Physics Department, Lancaster University, Lancaster; United Kingdom
- 88 Oliver Lodge Laboratory, University of Liverpool, Liverpool; United Kingdom
- 89 Department of Experimental Particle Physics, Jožef Stefan Institute and Department of Physics, University of Ljubljana, Ljubljana; Slovenia
- 90 School of Physics and Astronomy, Queen Mary University of London, London; United Kingdom
- 91 Department of Physics, Royal Holloway University of London, Egham; United Kingdom
- 92 Department of Physics and Astronomy, University College London, London; United Kingdom
- 93 Louisiana Tech University, Ruston LA; United States of America
- 94 Fysiska institutionen, Lunds universitet, Lund; Sweden
- 95 Departamento de Física Teórica C-15 and CIAFF, Universidad Autónoma de Madrid, Madrid; Spain
- 96 Institut für Physik, Universität Mainz, Mainz; Germany
- 97 School of Physics and Astronomy, University of Manchester, Manchester; United Kingdom
- 98 CPPM, Aix-Marseille Université, CNRS/IN2P3, Marseille; France
- 99 Department of Physics, University of Massachusetts, Amherst MA; United States of America
- 100 Department of Physics, McGill University, Montreal QC; Canada
- 101 School of Physics, University of Melbourne, Victoria; Australia
- 102 Department of Physics, University of Michigan, Ann Arbor MI; United States of America
- 103 Department of Physics and Astronomy, Michigan State University, East Lansing MI; United States of America
- 104 B.I. Stepanov Institute of Physics, National Academy of Sciences of Belarus, Minsk; Belarus
- 105 Research Institute for Nuclear Problems of Byelorussian State University, Minsk; Belarus
- 106 Group of Particle Physics, University of Montreal, Montreal QC; Canada
- 107 P.N. Lebedev Physical Institute of the Russian Academy of Sciences, Moscow; Russia
- 108 National Research Nuclear University MEPhI, Moscow; Russia
- 109 D.V. Skobel'syn Institute of Nuclear Physics, M.V. Lomonosov Moscow State University, Moscow; Russia
- 110 Fakultät für Physik, Ludwig-Maximilians-Universität München, München; Germany

- 111 Max-Planck-Institut für Physik (Werner-Heisenberg-Institut), München; Germany
- 112 Graduate School of Science and Kobayashi-Maskawa Institute, Nagoya University, Nagoya; Japan
- 113 Department of Physics and Astronomy, University of New Mexico, Albuquerque NM; United States of America
- 114 Institute for Mathematics, Astrophysics and Particle Physics, Radboud University/Nikhef, Nijmegen; Netherlands
- 115 Nikhef National Institute for Subatomic Physics and University of Amsterdam, Amsterdam; Netherlands
- 116 Department of Physics, Northern Illinois University, DeKalb IL; United States of America
- 117 ^(a) Budker Institute of Nuclear Physics and NSU, SB RAS, Novosibirsk; ^(b) Novosibirsk State University Novosibirsk; Russia
- 118 Institute for High Energy Physics of the National Research Centre Kurchatov Institute, Protvino; Russia
- 119 Institute for Theoretical and Experimental Physics named by A.I. Alikhanov of National Research Centre "Kurchatov Institute", Moscow; Russia
- 120 ^(a) New York University Abu Dhabi, Abu Dhabi; ^(b) United Arab Emirates University, Al Ain; ^(c) University of Sharjah, Sharjah; United Arab Emirates
- 121 Department of Physics, New York University, New York NY; United States of America
- 122 Ochanomizu University, Otsuka, Bunkyo-ku, Tokyo; Japan
- 123 Ohio State University, Columbus OH; United States of America
- 124 Homer L. Dodge Department of Physics and Astronomy, University of Oklahoma, Norman OK; United States of America
- 125 Department of Physics, Oklahoma State University, Stillwater OK; United States of America
- 126 Palacký University, Joint Laboratory of Optics, Olomouc; Czech Republic
- 127 Institute for Fundamental Science, University of Oregon, Eugene, OR; United States of America
- 128 Graduate School of Science, Osaka University, Osaka; Japan
- 129 Department of Physics, University of Oslo, Oslo; Norway
- 130 Department of Physics, Oxford University, Oxford; United Kingdom
- 131 LPNHE, Sorbonne Université, Université de Paris, CNRS/IN2P3, Paris; France
- 132 Department of Physics, University of Pennsylvania, Philadelphia PA; United States of America
- 133 Konstantinov Nuclear Physics Institute of National Research Centre "Kurchatov Institute", PNPI, St. Petersburg; Russia
- 134 Department of Physics and Astronomy, University of Pittsburgh, Pittsburgh PA; United States of America
- 135 ^(a) Laboratório de Instrumentação e Física Experimental de Partículas – LIP, Lisboa; ^(b) Departamento de Física, Faculdade de Ciências, Universidade de Lisboa, Lisboa; ^(c) Departamento de Física, Universidade de Coimbra, Coimbra; ^(d) Centro de Física Nuclear da Universidade de Lisboa, Lisboa; ^(e) Departamento de Física, Universidade do Minho, Braga; ^(f) Departamento de Física Teórica y del Cosmos, Universidad de Granada, Granada (Spain); ^(g) Instituto Superior Técnico, Universidade de Lisboa, Lisboa; Portugal
- 136 Institute of Physics of the Czech Academy of Sciences, Prague; Czech Republic
- 137 Czech Technical University in Prague, Prague; Czech Republic
- 138 Charles University, Faculty of Mathematics and Physics, Prague; Czech Republic
- 139 Particle Physics Department, Rutherford Appleton Laboratory, Didcot; United Kingdom
- 140 IRFU, CEA, Université Paris-Saclay, Gif-sur-Yvette; France
- 141 Santa Cruz Institute for Particle Physics, University of California Santa Cruz, Santa Cruz CA; United States of America
- 142 ^(a) Departamento de Física, Pontificia Universidad Católica de Chile, Santiago; ^(b) Instituto de Investigación Multidisciplinario en Ciencia y Tecnología, y Departamento de Física, Universidad de La Serena; ^(c) Universidad Andres Bello, Department of Physics, Santiago; ^(d) Instituto de Alta Investigación, Universidad de Tarapacá, Arica; ^(e) Departamento de Física, Universidad Técnica Federico Santa María, Valparaíso; Chile
- 143 Universidade Federal de São João del Rei (UFSJ), São João del Rei; Brazil
- 144 Department of Physics, University of Washington, Seattle WA; United States of America
- 145 Department of Physics and Astronomy, University of Sheffield, Sheffield; United Kingdom
- 146 Department of Physics, Shinshu University, Nagano; Japan
- 147 Department Physik, Universität Siegen, Siegen; Germany
- 148 Department of Physics, Simon Fraser University, Burnaby BC; Canada
- 149 SLAC National Accelerator Laboratory, Stanford CA; United States of America
- 150 Department of Physics, Royal Institute of Technology, Stockholm; Sweden
- 151 Departments of Physics and Astronomy, Stony Brook University, Stony Brook NY; United States of America
- 152 Department of Physics and Astronomy, University of Sussex, Brighton; United Kingdom
- 153 School of Physics, University of Sydney, Sydney; Australia
- 154 Institute of Physics, Academia Sinica, Taipei; Taiwan
- 155 ^(a) E. Andronikashvili Institute of Physics, Iv. Javakishvili Tbilisi State University, Tbilisi; ^(b) High Energy Physics Institute, Tbilisi State University, Tbilisi; Georgia
- 156 Department of Physics, Technion, Israel Institute of Technology, Haifa; Israel
- 157 Raymond and Beverly Sackler School of Physics and Astronomy, Tel Aviv University, Tel Aviv; Israel
- 158 Department of Physics, Aristotle University of Thessaloniki, Thessaloniki; Greece
- 159 International Center for Elementary Particle Physics and Department of Physics, University of Tokyo, Tokyo; Japan
- 160 Department of Physics, Tokyo Institute of Technology, Tokyo; Japan
- 161 Tomsk State University, Tomsk; Russia
- 162 Department of Physics, University of Toronto, Toronto ON; Canada
- 163 ^(a) TRIUMF, Vancouver BC; ^(b) Department of Physics and Astronomy, York University, Toronto ON; Canada
- 164 Division of Physics and Tomonaga Center for the History of the Universe, Faculty of Pure and Applied Sciences, University of Tsukuba, Tsukuba; Japan
- 165 Department of Physics and Astronomy, Tufts University, Medford MA; United States of America
- 166 Department of Physics and Astronomy, University of California Irvine, Irvine CA; United States of America
- 167 Department of Physics and Astronomy, University of Uppsala, Uppsala; Sweden
- 168 Department of Physics, University of Illinois, Urbana IL; United States of America
- 169 Instituto de Física Corpuscular (IFIC), Centro Mixto Universidad de Valencia – CSIC, Valencia; Spain
- 170 Department of Physics, University of British Columbia, Vancouver BC; Canada
- 171 Department of Physics and Astronomy, University of Victoria, Victoria BC; Canada
- 172 Fakultät für Physik und Astronomie, Julius-Maximilians-Universität Würzburg, Würzburg; Germany
- 173 Department of Physics, University of Warwick, Coventry; United Kingdom
- 174 Waseda University, Tokyo; Japan
- 175 Department of Particle Physics and Astrophysics, Weizmann Institute of Science, Rehovot; Israel
- 176 Department of Physics, University of Wisconsin, Madison WI; United States of America
- 177 Fakultät für Mathematik und Naturwissenschaften, Fachgruppe Physik, Bergische Universität Wuppertal, Wuppertal; Germany
- 178 Department of Physics, Yale University, New Haven CT; United States of America

^a Also at Borough of Manhattan Community College, City University of New York, New York NY; United States of America.

^b Also at Bruno Kessler Foundation, Trento; Italy.

^c Also at Center for High Energy Physics, Peking University; China.

^d Also at Centro Studi e Ricerche Enrico Fermi; Italy.

^e Also at CERN, Geneva; Switzerland.

^f Also at Département de Physique Nucléaire et Corpusculaire, Université de Genève, Genève; Switzerland.

- ^g Also at Departament de Fisica de la Universitat Autònoma de Barcelona, Barcelona; Spain.
- ^h Also at Department of Financial and Management Engineering, University of the Aegean, Chios; Greece.
- ⁱ Also at Department of Physics and Astronomy, Michigan State University, East Lansing MI; United States of America.
- ^j Also at Department of Physics and Astronomy, University of Louisville, Louisville, KY; United States of America.
- ^k Also at Department of Physics, Ben Gurion University of the Negev, Beer Sheva; Israel.
- ^l Also at Department of Physics, California State University, East Bay; United States of America.
- ^m Also at Department of Physics, California State University, Fresno; United States of America.
- ⁿ Also at Department of Physics, California State University, Sacramento; United States of America.
- ^o Also at Department of Physics, King's College London, London; United Kingdom.
- ^p Also at Department of Physics, St. Petersburg State Polytechnical University, St. Petersburg; Russia.
- ^q Also at Department of Physics, University of Fribourg, Fribourg; Switzerland.
- ^r Also at Faculty of Physics, M.V. Lomonosov Moscow State University, Moscow; Russia.
- ^s Also at Faculty of Physics, Sofia University, 'St. Kliment Ohridski', Sofia; Bulgaria.
- ^t Also at Graduate School of Science, Osaka University, Osaka; Japan.
- ^u Also at Hellenic Open University, Patras; Greece.
- ^v Also at Institutio Catalana de Recerca i Estudis Avancats, ICREA, Barcelona; Spain.
- ^w Also at Institut für Experimentalphysik, Universität Hamburg, Hamburg; Germany.
- ^x Also at Institute for Particle and Nuclear Physics, Wigner Research Centre for Physics, Budapest; Hungary.
- ^y Also at Institute of Particle Physics (IPP); Canada.
- ^z Also at Institute of Physics, Azerbaijan Academy of Sciences, Baku; Azerbaijan.
- ^{aa} Also at Institute of Theoretical Physics, Iliia State University, Tbilisi; Georgia.
- ^{ab} Also at Instituto de Fisica Teorica, IFT-UAM/CSIC, Madrid; Spain.
- ^{ac} Also at Istanbul University, Dept. of Physics, Istanbul; Turkey.
- ^{ad} Also at Joint Institute for Nuclear Research, Dubna; Russia.
- ^{ae} Also at Moscow Institute of Physics and Technology State University, Dolgoprudny; Russia.
- ^{af} Also at National Research Nuclear University MEPhI, Moscow; Russia.
- ^{ag} Also at Physics Department, An-Najah National University, Nablus; Palestine.
- ^{ah} Also at Physikalisches Institut, Albert-Ludwigs-Universität Freiburg, Freiburg; Germany.
- ^{ai} Also at The City College of New York, New York NY; United States of America.
- ^{aj} Also at TRIUMF, Vancouver BC; Canada.
- ^{ak} Also at Università di Napoli Parthenope, Napoli; Italy.
- ^{al} Also at University of Chinese Academy of Sciences (UCAS), Beijing; China.
- ^{am} Also at Yeditepe University, Physics Department, Istanbul; Turkey.
- * Deceased.